TURBULENCE MEASUREMENTS USING PULSED DOPPLER ULTRASOUND

A THESIS

Presented to

The Faculty of the Division

of Graduate Studies

by

Vijay Saxena

In Partial Fulfillment

of the Requirements for the Degree

Doctor of Philosophy in the

School of Aerospace Engineering

Georgia Institute of Technology

November, 1978

TURBULENCE MEASUREMENTS USING

PULSED DOPPLER ULTRASOUND

Approved:

D. P. Giddens, Chairman

J. I. Craig

A. M. Bush

Date approved by Chairman: 11/30/78

ACKNOWLEDGMENTS

First and foremost, I would like to thank Dr. Donald P. Giddens, my advisor, for his suggestion of the topic of the present research and for his invaluable guidance; but for his patient and persistent encouragement this report would never have seen the light of the day. Working with Professor Giddens was a very pleasurable and rewarding aspect of my graduate education.

My sincere thanks and earnest gratitude are due to Dr. James I. Craig for many stimulating and enlightening discussions, as well as for always finding time for me in his ever-so-busy schedule.

I am greatly obliged to Professors A. M. Bush, J. E. Hubbartt, and R. W. Schafer, the additional members of my reading committee, for their careful reading of the manuscript and many useful suggestions.

Discussions with and experimental expertise of Mr. A. M. A. Khalifa proved to be indispensable during the course of the research. Also, I am grateful to Mr. J. Caudell for coming to my rescue, whenever needed, by cajoling the electronic equipment to work.

I am obliged to thank Ms. Jackie Van Hook for her careful typing of this thesis at a very short notice and also for standing up to the trials of working with me.

I wish to thank my parents for their constant encouragement, and my numerous friends who made the business of living a pleasure. Finally, to all the skeptics in the world -- I MADE IT!!

TABLE OF CONTENTS

TABLE OF CONTENTS (Continued)

LIST OF TABLES

LIST OF TABLES (Continuation)

LIST OF ILLUSTRATIONS

LIST OF ILLUSTRATIONS (Continuation)

LIST OF ILLUSTRATIONS (Continuation)

LIST OF ILLUSTRATIONS (Continuation)

LIST OF ILLUSTRATIONS (Continuation)

SUMMARY

Pulsed ultrasound Doppler (PD) velocimeters have recently been developed for measuring flow disturbances and mapping velocity flow fields. This is especially advantageous in clinical situations where detection of turbulence may lead to an early detection of atherosscleroses. However, the most common demodulator used with these velocimeters, namely the zero-crossing frequencymeter (ZCF) has been demonstrated to be unsuitable for turbulence measurements. The phase-locked-loop demodulators also suffer from several disadvantages including poor performance at low velocities. In the present work, a new demodulating scheme is proposed by relating the statistical probability density functions of velocities inside the region of Doppler sensitivity (i.e., sample volume) to the Doppler shifted signal originating from this region. The first moment of the normalized power spectrum of the Doppler signal received from a sample volume is hypothesized to be the spatially-averaged velocity within it.

This demodulator is realized through the use of digital methods and therefore is called the Digital First Moment (DFM) method. Through the use of this DFM method the spatially-averaged velocity can be sampled to obtain the time history from which relevant information about the turbulent flow may be derived. The validity of the proposed model is tested, first in the mean, by its application to real pipe flows. Next, its performance limits and accuracy in velocity fluctuation measurements are evaluated through its application to a set of

Doppler signals simulating a variety of flow situations. Lastly, the DFM method is tried on actual turbulent pipe flows, and its results are compared with a phase-locked loop (PLL) demodulator, and an accepted standard, the Laser Doppler velocimeter. The PD/DFM combination is demonstrated to have a superior performance than the PD/PLL combination if various errors corrupting its performance are taken into account. It may be noted that these errors are not due to the DFM demodulator, but rather are dependent on the PD velocimeter being used, and therefore can be eliminated by suitable redesign. This and other possible future improvements are described.

NOMENCLATURE

$A(t)$	Amplitude modulating signal
c	velocity of propagation of sound
D	pipe diameter
d	piezo-electric crystal diameter
E^*	non-dimensionalized power spectrum
e	modulation factor
f	frequency
$F(\vec{r},\vec{v},t)$	time dependent point probability density function of velocity (in statistical fluid mechanics)
f_o	transmission frequency
f^*	cut-off frequency of a Doppler velocimeter
f_D	the Doppler frequency shift
$F(f)$	dimensional (measured) power spectrum
F_{max}	maximum frequency response
$g(\vec{r},\vec{v}_x,t)$	'reduced' probability density function of axial velocity (in statistical fluid mechanics)
$I(f)$	power spectrum of the ideal Doppler signal, i.e., ideal distribution function of velocities
$Jn(\beta)$	Bessel functions of the first kind
K_D	Doppler constant
K_v	VCO constant
k_*	cut-off wave number of a Doppler velocimeter

N_S^*	Strouhal's number
Q	coupling coefficient of the piezoelectric crystal
R	Range
R_{max}	maximum measurable range
$R_F(u)$	response function of a flow experiment setup
Re	Reynolds number
Re_{min}	Reynolds number based on the minimum resolvable length in the direction of the mean flow
SNR	signal-to-noise power ratio
T	the sample length of the Doppler signal
u	instantaneous flow velocity
u_{max}	maximum measurable velocity
U	the mean flow velocity
u'	fluctuations about the mean velocity, i.e., turbulence
u'_{rms}	the rms turbulence velocity
v(t)	instantaneous particle velocity
V	maximum particle velocity
$(v_m)_{rms}$	rms amplitude of A(t)
$(v_m)_{avg}$	average amplitude of A(t)
	Doppler spectrum broadening caused by:
$\Delta\omega_{u_o}$	volume averaged velocity (i.e., center frequency) fluctuations
$\Delta\omega_T$	variations in velocity across the sample volume

$\Delta\omega_L$	finite transit time of particles through the sample volume
$\Delta\omega_G$	mean velocity gradient across the sample volume
$\Delta\omega_\beta$	Brownian motion of the scatterers
$\Delta\omega_S$	electronic noise
$\Delta\omega$	Doppler ambiguity bandwidth
λ	wavelength of the transmitted beam
η	Kolmogorov microscale of turbulence
ρ	fluid density
μ	fluid viscosity
ϕ	angle between the transmitted and the received beam
ν	kinematic viscosity
θ	angle between the ultrasonic beam and the velocity vector (single transducer case)
θ_1	angle between the velocity vector and the transmitting crystal axis
θ_2	angle between the velocity vector and the receiving crystal axis
ω_c	carrier frequency

CHAPTER I

INTRODUCTION

1.1 Background and Motivation

Measurement of velocities in disturbed flows is a problem facing engineers today in a variety of disciplines. A description of the flow field in the vicinity of an airfoil is necessary for more accurate load prediction and efficient design of airplane wings and helicoptor rotors. Quieter and energy-saving engines and compressors can be developed if their internal flow characteristics are established. Measurement of atmospheric currents is useful in meteorology, and that of oceanic currents in oceanography. In the medical field determination of blood flow velocities through peripheral arteries is necessary for biomedical engineering studies of artherosclerosis -- an accurate knowledge can supply useful information for the study of the disease. Finally, knowledge about the fine structure of turbulence will help in making better and more general models for mathematical treatment of the problem.

One way to measure turbulence with high spatial resolution, and frequency response is to use small, heat sensitive elements with small heat capacity and response time. Hot-wire and hot-film anemometers were developed using this idea, and over the last several decades have proved to be the most popular instruments (Laufer 1956, Ling 1956, Wehrmann 1968). Despite their effectiveness, they suffer from several rather severe drawbacks, the major one being the necessity of probe insertion in the

flow being measured, which in small scale experiments can cause excessive interference. Their calibration is delicate and unstable, thus not reliable. Also, they are incapable of measuring recirculating flows due to their directional ambiguity, and they are likely to be damaged by naturally occurring particles in some flows.

The recently developed Laser Doppler velocimeters (LDV) overcome these difficulties, and in fact, with their sophisticated photon-correlation techniques are regarded nowadays as supreme tools for the study of fine scale turbulence (Yeh and Cummings 1964, Durst, et al. 1976). However, they too have their share of drawbacks; they are quite expensive, yield erroneous results with high particle concentrations, and due to their very nature, cannot measure flows in optically opaque vessels or fluids.

The ultrasound Doppler flowmeter, developed in the late fifties is becoming increasingly popular as a result of an awareness of key advantages it offers, and the availability of inexpensive and reliable instrumentation (Satomura 1959, Baker 1970, Light 1972). These devices have proved their worth in a wide variety of applications in engineering and medicine.

The present research derives its motivation from the study of blood flow near localized arteroisclerosis. Arteroisclerosis is a major cause of death in the United States, and therefore is the object of one of the most intensive research efforts in recent years. Hemodynamics has been recognized to be a major factor in the genesis and development of the disease. Clearly, it is desirable to measure blood flow through arteries in order to diagnose the disease. However, the

study of blood flow within the body (in-vivo) nontraumatically requires noninvasiveness of the probe, thus severely limiting the use of hot-film devices. Optical opaqueness of arteries renders the LDV inapplicable for invivo studies, although it could be used in studying flow patterns in models (in vitro). Doppler Ultrasound flowmeters, thus, seem to be the ideal choice for the study of blood flow both in research and in clinical environments.

Until recently, medical researchers have been using these ultrasound flowmeters as crude estimators of blood flow rate through peripheral arteries: the continuous wave (CW) type is used as an empirical estimator of blood flow rate (Miller and Histand, 1972(a)), and the pulsed (PD) type is used to directly map the velocity profile across the artery and calculate the resulting blood flow (Peronneau, 1971). Unfortunately, the blood flow through arteries does not decrease significantly until a severe constriction is formed, thus pre-empting this criterion for an early detection of arteriosclerotic disease. Velocity disturbances occurring downstream of an occlusion, even in its earliest stage of advancement, are measurable and may yield valuable information about the occlusion itself. In fact, there is a possibility that a certain degree of correlation may exist between the intensity (and power spectrum) of turbulence and the severity of stenosis generating it (Giddens et al. 1976, Histand and Greene 1976).

In addition to various clinical needs for such a technique, detection and characterization of flow disturbances is a largely neglected area of hemodynamics. The importance of turbulence cannot

be overlooked in the estimation of parameters such as pressure gradient and shear forces acting on the arterial wall. Also, as a noninvasive measurement technique for turbulence in optically opaque vessels ultrasound deserves more thorough and vigorous research efforts.

With biological systems it is estimated that the average radiation power level of any device should not exceed 50 mW/cm^2 (MacIntosh 1972, Wells 1974) in order to avoid hemolysis and damage to tissue structure. The power levels of ultrasonic devices are low enough so as not to cause these mal-effects. In addition, the use of acoustic energy does not necessitate insertion of the probe (i.e., it is non-traumatic), thus making these devices ideal for use in medicine.

1.2 The Flowmeter

1.2.1 A Historical Sketch

Though ultrasound flowmeters were first used for industrial purposes, medicine embraced it with great enthusiasm with the result that nowadays alomst all of the research on these devices is oriented toward blood flow measurement.

The possibility of application of ultrasound in medicine was first suggested by Kalmus' device, developed at the Scripps Institute of Oceanography for ocean current measurement (1954). Herrick and Anderson (1959) appreciated the advantages of Kalmus' method and produced a miniaturized unit. Franklin et al. (1959) developed a pulsed flowmeter unit ('sing around' type) in which pulses are sent alternately upstream and downstream through the flow. This gives a voltage proportional to the transit time, and hence proportional to velocity.

Because of the bidirectional emission of pulses, they also did not have the zero problem experienced by Herrick.

All these devices, however, were of the 'transit time' type. Their medical applications were at an early experimental stage in which the chest of an animal subject was opened and two transducers put snugly on the unopened artery 1-3 centimeters apart. Still, under optimal conditions they could measure volume of flow within a five percent error. Maximum noise and base drift corresponded to a flow velocity variations of less than 1 cm/sec (Franklin et al.,1959).

Satomura (1959) was the first to realize the feasibility of determining blood flow by measuring the Doppler frequency shift in the signal backscattered by erythrocytes in the flow. He and Kaneko (1960) constructed a flowmeter using this concept, and Franklin et al. (1961) demonstrated satisfactory use of such a continuous Wave (CW) type flowmeter in measuring blood flow velocity in an unopened dog aorta.

Baker et al. (1964 and 1965) described the first practical device intended for transcutaneous blood flow measurement in man. Since then, CW Doppler ultrasonic flowmeters have been increasingly improved and now are sold to clinics throughout the world. They have been successfully used by a number of investigators in studies such as the detection of fetal heart wall motion, localizing subcutaneous arteries transcutaneously, to evaluate their vascular patency (Strandness et al., 1967a), directional measurement of instantaneous mean blood flow velocity in a vessel (McLeod, 1967),

transcutaneously transmurally (Rushmer, et al. 1966, Miller and Histand, 1972 (b), Rushmer et al. 1965), intramurally with a catheter tip probe (Siegall et al., 1967), and for peripheral vascular disease (PVD) diagnosis (Strandness et al., 1967 (b)).

The Doppler system can also be easily applied to telemetry operations since the signal exists as a carrier plus a sideband and therefore can be directly transmitted without further modulation. This led to some interesting and unique applications; Van Citter and Franklin measured blood flow rates in free-ranging animals such as baboon, a dog running with a dog sled team, an elephant seal and a running giraffe (Van Citter et al., 1965 a,b and c, 1966, 1967).

Almost in parallel with the development of more effective instruments, clinicians began to ask more sophisticated diagnostic questions. The need for a more powerful method was slowly being defined: the CW Doppler flowmeter did not have any range perception -- everything moving within the reach of the acoustic beam contributed toward the final signal. Thus, vessel wall motion or the presence of two arteries in the beam path could lead to incorrect results. Also, since the Doppler process is sensitive to velocity, and not to the flow rate, the lumen diameter must be known or the flowmeter must be calibrated empirically for measuring flow rates (McLeod, 1970).

As a result of these limitations, the use of CW devices, for the most part, was restricted to a qualitative nature, whether the Doppler signals were processed and recorded as analog waveforms or the clinician based his conclusion on listening to Doppler signals. Thus, these

devices were not used as flow meters, but rather as flow detectors.

Many of the problems associated with the CW systems can be overcome if the ultrasound source is pulsed. By pulse modulating the carrier, position and velocity of the scattering particles can be simultaneously estimated. The entire velocity profile can be obtained, and the blood flow rate can be computed from the measured profile without resorting to any empirical calibration schemes. These pulsed, range-gated Doppler velocimeters (PDV) have been available since Baker described such an instrument (Baker and Watkins 1967, Baker 1970). Two other systems were also developed almost simultaneously (Wells 1969, Peronneau 1969). Since then, the instrument has prospered through the electronic revolution.

1.2.2 More Recent Advances

Multi-channel PD devices have been recently developed (McLeod 1974) which yield instantaneous values of velocities at several depths simultaneously, thus facilitating the construction of instantaneous velocity profiles.

Meindl's group at Stanford University has been quite active in the past in development of implantable flowmeters. These have been made successively smaller and more sophisticated. However, results of in-vivo experiments have not been reported (Dipietro and Meindl 1970, Bert et al., 1972, Allen et al. 1977).

The typical PD flowmeter described above, though a vast improvement over the CW type, suffers from several limitations. Two of the more significant ones and their cures are described below.

In their simplest form, ultrasound flowmeters are unable to sense direction due to their inability to distinguish between positive and negative frequency shifts. Improvements were tried on the CW type (McLeod 1967, Nippa 1974), and later extended to the PD type (Peronneau, 1969, Haase et al. 1973). McLeod (1967) observed that a phase detection in quadrature makes possible the identification and separation of the positive and negative Doppler shifts. Which of the two voltages leads the other depends solely on the sign of the Doppler shift. By using shifts ranging from 60° to 120° he was able to obtain flow rates in the aorta of a dog as it varies during the cardiac cycle. Nippa (1974, 1975), argued that a true velocity separation in the two channels is not achieved, only a signal proportional to differential or net flow. The scattered signal from CW type flowmeter, in the presence of bidirectional simultaneous flow consists of an ultrasonic carrier, f_0 and a positive Doppler shift $f_0 + f_u$, and a negative one $f_0 + f_1$. Thus $f_0 + f_u$ and $f_0 + f_1$ are upper and lower sidebands of f_0 respectively, and can be separated using the well established techniques in radio communication. They introduced a phase shift prior to the phase detection stage of the flowmeter, thus gaining capability of simultaneously measuring coexisting bidirectional flow. Their device gives two independent flow velocity voltages, one for forward and the other for the reverse flow. Using this flowmeter they demonstrated simultaneous measurement of blood flow in the carotid artery and the adjacent jugular vein (both lying in the acoustic beam path) on two different channels. In this case McLeod's device would give only the resultant differential

velocity.

Both the above flowmeters were of the CW type. Using similar techniques Peronneau (Peronneau et al., 1969) developed a directional PD velocimeter. Hasse et al. (1973) report construction of a directional PD flowmeter utilizing the freuqency offset technique. Here the received backscattered signal is compared with transmitted frequency, f_0 offset by Δf_0. This offset was provided by a digital phase-locked-loop circuit connected to the master oscillator, and was adjustable. The output of phase detector is then $f_D + \Delta f_0$. Thus zero flow corresponds to a Doppler frequency of Δf_0, forward flow has frequency shift greater than Δf_0, and shift frequencies less than Δf_0 indicate reverse flow. They claimed that such a method has some distinct advantages over the phase shift direction sensing method:

a) it requires much fewer electronic components and less complicity.

b) better accuracy is obtained with low flow velocities - the ZCF has been demonstrated to give maximum error near zero frequency due to the noise present in the input signal (Rice, 1945). With non-offset techniques, low velocities (i.e., near-zero frequencies) will result in large errors.

The conventional PD systems using a sinusoid as carrier are well suited to peripheral vascular measurements. However, they suffer from their inherent lack of simultaneous range and velocity resolution. It is known that the range-velocity error element for all radar systems is inversely proportional to the bandwidth-time duration of the pulse.

Clearly, in order to improve range-velocity resolution, this bandwidth duration product must be made as large as possible. In the conventional pulsed systems it is around 1.2 generally; hence it is not possible to simultaneously obtain good range and velocity resolution. The range resolution capability of the conventional RF system can be improved by narrowing the transmitted pulse (in order to reduce the listening time which governs the depth of the sample volume). But the necessity of maintaining sufficient average power in the transmitted signal could make the peak power prohibitively high for the biological tissue.

In order to overcome this time-bandwidth product limitation, a number of techniques such as pulse compression, pseudo-random phase coding of the signal, coherent pulse-to-pulse transmission, and pseudo-random noise technique have been tried in the microwave radar area (Jethwa et al. 1975, Skolnik 1962). However, all of these suffer from limitations such as:

a) ambiguous responses due to the necessity of employing periodic signals, and

b) a direct coupling between range and velocity resolutions. This comes from the fact that the maximum unambiguous range and the maximum unambiguous velocity are inversely related.

It is claimed (McGillem and Cooper 1969, Newhouse and Bendick 1973, Jethwa et al. 1975) that random signal pulsed Doppler Systems provide a solution to above problems. The transmission freuqency is derived from a wideband Gaussian white noise source thus permitting extremely large time-bandwidth products, and consequently alleviating

the range and velocity ambiguities associated with the periodic signals. In this case the bandwidth of the signal is primarily limited by the characteristics of the transducer used. The velocity and range resolution in these systems are independent of each other allowing us to control one without affecting the other -- a thing not possible with the conventional pulsed systems.

In summary, the random signal ultrasonic system has following advantages:

a) A much greater average power can be transmitted without sacrificing the range resolution, since it does not depend upon the pulse width of the transmitted signal as is the case with the conventional coherent Doppler system.

b) The signal-to-noise ratio of the random signal and the conventional coherent Doppler system using the same average power and spatial resolution are equivalent. However, the former has the advantage of complete freedom from ambiguous responses.

c) The range and velocity measurements can be improved simultaneously using this instrument. This is not possible with the conventional coherent Doppler systems.

d) Separate instruments using independent noise signal can be used to monitor different quantities on the same subject at the same time without mutual interference.

The main problem associated with the Random Signal Doppler Flowmeter is the continuous clutter noise due to the tissues surrounding the blood vessel and those located between the transducer and the blood

vessel of interest. Jethwa et al. (1975) suggest minimizing this problem by the use of low pulse repetition frequencies while the velocity ambiguities introduced by such a long pulse period can be eliminated by employing random signal pulse staggering. Clearly, however, this approach leads directly toward vastly more complicated systems than considered to date. The use of random PD velocimeter is also restricted due to the transducer response limitations (Luque et al., 1976).

1.3 Previous Studies in Ultrasound Doppler Signal Processing

After the rapid growth of hardware, and its apparent initial successful application to flow measurement, only recently efforts are being made to explain theoretically the Doppler process, and the functioning of associated demodulation techniques. This is necessary to develop and devise better methods to study fluid flow with a sound theoretical background keeping in mind the limitations and drawbacks of these devices.

In the presence of nonuniform flow profiles across the sample volume, there will be a range of Doppler shifts rather than a single one as predicted by the Doppler equation. Any attempt to understand the operation of Doppler flowmeters solely on the basis of this equation will result only in limited success because many important aspects of problem have not been taken into account. It is the power spectrum of the Doppler signal that contains the relevant information about the flow inside the sample volume, and it is this that must be considered

for obtaining any meaningful results from the returned Doppler signal.

Medical researchers have been analyzing the Doppler shifted signal in an attempt to predict stenoses. One method is to view its sonogram (a sonogram of a signal displays frequencies present with the trace blackening in proportion to the amplitude of the frequency). A sonogram thus contains the Doppler frequency information for simple visual inspection. Collins et al. (1976) studied these sonograms from diseased persons, and related the changes in them to arteriographic findings. Lin et al. (1976) suggested a way to continuously display the power spectrum using transfer properties of various optical elements. Here the Doppler signal was transformed to frequency domain and displayed on a ground glass plate. Sigel and colleagues (1970) were able to distinguish laminar and turbulent flows by observation of power spectra of the Doppler signal. In an in-vivo model they found that the high frequency content of the signal was greater for turbulent flow in comparison with the laminar flow. A significant part of this increase was interpreted as resulting from transverse velocity components moving within the vortices of turbulent stream. Yao and Needham (1970) and Gosling et al. (1970) studied changes in the Doppler power spectra visually in order to diagnose stenoses.

Winter, Wills and Morgan (1975, 1976a, 1976b) hoped that the variation in the autocorrelation function of the Doppler signal would give an indication about the flow disturbances. However, this method could only differentiate between disturbed and undisturbed flow, without

any quantitative information about the flow disturbances. Thus, it could best be used only as an indicator of flow disturbances.

In a similar approach, McLeod et al. (1977) proposed detection of flow disturbances from a Lissajous pattern derived from both channels of a (quadrature detecting) directional Doppler velocimeter. Owing to Rayleigh fading, laminar flow signals appear as a series of smooth spirals. In disturbed flow, small irregularities develop in the display to indicate the presence of phase (i.e., frequency) modulation and disturbed flow. This, again, at best is only an indicative scheme.

Green (1964) analyzed the effect of various causes which contribute toward the broadening of the power spectrum of Doppler signal from a CW Doppler flowmeter intended to measure ocean currents. The factors studied were Brownian motion of the scatterers, finite transit time of the particles through the transducer field pattern, and the angular divergence of the transducer beam. The motivation for his study was the fact that the low density of scatterers in the ocean produces scattered returned signals that are buried in noise. To reduce the effect of this white noise, system bandwidth must be reduced. Green concluded that by producing very narrow Doppler spectrum, a phase-locked-loop demodulator can be used (in the place of the zerocrossing demodulator commonly employed), thereby reducing the bandwidth, and increasing the effective SNR of the flow estimates. Non-uniform velocity distribution was neglected as this was not a significant factor in his study.

Even in the presence of a range of Doppler shifts, the frequency

to voltage converter gives only one output. The relationship of this output to the range of Doppler frequencies present in the signal depends on the detailed description of the demodulator. Flax et al. (1969, 1971) attempted to make a unified model of a flow with parabolic velocity profile, CW flowmeter, and zero crossing frequencymeter. Through a completely analytical approach, they predicted the power spectrum, and autocorrelation function of the ZCF output, and these were compared with experimentally observed results. However, several important factors were omitted in this pioneering work: first, the amplitude of the Doppler voltage spectrum was assumed to be proportional to the number of the scattering particles, N, at a given frequency. As a result, the power spectrum will be proportional to the number of the particles squared, N^2. This assumption was based on a deterministic scattering model, in which all particles were tacitly assumed to scatter with fixed relative amplitude, and phase (i.e., they are coherently distributed inside the sample volume). In Rayleigh scattering, commonly believed to occur with the ultrasound, however, these particles are independent of each other and scatter with random phase giving a power spectrum proportional to N rather than N^2. Secondly, the fact that the power spectrum is a density function (implying that the total power is the integral of the power spectrum over frequency) was neglected, thus leading to analytically erroneous spectra predictions. Thirdly, by completely ignoring the statistical nature of scattering, the contribution to the power spectrum by the finite transit time of scatterers through the incident beam was lost (Brody, 1972).

Nevertheless, this work is important in presenting a first analytical model of zerocrossing demodulator based primarily on Rice's early work (1945) in this field. They demonstrated the large variance obtained in the flow measurements by the use of ZCF, especially with pulsatile flows. Suggestions were made (Flax et al., 1974) to improve the system performance by either redesigning the transducer geometry to produce narrower Doppler spectra (making the ZCF adequate), or by employing a different kind of demodulator (such as phase-locked-loop) to track the peak of the power spectrum. However, neither of these possibilities was explored.

These tasks were taken up by Brody (1972, 1974), and his work probably is the most comprehensive theoretical treatment to date. He set out to answer the questions as to what does the CW flowmeter measure, and how to improve the demodulator performance so as to directly give flow rates (not velocities) through vessels. By recognizing the CW flowmeter as a type of sonar mapping system, he availed himself of the well known results of statistical communication theory, which in turn were used to develop a statistical model of ultrasound scattering by particles from which relevant characteristics of the Doppler signal were derived. Next, a generalized model of the flowmeter was formulated taking into account the geometry of transducers, transmitted waveform, and the velocity distribution of scatterers. The predicted Doppler power spectra were compared with the experimental results for several, but not all, transducer dimensions and orientations. The main contributions of this work can be summarized as:

a) A rigorous theoretical foundation is laid for treatment of the scattering process inside the sample volume for laminar flow.

b) Fluid flow estimation is demonstrated to be integrally related to the estimation of Doppler power spectra.

c) A scheme was proposed for predicting the bulk flow rates using a CW flowmeter without requiring empirical calibration, and regardless of velocity profile shape across the vessel.

d) Zero crossing demodulator was studied in even greater detail, and was found to be quite inadequate in predicting flow estimates, let alone velocities. An alternative analog device incorporating phase-locked tracking filters coupled with an average frequency estimator was suggested, but never implemented.

This study, too, leaves out several importnat factors, especially in relation to turbulence measurement using the PD. Finite transit time effects, though incorporated in the initial formulation, were later abandoned for the sake of theoretical and computational simplicity. With CW flowmeters this does not give rise to large errors as the transducer size used is very large in comparison to the wavelength of the radiation used. However, for turbulence measurements, the sample volume is made as small as possible resulting in quite nonuniform ultrasonic fields, thus making these effects prominent. Also, Doppler spectra were predicted only for steady laminar flow, thus restricting its usefulness

for the new interest in turbulence measurements (the study does not lend itself to be extended easily to turbulent flows).

Newhouse (1974, 1976a and b, Varner et al. 1975) studied the effects of the bandwidth of the transmitted signal and the finite transit time of scatterers through the sample volume of PD devices, and predicted methods to estimate flow rates through tubes. They concluded that the effect of finite bandwidth of the transmitted signal (used with random, and pseudorandom PD devices) over the average velocity inside the sample volume can be neglected if the power spectrum of the transmitted signal is symmetric. Thus the estimates were concluded to be within 'acceptable' variance limits. However, in practice this conclusion is suspect as the power spectrum of the transmitted signal is never symmetrical due to the response characteristics of transducers. A more dominant factor, finite transit time was found to give large broadening of the Doppler spectra even when the sample volume was filled with steady velocity with no gradient across it.

Griffith and Brody (1975, 1976) related the limitations on velocity resolution with ultrasonic flowmeters to the finite transit time. Experiments were conducted to demonstrate that the resolution in velocity ΔV depended on the value of velocity, V (i.e., on the transit time of scatterers through the sample volume) for a given transducer-flowmeter combination, and that the ratio $\Delta V/V$ was constant. Finally, they also defined a 'range-velocity resolution product' to quantify the performance of a given PD velocimeter.

Theoretical studies done in relation to the recently developed

technique of Laser Doppler Velocimetry, can be applied to problems with ultrasonic flowmeters. Different methods of velocity detection (cross beam versus single beam) and inherent difference in the nature of light and sonic beams limit the applicaton of the results obtained with LDV directly to PD devices; nevertheless, some qualitative parallels can be established. In this connection, work of Edwards et al. (1971) and George and Lumley (1971, 1973) is notable. The latter investigated the spectrum broadening caused by the finite transit time effect and turbulence in the sample volume and predicted ambiguity limits beyond which turbulence cannot be measured.

Most recently, Fox (1978) has designed a cross beam type ultrasonic flowmeter analogous to the LDV. Theoretical expressions have been derived for expected Doppler shifts and spectral broadening for different flow conditions. When compared with flow inside a turntable, these predictions were found to be satisfactorily accurate. This approach, however, is still in experimental stages, and cannot yet be used for direct turbulence measurements.

1.4 Purpose of Study

The most common method of deriving velocity informaton from the Doppler Signal is the use of zero-crossing frequencymeters. From the literature survey of the last section, it is apparent that though their performance is satisfactory for rough flow rate estimation, they are unsuccessful in measuring velocity disturbances. Also, they have been demonstrated to have poor performance with pulsatile flows (Flax

et al. 1971). Recently, phase-locked-loop demodulators have been tried, generally with more success than the ZCF. However, their performance predictions are erroneous at smaller velocities, and also it is not quite clear as to what velocity they measure inside the sample volume. Thus, any demodulating scheme has two basic questions associated with it. First, to what does its output correspond - is it the mean velocity, velocity from the center point, or the maximum velocity of the sample volume? Secondly, how can its performance be improved, i.e., how to devise a good estimator of velocity in order to measure turbulence.

In an effort to answer these questions, the present study proposes a new demodulating scheme. The first question is answered directly, as we try to measure the spatially-averaged velocity in the sample volume. Also, this research thrusts toward achieving higher frequency response, and greater accuracy in velocity measurements in a large velocity range. To these ends we shall:

1. Hypothesize a theoretical model of the sample volume —— we shall provide substantiating arguments from statistical fluid mechanics as the basis for our hypothesis that the instantaneous power spectrum of the Doppler signal originating from the sample volume corresponds to the distribution pattern of velocities inside it. As a consequence, the mean (i.e., the first moment) of the normalized power spectrum is indicative of the instantaneous spatially-averaged velocity inside the sample volume.

2. Devise a digital scheme for the realization of the above model -- in order to sample this instantaneous spatially-averaged velocity of the sample volume at rates necessary to yield its time history with sufficiently high frequency response, digital techniques are resorted to. This recorded time history of the average velocity can later be used to derive desired information about the turbulent flow.

3. Test the validity of the concept, and evaluate the performance limits of the proposed demodulator by its application ot synthesized Doppler Signals simulating different flow situations of increasing complexity. This yields exact error margins of operation of the proposed velocity estimator since all the parameters of the flow are known and controllable. These simulated flows are important to study because they can be made to have an 'ideal' Doppler signal uncontaminated by the effects if i) nonidealities of the actual sample volume, and ii) Doppler ambiguity. Thus, any limitation of the DFM concept which are not related to the scattering process and sample volume size can be readily isolated.

4. Finally, apply this theoretical model and its digital realization to an existing PD velocimeter in measuring actual turbulent pipe flows. This will give us some insight into the limitations for practical use of the proposed scheme. Also, it will give us some experience so that a reasonable judgement about the model and some recommendations for the improvement of the proposed demodulator can be made.

It should be noted, thus, that the scope of this research is

limited to hypothesizing and testing of a model. It is neither proposed nor tried to provide an end product for routine use in turbulence measurements.

1.5 Contributions

The main contribution of this work lies in the fact that a new model for the velocity distribution in the sample volume is proposed, thus affording a greater insight into the flow. The validity of this model encourages one to use not only the first moment but also the higher moments in an effort to describe more accurately (and more completely) the flow inside the sample volume. The decision to implement the above model digitally is especially advantageous since digital methods tremendously enlarge the scope of signal treatment. Any demodulator bandwidth can be achieved (giving corresponding accuracy and maximum frequency response in velocity). Also, the measurement of higher moments of Doppler power spectrum is greatly facilitated. An important by-product of this work is the construction of a "Doppler Synthesizer" capable of generating Doppler signals simulating several different flow situations occurring in nature (and some others that don't). This makes further expansion of the proposed demodulator, and testing of any other much simpler without resorting to actual time-consuming, and often messy, flow systems.

CHAPTER II

INSTRUMENTATION

2.1 The Ultrasound Doppler Flowmeter

2.1.1 Principle of Operation

Ultrasonic Doppler flowmeters utilize a classical phenomenon for their operation, namely the Doppler Effect. Whenever there is relative motion among the source, observer, and the propagating medium, the frequency of the signal received by the observer will be different from its frequency at the source. In the special case of a moving medium with source and observer fixed this difference in frequency - the Doppler shift - is given by

$$f_D = \frac{f_o\, u(\cos\theta_1 + \cos\theta_2)}{c} \qquad (2.1)$$

with symbols as defined on page xiv).

Thus, if sound-scattering particles are present in a moving fluid (in case of blood, these are erythrocytes) the velocity of the fluid can be detected by measuring the shift in frequency of the transmitted signal. In the case of blood flow, this frequency shift falls within the audio range due to the carrier frequency employed and the range of typical blood velocities, thus facilitating a qualitative characterization of flow by listening to it on loudspeakers.

For the special case with both the transmitting and receiving

crystals inclined at the same angle to the velocity vector, or the same crystal doing both transmitting and receiving, the above equation reduces to the well-known form,

$$f_D = \frac{2uf_o \cos \theta}{c} \qquad (2.2)$$

where

$\theta = \theta_1 = \theta_2$ is the angle between the incident beam and the flow direction (Figure 1).

Continuous wave (CW) type instruments operate with two separate transducers, one for continually insonating the flow with an acoustic beam, and the other for receiving the backscattered signal from the particles in the flow. Since all the scatterers in the path of the beam reflect ultrasound, the received signal is a sum of signals from these particles, and there is no way of discerning the distance from the transducer of any given scatterer, i.e. all range information is lost, and at best the CW flowmeter is capable of detecting only average velocities. In fact, there has been some controversy among researchers (Rushmer et al. [1966] as to what actually it does measure. Does it measure velocity at one point in the vessel (e.g. center) or, does it estimate velocity averaged over the diameter of the vessel? Another major difficulty with the use of CW flowmeters is poor signal to noise ratio (SNR) that occurs in measuring pulsatile flow (Flax et al 1970). In an attempt to measure velocity averaged over the lumen diameter,

large transducers were used to insonate a significantly large portion of the vessel; however, a decrease in SNR and an increase in the variance of the estimate of the flow was noted at the output of the ZCF (Brody, 1972).

Sometimes, however, it may be desirable to have range resolution. Pulsed Doppler (PD) flowmeters operating in a radar-like range-gated mode allow measurements to be made at specific depths, i.e., they have range sampling capability making it a more attractive mode of operation for velocity measurements. Specifically, PD flowmeters can be used for the following applications:

i) bulk flow rates in small diameter tubes,

ii) determination of blood vessel caliber and depth below the skin,

iii) cross-sectional velocity profiles in the larger tubes, and

iv) even three-dimensional mapping of the flow field.

In addition, the PD approach can significantly reduce the effects of interfering signals by spatially selecting a sample volume for measurement and thus rejecting such artifacts as beat by beat motion of vessel walls or measurement of other moving objects in the acoustic path.

No fewer than three instruments have been developed using this principle (Baker 1970, Wells 1969, Peronneau 1969). Some make use of a single crystal as both transducer and receiver and others use two different transducers; but the basic principle of operation is the same. The transmitter is excited for a very short period of time (0.1 - 1 μsec),

thus sending an acoustic pulse through the flow of fluid containing scatterers. As this pulse of ultrasound traverses across the tube, it contains different scatterers at different times, and as a consequence, reflects signals of different frequency at different times. After an appropriate delay after the transmission of the pulse, the returned signal is received for a short while (0.5 - 3 μs), thus yielding the frequency shifts caused by the particles insonated by the acoustic energy during the time the receiving gate is open. This delay determines the depth location of the sample volume from the transmitter, thus providing the range sampling capability. For the delay time, t, between the transmission and the reception of the pulse, the range, R, is given by

$$R = \frac{t.c}{2} \tag{2.3}$$

where c is, again, the sonic velocity in the fluid.

If the scatterers are small enough, they scatter the incident acoustic energy in the Rayleigh mode, i.e., as point radiators. Therefore, only part of the transmitted energy is backscattered toward the receiver, necessitating amplification of the received signal. This amplified signal is then compared with the delayed version of the transmitted signal yielding the Doppler frequency shift, f_D. However, due to extremely short pulse lengths, this constitutes essentially an instantaneous phase measurement of the Doppler shift; and therefore, in order to properly determine the actual shift frequency this phase

measurement must be repeated at a rate (sampling frequency) at least twice the maximum frequency shift expected. This requirement comes about due to a fundamental theorem of information theory (Shannon's Sampling Theorem) and consequently fixes the minimum transmitting pulse repetition frequency (PRF), f_p to be such that

$$f_p \geq f_{D_{max}} = \frac{4 f_0 V_{max} \text{Cos } \theta}{c} \tag{2.4}$$

This PRF is constrained by another requirement -- if a maximum beam range, R_{max}, is desired giving a delay time of $2R_{max}/c$) and all significant returns are to be received prior to the transmission of a new pulse, the maximum PRF, in absence of the secondary reflections is then

$$f_p \leq \frac{c}{2R_{max}} \tag{2.5}$$

Combining the above two relations yields the 'range-velocity' constraint,

$$U_{max} R_{max} \leq \frac{c^2}{8 f_0 \text{ Cos } \theta} \tag{2.6}$$

This constraint is graphically illustrated in Figure 2 for a sonic velocity of 1500 cm/sec and transducer angle, $\theta = 45^{o}$. For a given carrier frequency, f_0, operation is possible only in the u-R zone to the left of

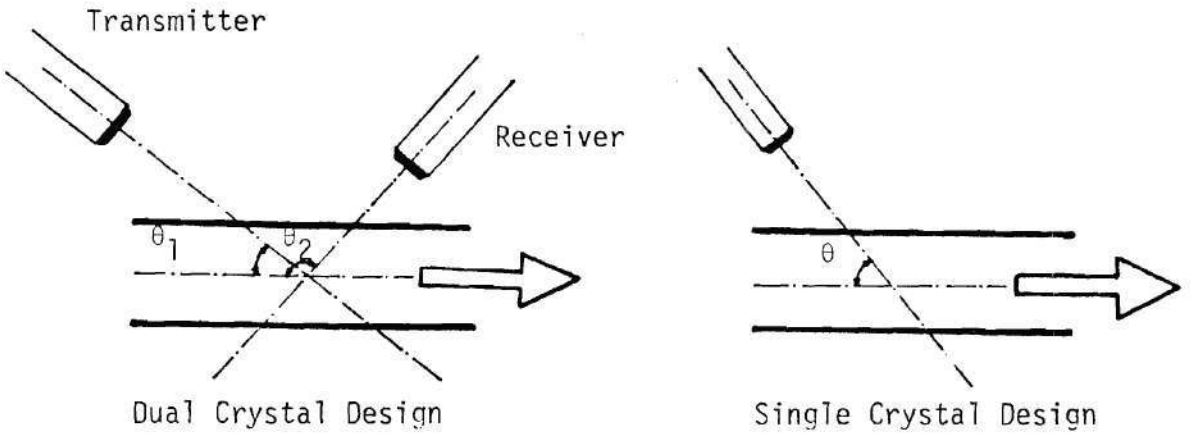

Figure 1. Principle of Operation of Doppler Ultrasound Flowmeters

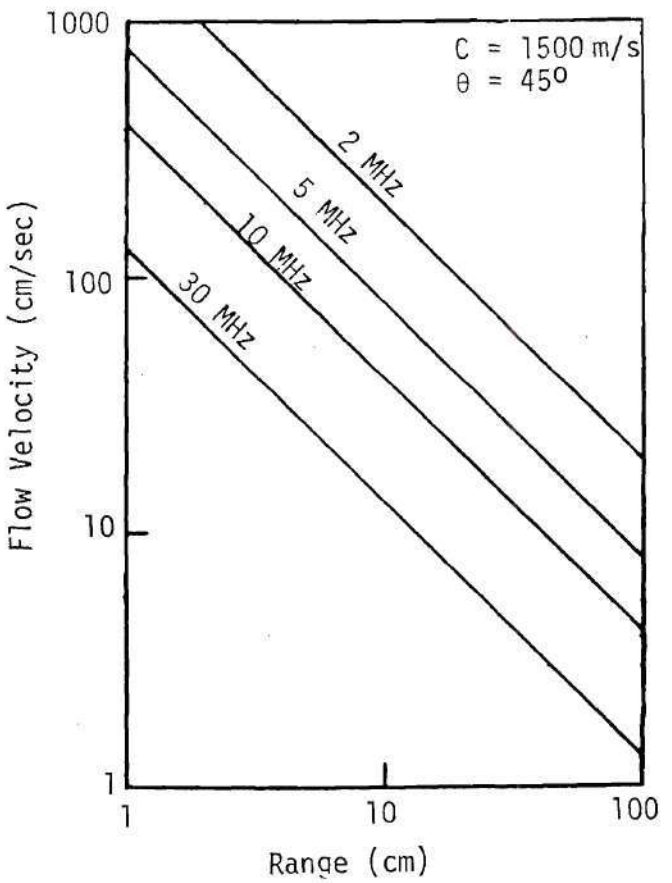

Figure 2. Range-velocity Constraint Illustration for a Pulsed Doppler Velocimeter

the corresponding line. Thus benefits of reducing range ambiguities by pulsing the carrier have their price: although CW flowmeters has very high frequency resolution (minimum ambiguity in velocity), the pulsed system, by necessity, must have poorer Doppler resolution (increased ambiguities in velocity). The design problem of PD, then focuses on finding a pulse rate that, when used with the target for which it is designed, achieves the desired resolution in both range and velocity.

2.1.2 The Flowmeter - Block Diagram

The basic function of all PD devices is to emit an ultrasonic pulse at a pre-selected interval, receive the backscattered signal, and sense the frequency shift by comparing it with a delayed version of the transmitted pulse. To this end, a variety of instruments have been designed; we shall attempt here to describe the interconnections of various essential functional elements with the help of a simplified block diagram (Figure 3).

CW Doppler devices cannot distinguish distances and, conversely, incoherent pulse echo techniques cannot give a direct measure of the velocity of the target. The phase-coherent pulsed Doppler system tries to incorporate into one instrument the primary characteristics of both. The essential requirement of a phase-coherent system is that each burst of ultrasound transmitted be derived from a master oscillator so that the basic rate and the related harmonics have a fixed phase relationship. If this is not done, mixing and beating will occur among the repetition rate harmonics and the Doppler signal. The

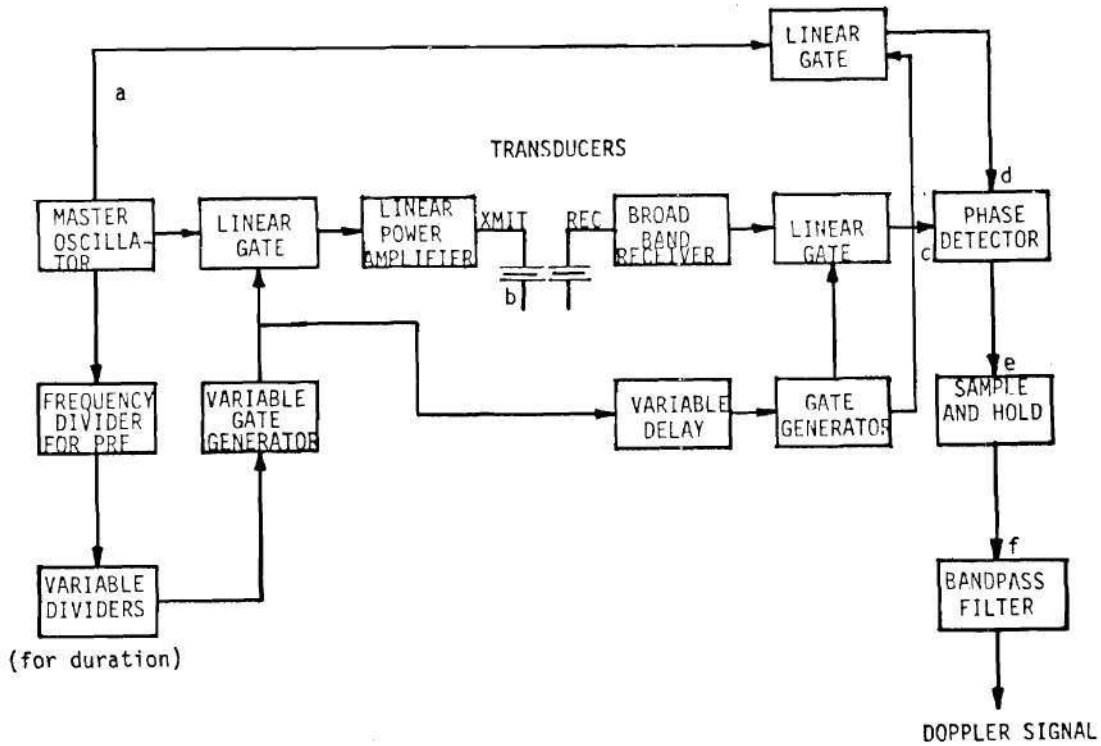

Figure 3. Block Diagram of a Pulsed Ultrasound Doppler Velocimeter

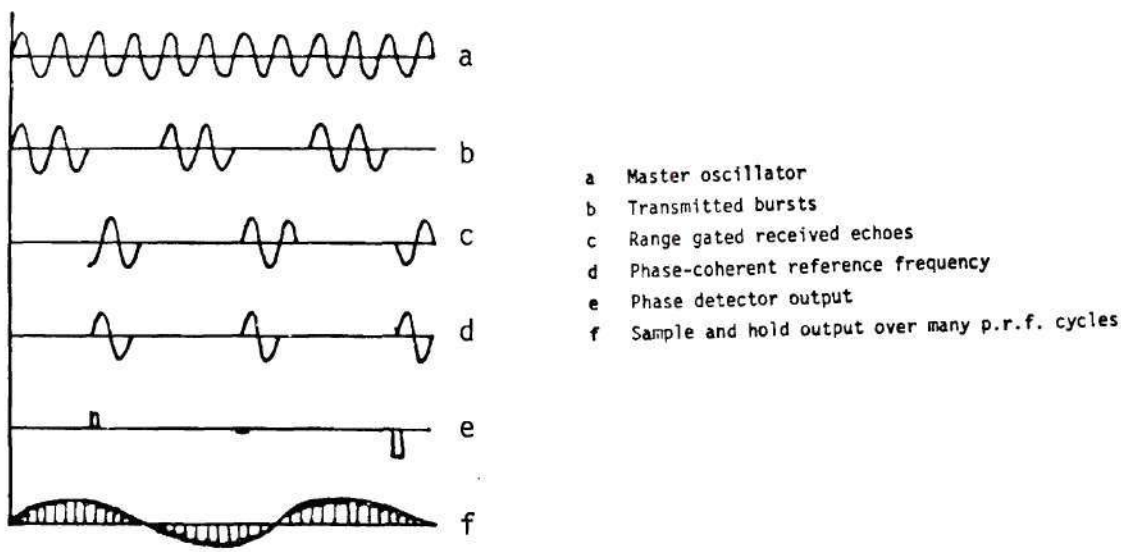

Figure 4. Signal at Different Stages of the Block Diagram in Figure 3.

coherent type of PD flowmeter consists of:

1. Master Oscillator -- This is the heart of the system. Primarily, it generates the transmission frequency, f_0, and it is from this that all the frequencies used in the system are derived. The selection of this transmission frequency represents a compromise between resolution, useful depth penetration, and the maximum velocity to be measured. The following factors must be taken into consideration while making this selection which typically is in the 2.5 to 10 MHZ range:

   a) The requirement of having sufficient power at the receiving end. However, the average transmission power cannot exceed 50 mW/cm^2 with biological systems (Wells 1974, MacIntosh 1972). Attenuation losses through the tissue are proportional to f_0^2, and the intensity of the backscattered signal in Rayleigh scattering is proportional to f_0^4 (Newhouse et al, 1974).

   b) Improved velocity resolution depends on the highest possible f_0; but noise and losses increase rapidly with f_0.

   c) An upper limit on f_0 is needed to measure maximum velocity for a given maximum range.

   d) Increased depth of observation demands lower f_0.

   e) Higher f_0 requires smaller transmitting crystal dimensions to maintain unidirectionality of the acoustic beam; but there is a physical limit to constructing crystals of small dimension.

2. Pulse Generation -- Pulse repetition frequency and the duration of the pulse are also derived from the master oscillator. The repetition period can be chosen in pre-selected intervals by using digital flip-flop dividers (Baker and Watkins, 1967). The number of flip-flop stages determines the PRF. The duration of the pulse is also varied by the same technique. The pulses are fed to a linear transmission gate. Whenever the gate is opened, a pre-selected number of cycles of the master oscillator pass through to a linear power amplifier. Thus, the amplifier output is a train of pulses which is phase-coherent with the master oscillator.

The selection of the PRF is dependent upon two requirements:

i) It should be greater than twice the maximum Doppler Shift expected (from the requirement of the sampling theorem); and

ii) It should be small enough so that received bursts occur before the next transmission.

The duration of a single pulse comes from the following consideration: if there are n cycles (of f_0) in a pulse, n should be small enough to give adequate spatial resolution, but not so small that considerable spectral broadening occurs due to finite transit time across the beam by the flow particles. Experimentally $n = 4$ is found to be quite satisfactory (Newhouse et al., 1974).

3. Transducers -- The resulting train of pulses issuing from the gate is the input to the transmitting piezoelectric crystal which in turn produces ultrasonic pulses. Some consideration of the crystals used is due here as they are the contact between the driving circuitry

and the fluid flow. The transducer should ideally have the sensitivity of the lightly backed narrow-band CW Doppler units and range discrimination of the wide bandwidth units (Baker, 1970). The transducer bandwidth is the primary factor in setting the discreteness of the Doppler range window. A broad-band, low Q transducer permits the transmission and reception of short bursts with fast turn on-turnoff characteristics (Baker and Watkins, 1967). The coupling coefficient, Q of the crystals used in PD units is as low as 1.5 - 2.5. The area of the transducers is kept to a minimum for a good spatial resolution, usually 2 - 5mm^2. The efficiency of a carefully constructed transducer is estimated to be about ten percent (Baker, 1970).

There are some arguments in favor of using the same crystal for both transmitting and receiving purposes: use of one crystal in the pulse mode avoids focussing and matching problems and simplifies transducer design. Lateral resolution can be held more closely constant over the range of interest. Furthermore, the large carrier component due to feed-through in the dual crystal design is not present so that the received signal can be amplified significantly without distortion and intermodulation (Nippa, 1974).

As the produced burst leaves the transmitting crystal and travels through the flow, a continuous train of echoes is produced. The receiving crystal picks up these echo reflections and converts them into an electric signal.

4. Received Signal Porcessing -- A high frequency amplifier and limiters are first used to bring received signal echoes up to a level for phase detection. The received signal passes through a linear

transmission gate and a sample of the Doppler shift in each echo return is derived by gating the receiver output. This gate, again, is operated by the master oscillator through a set of flip-flops whose number determines the time interval the receiving gate is open.

At the phase comparator the linear gate output is fed into one port and, simultaneously, a sample of the master oscillator signal is fed into the reference port. This reference signal is also delayed to provide for the desired range. By this process a train of short pulses at the PRF are developed at the comparator output port. The voltage of each pulse is porportional to the instantaneous phase difference between the transmitted and received bursts. The amplitude envelope of this pulse train corresponds to the time varying Doppler signal.

The pulse train is input to a sample and hold circuit producing a voltage that oscillates at the Doppler frequency. This raw Doppler signal is low in amplitude and contains harmonics of the PRF. In addition to the Doppler shifted frequencies from the flow, it also contains Doppler shift produced by the motion of hand-held transducer and vessel wall motion which are large in amplitude and low in frequencies. These could easily block high gain audio amplifier used to amplify the Doppler signal.

Therefore, a bandpass filter is inserted before this audio amplifier. The high pass sections come first to remove the large amplitude- low frequency spatial leakage components. Then comes a group of low pass filters that remove the high frequency PRF components

from the Doppler signal. Usually the roll-off frequency is the highest PRF that avoids range ambiguities; however, since the highest Doppler shift is almost always much less than the PRF, the filter roll-off frequency can be set to a value just above the highest expected Doppler shift rather than at the PRF/2 (Baker and Watkins, 1967).

The output of these filters is the Doppler Signal which is amplified by an audio amplifier for further quantitative or qualitative analysis.

2.1.3. Operating Parameters

The PD velocimeter used in this work was constructed in the instrumentation laboratory of the Aerospace Engineering School using circuits provided by F. D. McLeod. It is a typical quadrature detecting bi-directional device. The main data concerning its operation are given below:

Transmission frequency, f_0 = 7.7 MHz

Pulse Duration = 4, 8 and 16 cycles of the above

PRF = f_o/160, 320 and 640 Hz, i.e.

= 48.12, 24.06, 12.03 KHz

Listening gate times = 0.5 to 3 sec

Delay = 0 to 20 secs

= 0 to 15 sinθ mm

With the speed of propagation of sound,

$$c = 1.5 \times 10^5 \text{ cm/sec}$$

The Doppler equation (2.2) gives

$$f_D = 102.6\ u \cos\theta \qquad (2.7)$$

and, with angle of probe,

$$\theta = 45^o,$$

$$f_D = 72.6\ u\ \text{Hz}$$

For the given PRF's, there are corresponding maximum ranges according to the Equation (2.5) and then corresponding maximum velocities according to the Equation (2.6) that can be measured unambiguously. These are listed in Table 1.

Table 1. Maximum Measurable Range and Velocity Combinations Available with the PD Flowmeter Used

PRF_{KHz}	$R_{max_{cm}}$	$V_{max_{cm/sec}}$
12.03	6.23	58.6
24.06	3.12	117.2
48.12	1.56	234.4

In addition the flowmeter has three extra features: a variable gain setting which amplifies the received signal before phase detection, a unique variable slope setting provided to give constant gain with varying range (i.e., varying attenuation of the returned signal), and an optional frequency offset of 7 KHz to the Doppler signal. The latter

is useful with low velocities giving smaller Doppler shifts which, when fed directly into the zero crossing frequencymeter, may yield erroneous results. Also, the phase locked-loop demodulator will fail to lock if the input frequencies are below its range of operation.

2.1.4 The Probe

The probe used in the experiments was constructed in the Biomechanics laboratory and consists of (Figure 5):

1. a single transducer made of lead zirconate which acts both as transmitter and receiver,
2. a plexiglass acoustic insulator to decouple the crystal from the probe casing. This also acts as an electric insulator,
3. backing block of Devecon F on the rear side of the crystal which is chiefly responsible for the bandwidth and sensitivity of the transducer,
4. a brass metal case,
5. a co-axial cable of the minimum required length, and
6. the RTV filling material.

2.2 The LDV System

A DISA 55L Mark II system was employed in the flow studies to provide a reference against which the ultrasound results could be compared. This system consists of a 15 mW He-Ne Laser source (λ = 632.8 nm), beam splitter, an acousto-optic modulator (Bragg cell), and focussing lens on one side, and a photomultiplier tube (operated at 1600V) on the receiving end, whose output was processed through a

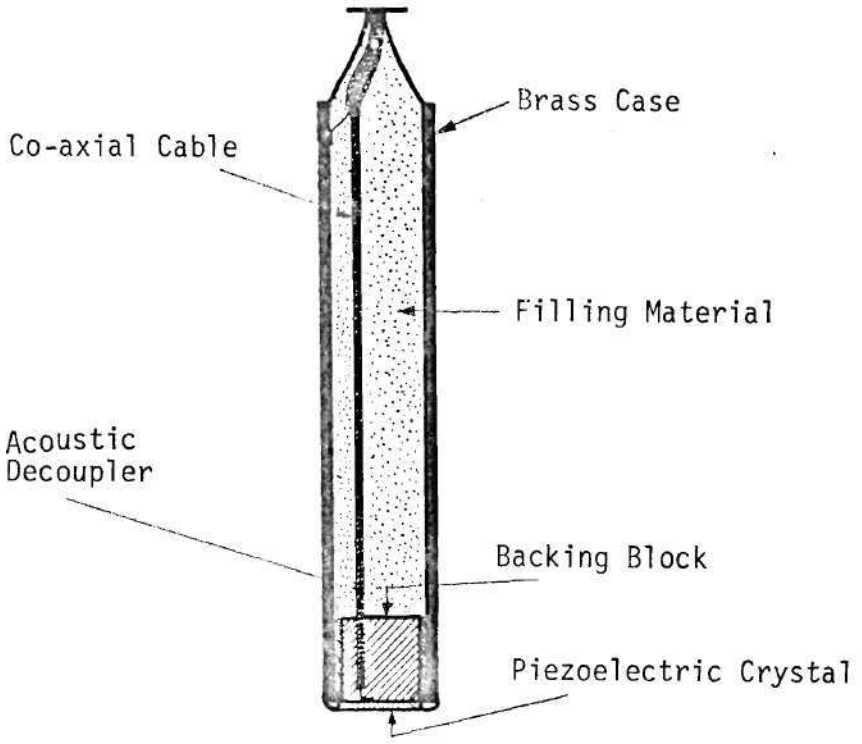

Figure 5. The Ultrasound Probe

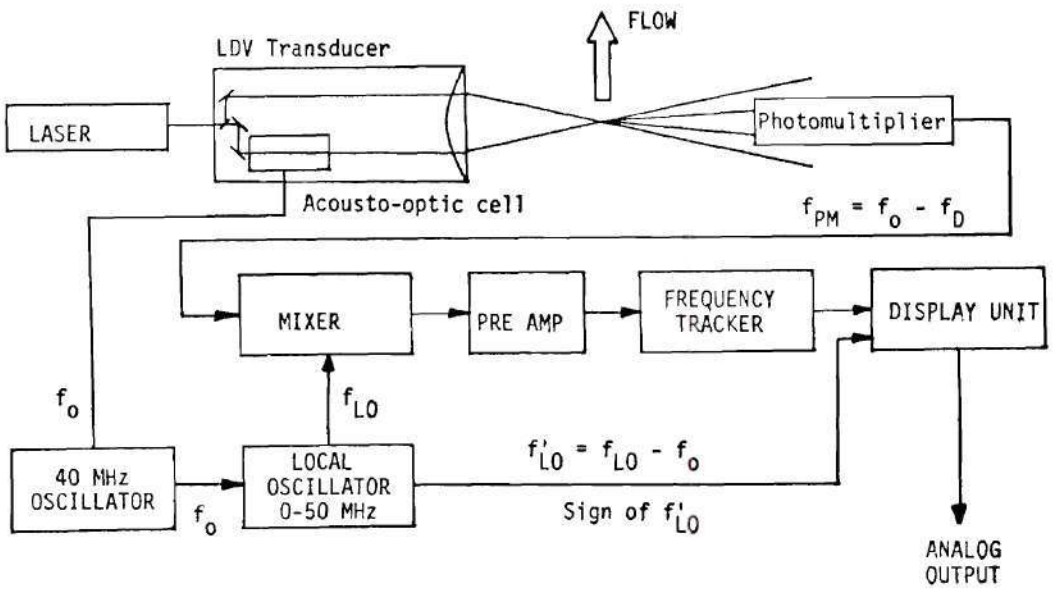

Figure 6. Block Diagram of Laser Doppler Velocimeter

frequency translator and a frequency tracker. The Bragg cell shifted one of the beams by 40 MHz, thus providing direction sensing capability.

The block diagram (Figure 6) of the LDV demonstrates how the system combines the fixed optical frequency translation (f_0 = 40 MHZ) of the laser beam with electronic mixing of the detected signal ($f_0 - f_D$) and an electronic local oscillator frequency (f_{LO}) to produce a total frequency span of -10 to +40 MHZ. The fixed optical frequency shift introduced by the Bragg cell is derived from a 40 MHZ oscillator. This 40 MHZ oscillator also drives the local oscillator, so as to eliminate relative drift of these two frequencies.

The photomultiplier picks up Doppler shifted light from the point of measurement in the flow. In addition to the normal Doppler signal the detected signal also contains the frequency translation due to acousto-optic cell, resulting in a photomultiplier output frequency of $f_{PM} = f_o - f_D$. In the mixer the photomultiplier signal combines with the signal from local oscillator (f_{LO}), and the difference frequency ($f_{LO} - f_{PM}$) is fed to the pre-amplifier.

The tracker mixes the preamplified signal ($f_{LO} - f_{PM}$) with the signal f_{VCO} from a voltage controlled oscillator. The difference frequency ($f_{VCO} - f_{LO} + f_{PM}$) is automatically centered at the middle frequency of a relatively narrow bandpass filter in the tracker. This is done by means of a fast servo loop that controls the value of f_{VCO} so that the relation $f_{VCO} - f_{LO} + f_{PM} = f_{IF}$ is satisfied. The display electronics counts the frequency of the VCO signal ($f_{VCO} = f_{LO} - f_{PM} + f_{IF} = f_{LO} - f_0 + f_{IF} + f_D$). Using digital techniques, the nonvarying

component ($f_{LO} - f_0 + f_{IF}$) is subtracted from f_{VCO}, leaving the mean Doppler frequency, f_D which is multiplied by a calibration factor to give the mean flow velocity. This mean velocity is digitally displayed on a LED panel, and also is available in the analog form.

The translation frequency allows the operator to select the flow velocity range which most efficiently covers the measurement in question. The range can be translated so that zero velocity is mid-scale. This allows measurement of flow fluctuations around zero. When detailed studies of flow fluctuations around a mean velocity are required, the velocity range can be selected to cover only the actual fluctuations resulting in increased resolution and accuracy.

2.3 Minicomputer Based Processing System

The proposed digital method for processing the Doppler signal was implemented in a dedicated minicomputer based signal analyzer (HP 5451B Fourier Analyzer). This instrument is built around a HP 2100S minicomputer and includes a dual channel analog-to-digital converter (ADC), a graphic display terminal, and a high-speed rigid disc mass-storage (5M-byte capacity). The system can be used to acquire and display time series data, and then by means of an operator keyboard, it is possible to carry out various time series computational functions directly. These operations can be enetered and executed singly or they can be storedin the machine as a program and executed automatically. The key computational functions that can be carried out are:

- Fourier Transform (either direction)
- Cross or Auto power spectrum
- Complex conjugate multiplication
- Convolution
- Cross or auto correlation
- Histogram
- Transfer and coherence function
- Log, linear, polar, rectangular, complex display
- Arithmatic operation
- Windowing - user defined or built-in hanning

In addition, it is possible to define (or dynamically redefine inside a program) the basic time series length (sample or blocksize) from 64 to 8192 data points using the available 32k-byte memory. The programming 'language' is rudimentary, but does include a conditional branching, as well as a counting or looping capability, and the ability to define and use variable parameters as instruction operand. In addition, provision is also made to insert and call special-purpose user programs in the operating system of the machine with the help of user-callable subroutines.

The Fourier Transform is implemented by means of the FFT algorithm, and for maximum speed, this as well as several other critical algorithms are programmed in a high speed Writable Control Store (WCS). Thus, they appear as an instruction of machine instruction set, and provide for high speed computation. For example, the machine can continuously sample and compute the power spectrum up to 5 KHZ for a single input

on the real-time basis. This is based on a time of 125 ms to compute a one-dimensional 1024 point FFT.

The disc software divides it into eight different kinds of files that can be treated as different physical units as far as the operator is concerned. These files store the data blocks, (i.e., time series), keyboard programs, ASCII headers for identifying different records on file, and the operating system of the machine; but most importantly, by the use of Direct Memory Access (DMA) it facilitates high-speed storage of up to four channel input simultaneously in the ADC throughput file. The maximum data flow rate in such an operation is 81 k-bytes/second on real-time basis. This ADC throughput file occupies almost half of the disc storage and provides for approximately one minute of data in real-time with the sampling rate used in this work.

CHAPTER III

FORMULATION

This work hypothesizes a correspondence between the power spectrum of the Doppler signal and the velocity distribution of scattering particles within the sampel volume using tools of statistical fluid dynamics. This done, a digital scheme shall be considered to compute the "instantaneous" spatially-averaged velocity within the sample volume. Our considerations, thus, can easily be dichotomized into statistical and sampling considerations.

3.1 Statistical Model

In the statistical treatment of turbulence, the velocity of flow is assumed to be a random variable having a time-dependent probability distribution function (pdf). The one point distribution, $F(\vec{r},\vec{v},t)$ is defined such that the probability of finding a fluid element in spatial volume $d\vec{r}$ about point $\vec{r}$, and in velocity volume $d\vec{v}$ about $\vec{v}$ at an instant of time t is $F(\vec{r},\vec{v},t)\, d\vec{v}\, d\vec{r}$. By using this distribution function, various time-dependent mean quantities can be defined by the use of statistical moments. For example, the mean velocity in volume $d\vec{r}$ about $\vec{r}$ is given by,

$$\vec{U}(\vec{r},\vec{t}) = \int_{-}^{+}\int_{\infty}^{\infty}\int \vec{v}\cdot F(\vec{r},\vec{v},t)\,d\vec{v} \qquad (3.1)$$

In particular, a single macroscopic velocity component say, $\vec{U}_x$, can be written as

$$\vec{U}_x(\vec{r},t) = \int_{-\infty}^{+\infty}\int\int \vec{v}_x \cdot F(\vec{r},\vec{v},t)d\vec{v}$$

or

$$\vec{U}_x(\vec{r},t) = \int_{-\infty}^{+\infty} \vec{v}_x \cdot g(\vec{r},\vec{v}_x,t)d\vec{v}_x \qquad (3.2)$$

where $g(\vec{r},\vec{v}_x,t)$ is a "reduced" distribution function, defined as the probability that a fluid element in volume $d\vec{r}$ about $\vec{r}$ shall have the x-component of velocity in $d\vec{v}_x$ about $\vec{v}_x$.

Thus, if we consider a small sample volume $d\vec{r}$ in an experiment, and take an "instantaneous snapshot" of x-velocity components of fluid elements contained within this sample volume, we may construct the reduced pdf, $g(\vec{r},\vec{v}_x,t)$ for that "instant". (Of course, the actual measurement of velocity will require a finite time). Equation (3.2), then could be used to yield a $\vec{U}_x(\vec{r},t)$, which we may call an "instantaneous" space ensemble average within the sample volume $d\vec{r}$. Implicit in the above discussion is the assumption that although the fluid volume $d\vec{r}$ is small in comparison to some characteristic dimension of the flow, it is still large enough to contain sufficiently great number of fluid elements to make its statistical treatment meaningful.

Thus, starting from a time t if we take a series of these snapshots, and construct the corresponding macroscopic velocity component $\vec{U}_x(\vec{r},t)$ as described above, there will be a strong variation in these velocity values with time in a turbulent flow. For a flow which is steady in the mean, the average of these velocities in time, $\vec{U}_x(\vec{r})$, is the mean velocity as usually defined in turbulent flow through Reynolds' decomposition. In effect, an assumption of ergodicity is being made which allows the correspondence of averages of numerous space ensemble mean values over a small sample volume, and a 'long' time average made at a single point. Reasonably, this correspondence will improve with increasing number of snapshots, i.e., with increasing averaging time. Further, we assume that constructing a discrete function $\vec{U}_x(\vec{r},t)$ by space emsemble averaging over a small sample volume $d\vec{r}$ at t_i and repeating this for many values of i (with pre-selected, but small, dt, the duration of *snapshot) gives the* same energy spectrum as obtained by measuring $\vec{U}_x(\vec{r},t)$ directly for a long time. It is this pivotal assumption that we apply to the PD velocimeter sample volume.

3.2 Application of the Model to PDV

In this work the evaluation of the 'reduced' pdf and the 'instantaneous' space-averaged velocity will be done through the use of the Doppler signal from a PD velocimeter, which is generated by moving scatterers within the sample volume. When the particles are small in comparison to the wavelength of the incident radiation, each particle acts as a point radiator, i.e., we have Rayleigh scattering

such that

$$\text{Attenuation} \propto (\text{volume of scatterers}) \cdot f_0^4$$

where f_0 is the radiation frequency. Each scatterer, therefore, can be considered to be an isotropic radiator (Flax et al., 1971). If the particles are homogeneously distributed within the sample volume, we could hypothesize, within reason, that the frequency of the total received Doppler signal is related to the velocity of the particles, and the amplitude is related to their concentration (Flax et al. 1969, Arts and Roevros 1972).

Furthermore, if the scatterers were organized in a periodic spacing (coherent), we could add the voltages resulting from each of them to give the voltage of total Doppler signal. Since, they are randomly distributed within the sample volume (incoherent), we add the power resulting from each particle to yield the total power of the Doppler signal (Brody, 1972). Thus, assuming that

a) each scatterer is exposed to approximately the same power level of ultrasound in the sample volume,

b) each scatterer reflects the same fracton of the incident ultrasound power,

c) the received ultrasound power level is proportional to the number of scatterers acting as primary radiators (i.e., secondary and higher order reflections are ignored), and

d) the velocity of a scatterer is the same as the velocity of the fluid at the point it occupies, we can hypothesize that

each particle contributes equally to the power of the Doppler signal but at different frequencies corresponding to its respective velocity. With this in mind, then, it is reasonable to expect the power spectrum of the Doppler signal and the velocity distribution pattern within the sample volume to correspond closely. Because of the large concentration of the particles used with the PDV (in blood, $5 \times 10^6/mm^3$) we extend this assumption to an instantaneous basis; and the periodic continuous sampling of the power spectrum of the Doppler signal, I(f), gives us data about the desired 'snapshots' of the reduced pdf, $g(\vec{r},\vec{v}_x,t)$

$$g(\vec{r},\vec{v}_x,t) = \frac{I(f)\ df}{\int_0^\infty I(f)\ df} \tag{3.3}$$

which then gives the desired discrete 'snapshots' of the x-component of the mean velocity within the sample volume from Equation (3.2)

$$\vec{U}_x(\vec{r},t) = K_D \frac{\int_0^\infty f \cdot I(f)\ df}{\int_0^\infty I(f)\ df} \tag{3.4}$$

where K_D is the so-called Doppler constant obtained from Equation (2.2)

$$K_D = \frac{c}{2f_0 \cos\theta} \tag{3.5}$$

with all quantities defined as before. For simplicity in notation it has been assumed that no negative velocities exist so that the lower limit in the frequency integration is zero. This is not a fundamental limitation since an arbitrary frequency offset can always be introduced to insure that no negative (offset) Doppler frequencies occur. Application of our statistical model implies that the power spectrum of turbulence derived from the discrete values of $\vec{U}_x(\vec{r},t)$ obtained from the sample volume (for a large number of snapshots) corresponds closely to the one obtained by directly recording the instantaneous velocity at a point for a long period of time.

3.3 The Sample Volume

The above description springs from our faith in the fidelity of the Doppler signal, i.e., it is really a correct indicator of the velocity distribution among the scatterers moving within the sample volume (or, in other words, it is really the sum total of signals from the individual scatterers). On the whole, this faith is well founded; however, certain factors must be kept in mind while applying the Doppler signal for the statistical interpretation of the flow field.

First, there is the qustion of the sample volume. In a statistical description the sample volume should be small compared to some characteristics diemnsion of the turbulent flow, and yet large enough to accommodate a large number of fluid elements, thus making its

statistical description meaningful. The size of the sample volume from which the Doppler signal originates depends on the dimensions of the transmitting crystal, listening gate time, and the transmission frequency. In most of the cases, it does not exceed 6 mm^3, small compared to the dimension of the tube (1 inch); but still large enough to hold a large number of scattering particles due to the particularly heavy seeding used with the PD devices (in blood, 5 x $10^6/mm^3$). Thus, a reasonable correspondence between the sample volumes of statistical turbulence and that involved with the Doppler process can be assumed. (It should be noted in passing that it is the fact of the heavy concentration of the scatterers used with the PD devices that makes the abovementioned statistical treatment possible. With the LDV, for example, the seeding is necessarily very dilute, and we are reduced to counting the photons emitted as individual scatterers traverse across the fringe patterns.

A second factor to be kept in mind is the distortion of the 'ideal' Doppler signal due to several 'non-idealities' inside the sample volume:

a) non-ideal geometry and insonation of the emitted pulse,

b) nonuniformity of the scattering particle size and distribution,

c) Rayleigh fading due to secondary reflections from the scatterers,

d) various sources of electronic noise, and

e) the distortion caused by the actual measurement process itself.

The effect of each of these factors upon the received Doppler signal is briefly discussed next.

a) With PD flowmeters, the flow velocity is measured over a finite volume (the sample volume). This is analogous to the averaging effect observed when using a pitot tube or hot-wire anemometer. The size and shape of this sample volume becomes important in relation to the accuracy with which the local flow velocity at a poitn can be measured, for the spectral content of the backscattered signal is greatly effected by the sample volume geometry and intensity distribution.

The ultrasonic pulse emitted from a piezo-electric crystal does not have the ideal uniform geometry and shape but due to the inertia of the transmitting crystal, has teardrop like shape (Figure 7). The

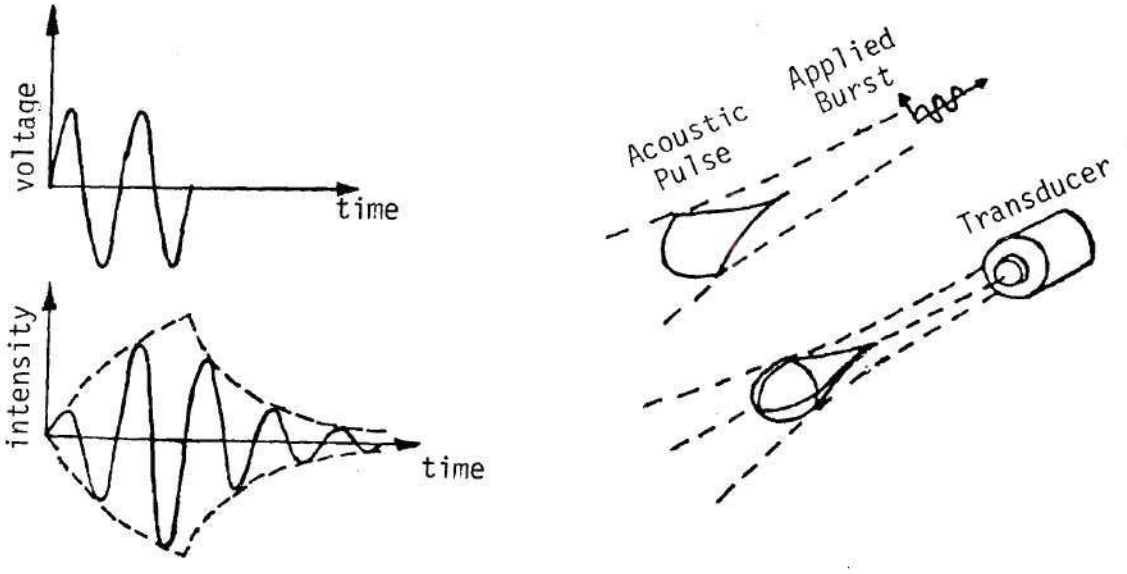

Figure 7. The Non-ideal Sample Volume

initial exponential rise corresponds to the transient response of the crystal to the electric excitation applied to it, and its taper is due to the 'ringing effect' when the crystal dissipates the stored energy exponentially in free response. In addition to distorting the geometry and intensity distribution within the pulse, this transducer ringing increases the length of the sample volume, and thus reduces the spatial resolution of the PD device.

The peak cross-sectional acoustic intensity within the pulse has been found to occur at its center and to vary along its length in an exponential rise and decay fashion corresponding to the teardrop shape of the pulse. Moving radially outward from the beam center, the intensity varies parabolically at all the cross sections (Jorgensen and Garbini 1974). The exponential rise and decay curve defining both geometry and intensity distribution are truncated in length to provide a finite sample volume. The size of the pulse also changes as it moves along the acoustic beam due to the beam divergence; however, it remains similar to its original shape (Jorgensen and Garbini 1974). Thus, at different ranges we shall have different levels of insonation within the sample volume.

Baker and his coworkers (Baker and Yates 1973, Baker et al., 1971) studied the sample volume experimentally using a fine jet, and also pulse echo techniqeus. They then predicted the distorted velocity profiles from the assumed parabolic one, and demonstrated the accuracy of these predictions through experiments. Next, Jorgensen, et al., (1972, 1973, 1974) studied analytically the effect of velocity gradient

across the sample volume, and suggested a deconvolution scheme to retrieve a correct velocity profile from the measured one in order to calibrate the flowmeter. This scheme was tried on several simulated velocity profiles with assumed convolving functions, and it appeared to give excellent results. However, in real flow situations the convolving function was assumed to be only a two-dimensional intensity distribution. In addition, the trigger level of the ZCF was found to be quite an interesting parameter - high trigger levels have the effect of reducing the sample volume size (by cutting-off the tail end of the pulse), thus increasing spatial resolution. However, this high trigger level reduces SNR resulting in reduced accuracy of the ZCF.

b) The assumption of uniform distribution of identical scattering particles within the sample volume may be violated in certain cases. This would lead to degrading the correspondence between the normalized power spectrum of the Doppler signal and the pdf of velocities in the sample volume. This effect is also a function of the experimental set up and therefore, difficult to deal with theoretically. Nevertheless, if the concentration is large and reasonably uniform-sized particles are used, this assumption seems reasonable. In particular, for the application to blood flow studies these conditions are fulfilled. The red blood cells are very uniform in size and shape, their concentration is quite large, and the left ventricle of the heart provides a chamber for thorough mixing.

c) First order scattering means that each scatterer acts

independently of all others (Middleton, 1967); the radiation scattered by one particle does not interfere with and is not rescattered by any other particle. If the received scattered signal is proportional to the number (or density) of scattering particles one can infer only primary radiators; on the other hand, the occurrence of multiple scattering is a function of the density of scatterers (Green, 1966).

In an effort to determine the scattering process by human blood, Reid et al. (1969) conducted experiments and reached the following conclusions:

i) the scattering intensity is proportional to hematocrit in the hematocrit range of 7 - 40 percent;

ii) scattering is isotropic;

iii) the red cell is the major source of scattering, and its scattering cross section $\simeq 10^{-4}$ times its geometrically projected area; and

iv) the scattering energy increases with 4th power of frequency.

These findings, especially (i) and (iv) are compatible with the commonly held belief that the ultrasound scattering by blood follows a Rayleigh scattering law (Stratton, 1941).

d) The Doppler signal also suffers from electronic noise. Noise is considered to be that part of the signal that conveys undesired information. Here, it could be of two types: additive Gaussian white noise, which is externally generated, and the noise generated by the flowmeter from such mechanisms as receiver input noise, transformer noise, coupling between transmitting and receiving crystals (leaking noise),

and reverberation or "clutter" noise (Haase et al. 1973, Light 1972). The latter is peculiar in that its effects cannot be overcome by increasing the transmitted signal power. To combat clutter, a better design of the electronic components is necessary.

Noise that is independent of the transmitted signal is referred to as externally generated noise, and is assumed to be additive, white, and Gaussian, and can be overcome by increasing the power of the transmitted signal. However, this approach is frequently impractical due to the low radiation requirements for the physiological systems.

In most demodulators, a minimum SNR is required at the input to obtain the desired level of performance; the greater the bandwidth of the demodulator, lesser the minimum SNR required at the input. To achieve optimal noise immunity, then, the demodulator bandwidth must be minimized. But this results in restricting the range in which the velocities can be measured (Brody, 1972).

The effect of electronic noise is, again, empirical, and is a result of non-idealities of Doppler instrumentation. It should be noted that all of the factors discussed so far are functions of individual experimental set-ups that do not lend themselves easily to theoretical analysis. For the sake of clarity and simplicity, their effects can jointly be considered as a 'response function' of the experiment convolving with the ideal instrument response to give the distorted (spectrum-broadened) Doppler signal.

e) In contrast with the factors discussed above, some spectral broadening arises as a direct consequence of the measurement process itself and, therefore, can not be eliminated by idealization of the

flowmeter and the experimental set-up. Let us assume that the first four effects were negligible, i.e., we have a steady flow of constant velocity across the sample volume containing uniformly distributed, constant diameter spherical particles moving with the flow. Also, the ultrasound pulse is assumed to have an ideal, cylindrical shape with uniform sonic intensity inside it.

If we could observe the signal coming from a particular scatterer (or a group of scatterers) for a long time. the power spectrum of the Doppler signal would be single line at f_D, the Doppler shift corresponding to the velocity of the scatterer. However, we have a finite sample volume from which the returned signal is observed only during the time the pulse takes to cross it. The net effect is to multiply in the time domain the constant shift signal by a "box car" sampling function at a given repetition rate. Thus, the original Doppler line spectrum is convolved with this box car sampling function, resulting in a broadening or smearing of the line spectrum. For example, for a 1m/sec velocity through a 1mm wide volume the spectral broadening amounts to about 1KHz for the basic 10KHz shift frequency. (Newhouse et al., 1974).

Additionally, in order to determine range the receiver is turned on only during the time the pulse is traversing across the sample volume. As a consequence, the insonation over the sample volume increases linearly with time as pulse enters the volume and decreases accordingly as it exits. The result is to multiply the "ideal" returned signal by a triangle shaped sampling function, or equivalently,

to convolve it with corresponding spectral function (Peronneau et al., 1974). This again results in the smearing of the ideal line spectrum.

3.4 The Response Function

Thus, it is possible to determine a correction function for the last case; but not for the other effects which can be determined only after the measurement of the actual instrument response. However, we can combine all these corrections into one response function, R_F for a certain instrument-transducer combination. The determination of this response function is then done best by experimentation.

The response function, $R_F(u)$ convolves with the "true" distribution function, $I(f)$ to produce the measured distribution function--

$$F(u) = \int_{-\infty}^{+\infty} I(f) \cdot R_F(u-f)\, df \qquad (3.6)$$

The response function is a function of velocity as well as the position within the sample volume. This can be measured by filling the sample volume with constant velocity particles so that R_F = function of u. Then, for uniform laminar flow through the sample volume at different velocities (whose ideal Doppler power spectra are only single lines on the frequency axis) by measuring the corresponding broadened power spectrum of Doppler signal, the response function at those velocities is known (Figure 8).

In the case of a turbulent flow spectral broadening results from temporal velocity fluctuations. The next figure demonstrates how the response function further broadens this spectrum (Figure 9). Let the

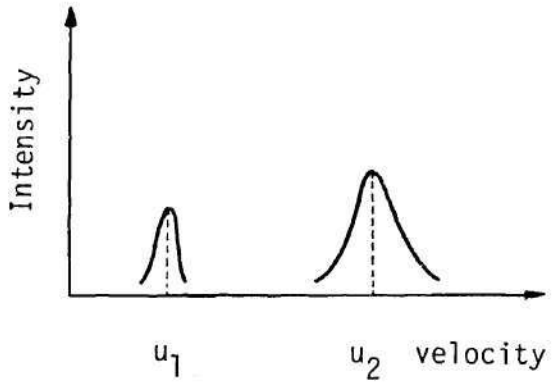

Figure 8. Response Function Effect in Laminar Flows

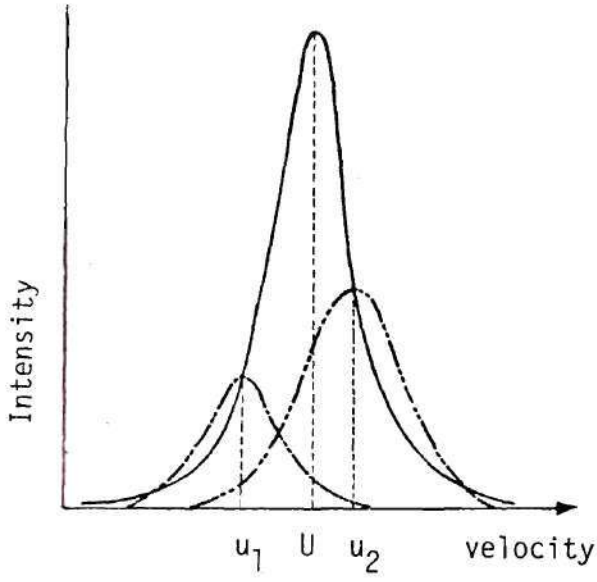

Figure 9. Response Function Effect in Turbulent Flow

true distribution be I (f) in the figure (not necessarily Gaussian), then for any frequency, f (corresponding to a velocity, u) there is a response function effect as shown. If we assume that it applies locally for each value of u, the measured profile, as a result of convolution, is expressed as

$$F(u_i) = \sum_{f_j} I(f_j) * R_F(u_i - f_j)\, \Delta f_j \qquad (3.7)$$

and, for all velocity space, this may be written as a matrix equation

$$[F] = [I] * [R_F] \tag{3.8}$$

If R_F and F are known, we may obtain [I] by matrix inversion.

3.5 Doppler Ambiguity

In addition to the Doppler spectral broadening caused by the non-ideal sample volume and sampling, some broadening also arises due to fluctuating particle velocities, the finite transit time of particles through the sample volume, and the mean velocity gradients across the sample volume. This provides a major limitation in experimental measurement of instantaneous velocity; and is unavoidable in single point measurement regardless of the detection system used. Several researchers have investigated this limitation in connection with the laser Doppler velocimeter, the most prominent being W. K. George (1971, George and Lumley 1973). Results of his theory incorporating effects of this limitation on the measurement of instantaneous fluctuating velocities shall be outlined here. Later, these will be used to predict the performance limitations of our velocimeters (both laser and ultrasound).

The total bandwidth of the Doppler spectrum is given by

$$(\text{Bandwidth})^2 = \Delta\omega_{u_o}^2 + \Delta\omega_T^2 + \Delta\omega_L^2\ \Delta\omega_G^2 + \Delta\omega_\beta^2 + \Delta\omega_S^2 \tag{3.9}$$

where the various terms were defined earlier (pp. xiv).

Since we are interested in measuring only the time varying spatially-averaged velocity of the sample volume, $\Delta\omega_{u_o}$ is the only information we seek for turbulence measurement -- all other terms

present spurious information. In analogy with Radar technology, this latter Doppler broadening arising from sources other than fluctuations of the center frequency is termed 'Doppler Ambiguity'.

The terms $\Delta\omega_\beta$ and $\Delta\omega_s$ are negligible in a typical experiment. Since $\Delta\omega_G$ increases linearly with the mean velocity gradient and the sample volume size, for the core region of the pipe flows it is negligible in comparison with other terms (George 1971). Thus, Doppler ambiguity bandwidth, $\Delta\omega$ is given by

$$(\Delta\omega)^2 = (\Delta\omega_T)^2 + (\Delta\omega_L)^2 \quad . \tag{3.10}$$

$\Delta\omega_T$ increases linearly with the highest frequency of turbulence, and the largest dimension of the sample volume. It should be noted here that due to the finite size of the sample volume, the velocity fluctuations of smaller spatial extent than the largest dimension of th sample volume (i.e., those of higher frequencies) are severely attenuated. $\Delta\omega_L$ is inversely proportional to the transit time of particles through the sample volume; i.e., it increases with mean velocity and decreases with sample volume size.

This Doppler ambiguity manifests itself in the measured power spectrum of turbulence as a corrupting quasi-white noise (i.e., its power spectrum is of constant amplitude, and extends in frequency range of 0 to $\Delta\omega$). This corrupts the power spectrum of turbulence at all frequencies - the degree of contamination depending on relative spectral heights of the turbulence and ambiguity spectra. The limit in measurement of turbulence frequencies is reached when the turbulence power

spectrum height is equal to the height of the Doppler ambiguity spectrum. Beyond this limit, called the cut-off frequency, the rapidly rolling-off turbulence power spectrum is dominated by the constant ambiguity power spectrum and as a result, the measured turbulence power spectrum becomes flat at the cut-off frequency and extends until the Doppler ambiguity bandwidth, $\Delta\omega$.

This cut-off frequency is given by (George and Lumley, 1973)

$$f^* = \frac{k^* U}{\eta} \tag{3.11}$$

where U is the mean velocity of the flow, and η the Kolmogorov microscale of turbulence. The wave number, k^* is obtained from

$$k^* = 1.27\ (Re_{min} \sin 1/2\ \phi)^{-1/2} \tag{3.12}$$

with ϕ as the angle between the transmitter and receiver, and Re_{min}, the Reynolds number based on the smallest length that can be resolved in the mean flow direction. Theoretically, it is the distance between the 'crests' of the transmitted wave (i.e., the wavelength λ). However, recalling that all turbulence components of smaller extent than the sample volume size are severely attenuated, the minimum sample volume dimension in the direction of the mean flow should be used.

Clearly, the higher the transmission frequency, the higher will be the cut-off frequency prediction. Thus the LDV is apt to have a higher frequency response in velocity fluctuations measurements than the PDV. In fact, the performance of the PDV is severely limited by Doppler ambiguity, as shall be seen in Chapter VI.

3.6 Digital Demodulator

A digital scheme for deriving velocity information from the Doppler signal was chosen for turbulence measurements in pipes. The application of the digital processing directly to the Doppler signal is attractive due to the following reasons:

a) It may be judged as the most straightforward method of studying the statistical characteristics of the flow. As outlined in Section 3.2 the mean of the normalized power spectrum of the Doppler signal gives the 'instantaneous' spatially-averaged velocity, and what could be more direct than determining this velocity by taking the first moment of the Doppler power spectrum digitally? We shall call this scheme the Digital First Moment (DFM) method.

b) Resorting to digital procedures extends the possibility for further processing without investing an inordinate amount of effort in each improvement. This is particularly attractive as the present work is confining itself to the DFM method, but could later be extended to include more exotic methods of signal treatment.

c) The Doppler signal is developed as the result of mixing the range-gated returning pulse echoes with the local ultrasonic oscillator output. The signal is basically a frequency modulated one with its 'carrier' frequency proportional to the mean velocity, and its random frequency fulctuations corresponding to velocity perturbations inside the sample volume. Conventional FM demodulation techniques could be employed to extract the velocity data were it not for several unconventional aspects:

(i) the 'carrier' frequency may vary considerably as the mean flow varies.

(ii) the degree of modulation (modulation index) may be large, especically for highly turbulent flow.

(iii) as discussed in Section 3.3, there may be significant spectral broadening of the Doppler signal.

The key element in developing the DFM method is the use of what are commonly known as "time series analysis" techniques. The term "Time series" appears to have originated in the field of statistics but following the pioneering work of Wiener (1949), it has been used to describe discrete or continuous sequences of quantitative data assigned to specific moments in time or points in space. In the present work spectral analysis techniques from this general area provide the critically important means to extract the velocity data from the Doppler signal in the manner suggested by Equation 3.4.

3.7 Sampling Considerations

In its basic form the DFM method consists of digitizing the Doppler signal to produce a discrete time series. Time series techniques for spectral analysis are then applied to determine a second time series which is the measured flow velocity. Bearing in mind that it is the frequency of the Doppler signal that conveys to us the relevant information about the flow, it is not surprising that the accuracy and the frequency response of the measured velocity are directly related to the Doppler signal digitizing rate. There are,

however, conflicting requirements imposed on this rate as a result of Equations 2.1 and 3.4. Each point in the resultant velocity time series is determined by calculating the first moment of the Doppler series power spectrum. As a minimum this requires a finite sample time, T, containing N digitized values of the Doppler signal. To follow the velocity closely as a function of time, we also wish to have a short sample time. Yet, decreasing the observation window duration results in degradation of Doppler frequency resolution and contributes to spectral broadening which, in turn, affects the velocity accuracy.

To illustrate this, consider a particle velocity which is varying according to

$$v(t) = V \sin 2\pi f_v t \tag{3.13}$$

as shown in Figure 10 and let T be the duration of the Doppler sample. During T the velocity is changing which results in Doppler spectrum broadening. Clearly, the maximum change will occur at the position of the maximum slope and is given by

$$\Delta U_T = 2\pi V f_v T \tag{3.14}$$

Further, if we assume adjacent, non-overlapping samples, then resolution of the velocity fluctuation frequency f_v, requires at least two velocity points per cycle (from Shannon's sampling theorem). Since each T (length of sample of the Doppler signal) will give one point in the velocity time series, the maximum measurable frequency in

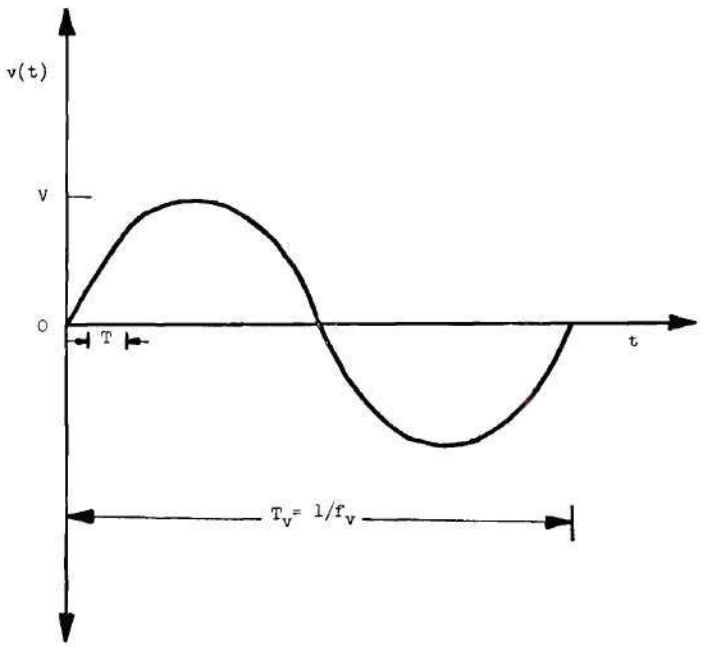

Figure 10. A Component of Turbulence

velocity is given by

$$F_{max} = \frac{1}{2T} \tag{3.15}$$

This sample length T also determines the frequency resolution at which the Doppler signal is measured:

$$(\Delta f_D)_{min} = \frac{1}{T} \tag{3.16}$$

which, in turn, is related to smallest resolvable velocity by the Doppler equation (2.1)

$$(\Delta v)_{min} = \frac{c}{2f_o \cos\theta} \quad (\Delta f_D)_{min} \quad . \tag{3.17}$$

If the velocity variation over T, Δv_T, given by Equation (3.14) is smaller than $(\Delta v)_{min}$, it can not be accurately resolved. Also, if $\Delta v_T >> (\Delta v)_{min}$ there will be considerable spectral broadening and the accuracy of Equation (3.4) in determining v as a function of time will suffer. We would thus like to have $(\Delta v)_T \simeq \Delta v_{min}$ for optimum accuracy. Use of Equations (3.14), (3.16) and (3.17) then gives the desirable value of sample length of the Doppler signal:

$$T \simeq \sqrt{\frac{c}{4\pi f_o V f_v}} \tag{3.18}$$

Let us summarize: In order to accurately measure a component of turbulence of peak velocity V and frequency f_v within a prescribed velocity accuracy the Doppler sample length, T, should be chosen with the above-mentioned criterion in mind. For a fixed sample length, the measurement errors can be expected to increase with increasing $V \cdot f_v$ product. The extent of this error can be estimated by proper experiments which are to be detailed later.

Also, for a fixed sample length, T, the maximum measurable frequency, F_{max}, of velocity fluctuations is fixed by Equation (3.15). Any attempt to measure velocity fluctuations beyond this limit, will result in aliasing, thus distorting the velocity power spectrum.

3.8 Present Approach

The flow chart in Figure 11 shows two alternate approaches to the problem of turbulence determination using the proposed demodulator. The present work will confine itself to the right leg of the chart.

The objective here is to test the validity of the model and evaluate the performance of the digital demodulator. For this, we shall treat the raw Doppler signal without any response function correction as shown in the right branch of the flow chart, i.e., once a short sample of the Doppler signal is received, the so-called 'snapshot' of the reduced pdf $g(\vec{r},\vec{u}_x,t)$ is found from the power spectrum $F(f,t)$ without any response function corrections. Thus, by continuously sampling the Doppler signal and finding the first moment of the normalized power spectrum, a series of samples of spatially-averaged velocity $u(t)$ is constructed. The turbulence energy spectrum, turbulence intensity and mean velocity may be obtained from further processing of this discretized mean velocity, $u(t)$. Since here we are confining ourselves to only the first moment of the power spectra, the errors introduced by not considering response function effects are minimal -- the first moment is not very sensitive to small changes in power spectrum shape which may be caused by response function corrections.

It may be pointed out here, that other workers have confined themselves to the right most part of the right leg, namely, qualitative comparison of Doppler power spectra for laminar and turbulent flows, and that only in the mean (not 'instantaneous'). This work, then, represents a new approach to Doppler signal processing.

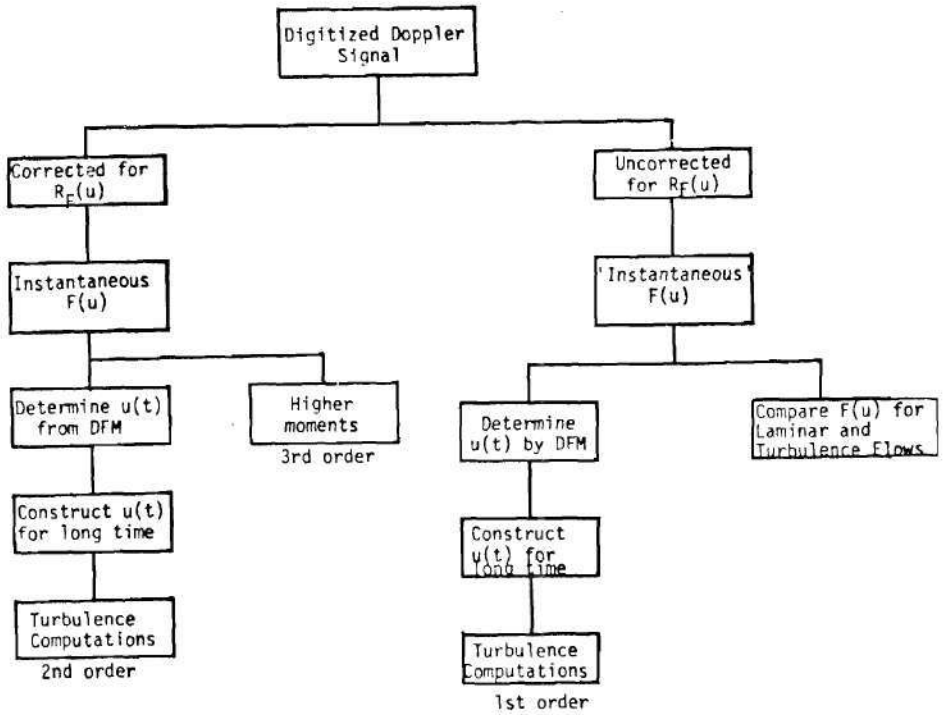

Figure 11. Flow Chart of Different Digital Approaches

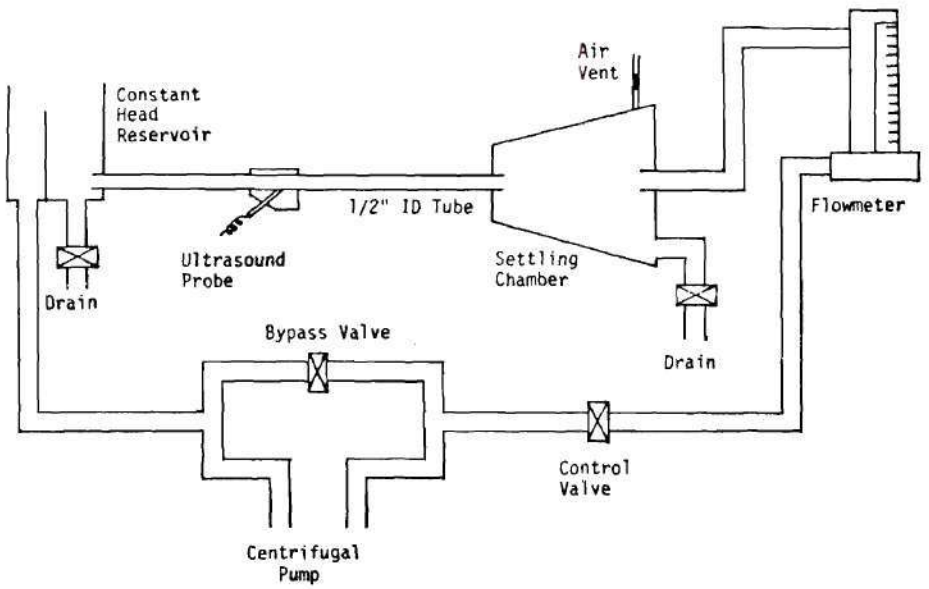

Figure 12. The Flow System - Preliminary Experiments

CHAPTER IV

PRELIMINARY EXPERIMENTATION

4.1 Purpose

Flow experiments were conducted in order to test the validity of the basic assumptions as outlined in the previous chapter, namely that the velocity signal derived from the spectral averaging of the Doppler signal is, in the statistical sense, the same as that found by observing the velocity directly. Here this concept shall be tested only in the mean for turbulent pipe flows.

4.2 The Flow System

A closed-loop flow system was employed in these experiments (Figure 12). A pump was used to circulate water through gravitational volume flowmeter, settling chamber, a 1/2 inch diameter plexiglass tube, and a constant-head reservoir. A plexiglass test section was inserted on the plexiglass tube midway between the settling chamber and the constant-head reservoir. This allowed the placement of an ultrasound probe at 45^{o} angle to the flow in contact with the inner surface of the tube, thus preventing unnecessary attenuation and reflection of the acoustic pulse while travelling through the walls of the tube. A main control valve, with a bypass flow control valve allowed control of the flow rate (hence velocity) through the test section, a rough estimate of which could be made by the gravitational flowmeter.

The scattering particles used were silicon carbide particles of 1 micron diameter, chosen because of their good scattering properties.

4.3 Procedure

The flow system was started with clean water. With the Doppler signal being monitored on the oscilloscope, silicon carbide particles were added until the signal dropout was minimized. The gain and slope settings were increased until the output of the zero-crossing frequency-meter in the ultrasound instrument no longer changed with further increase in these values. A delay appropriate for velocity measurement at the centerline of the tube was chosen.

The system was run at different velocities and the returning Doppler signals were processed using:

a) a zero crossing frequency meter (ZCF)

b) a phase-locked loop (PLL) detector, and

c) the DFM scheme.

The ZCF used was that employed by McLeod in the PDV design and was constructed as an integral part of the ultrasound system. The PLL used was incorporated in a frequency tracker (DISA 55L27) which was a component of the signal processing system of a DISA Laser Doppler Velocimeter. Its operational range varied from 15 KHZ to 50 MHZ with discrete selectable bandwidths of 0.5 percent to 8 percent. The outputs of the above two demodulators was averaged over long periods of time in the Fourier Analyzer to yield the mean.

The DFM scheme was incorporated in the Fourier Analyzer. At this preliminary stage of the work where only mean velocity values were

to be tested, it was deemed unnecessary to develop a real-time capability, which entails a substantial amount of effort. Thus the random Doppler signal (incorporating random velocity fluctuations) was sampled non-continuously. However, a large number of samples will fulfill the need of computing the mean velocity.

The above scheme was implemented in two ways. First, the spatial-averaged velocity from each Doppler signal sample calculated and stored. These values were used to give the mean. Then the Power spectra of these above Doppler signal samples were averaged, the average power spectrum being used to give the mean velocity.

These two estimates of mean velocity will be labeled DFM (a) and DFM (b), respectively from now on.

4.4 Results

The average velocities obtained from the three signal processing schemes are compared in Table 2 for the same Doppler data. Only two methods could be compared simultaneously since the ADC in the Fourier Analyzer provided for digitization of only two input channels. The mean velocities thus obtained appear to be in reasonable agreement.

Since measurement of mean velocities in steady flow does not require the simultaneous use of demodulators provided averaging is done over long time periods, the above three schemes were tried one after another on consecutive stretches of the Doppler signal. Their results, shown in Table 3, are in reasonable agreement thus encouraging us to attempt further application of the DFM method. The comparatively large

discrepancies at the low velocity end can be attributed to several factors:

a) It was difficult to maintain good, steady flow at low velocities due to the unstability of the pump employed,

b) The scatterers tend to settle faster because of their low momenta, thus degrading the quality of the Doppler signal,

c) The ZCF has poor performance at the low frequency end of the Doppler spectrum, and

d) The PLL has difficulty in locking onto such low frequencies, since it was designed for use with frequency shifts in range of 15 KHZ - 50 MHZ.

Figure 13 shows the averaged power spectra of the Doppler signal at different velocities (averaging time: 30 seconds). The shape of this power spectrum is affected by transducer design, flow profile across the sample volume, particle transit time, and far field beam divergence. The design factors being constant, the above figure then shows the variation in the Doppler spectrum shape due to variations in velocity.

Figures 14 and 15 display the effect of averaging on the Doppler power spectrum for two different velocities. As expected, averaging tends to smoothen the power spectrum, and also leads to velocity predictions converging toward its average value as demonstrated in Table 4.

4.5 Drawbacks and Modifications

The major drawback of the DFM method as used so far was that the sampling of the Doppler signal was not continuous. This comes about

Table 2. Comparison of Mean Velocity (cm/sec) in Pipe Flow Measured by Different Methods in Simultaneous Use

DFM		ZCF	PLL
a	b		
95.0	91.0	93.2	-
97.4	99.8	-	100.8
46.9	44.5	46.1	-
46.8	44.5	-	48.9
23.8	20.7	25.3	-
23.8	22.6	-	25.3

Table 3. Comparison of Mean Velocity (cm/sec) in Pipe Flow Measured by Different Methods

DFM		ZCF	PLL
a	b		
6.18	5.91	4.91	6.07
10.5	10.5	9.24	10.4
17.2	16.7	15.6	17.9
26.7	25.9	24.1	28.0
36.9	37.7	33.3	39.6
50.3	52.0	47.1	54.4
75.2	78.8	70.8	82.0
100.4	105.8	98.3	109.5

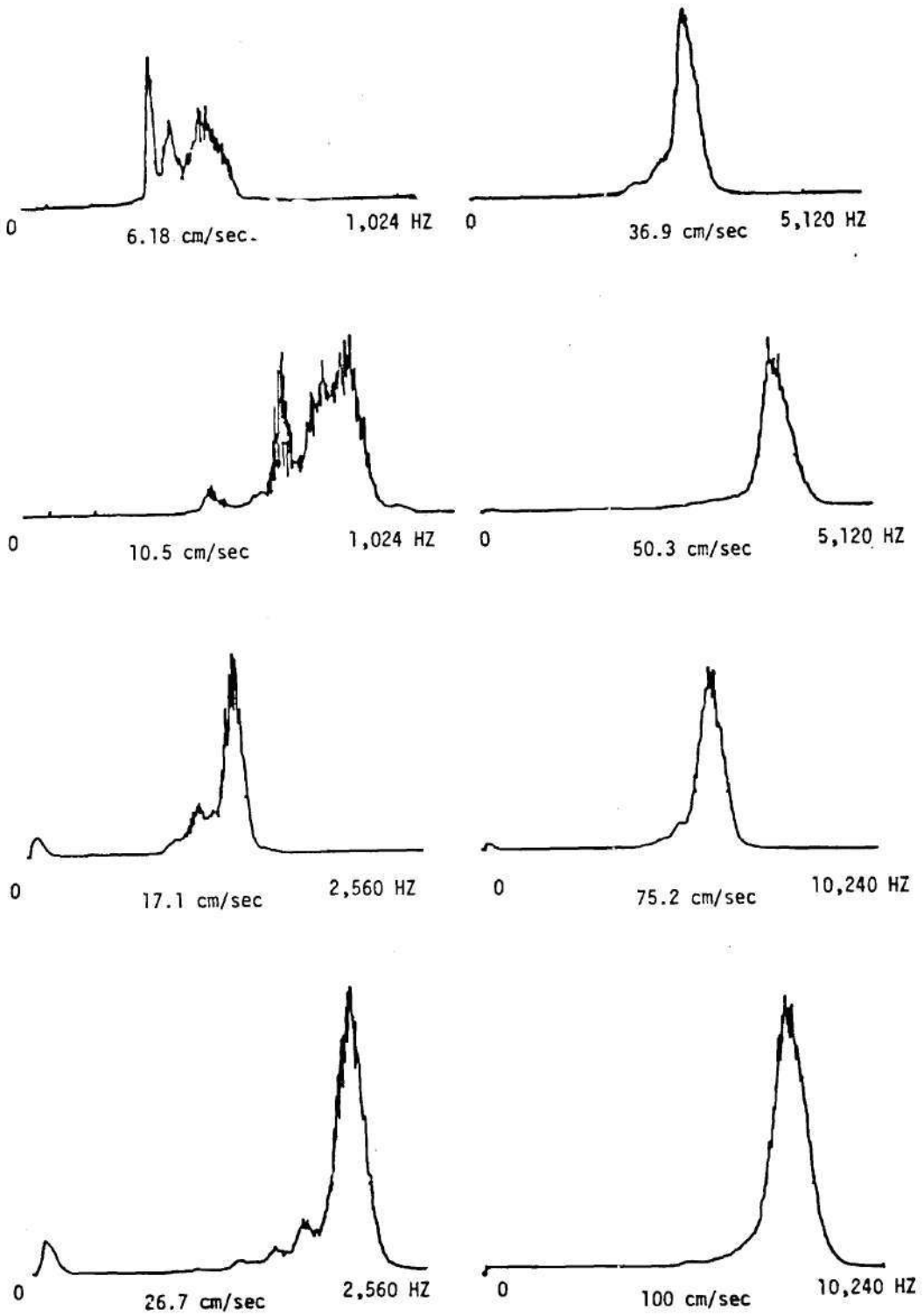

Figure 13. Averaged Doppler Power Spectra at Different Velocities (Averaging Time = 30 seconds)

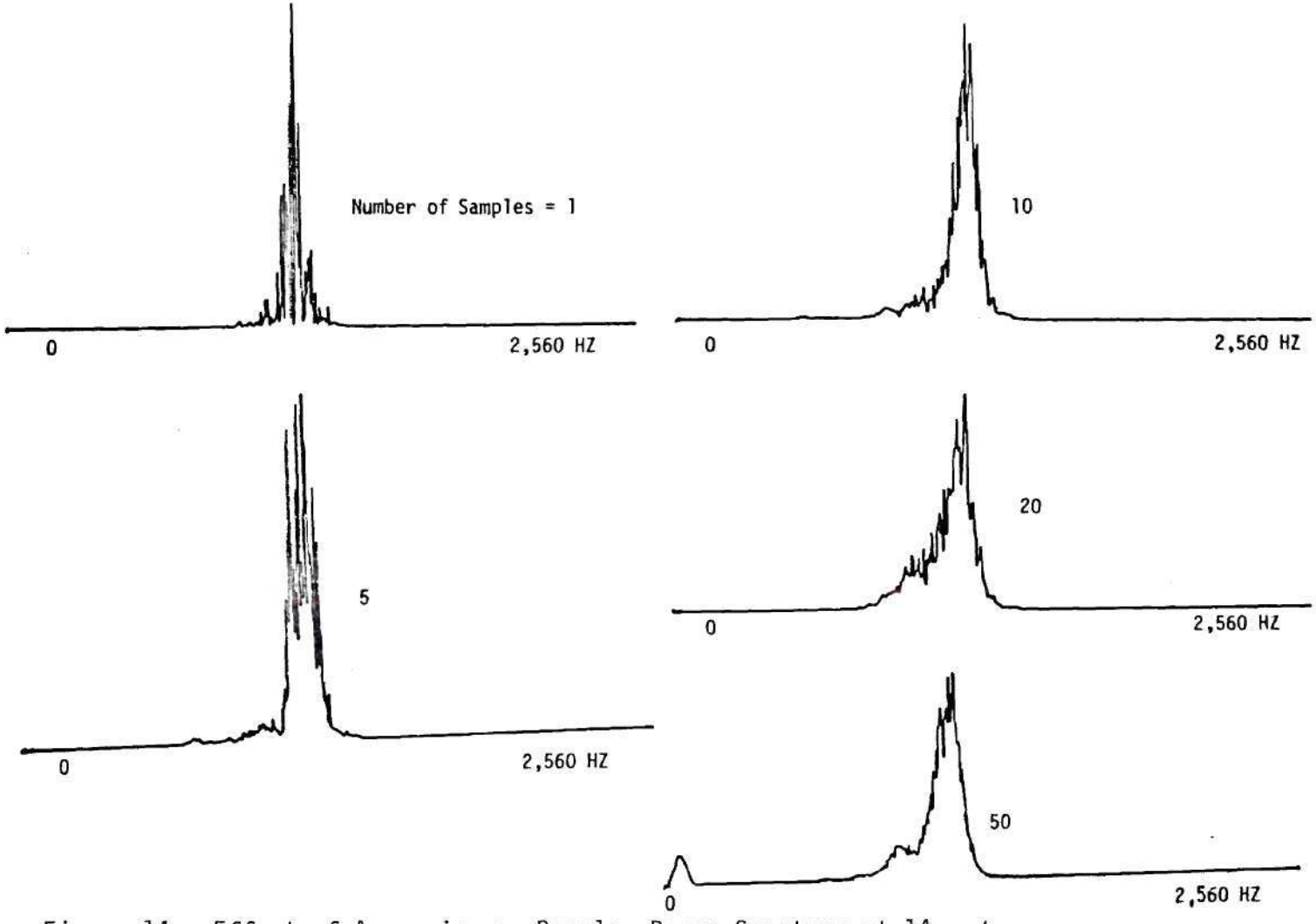

Figure 14. Effect of Averaging on Doppler Power Spectrum at 14 cm/sec (Each sample is 0.2 second long)

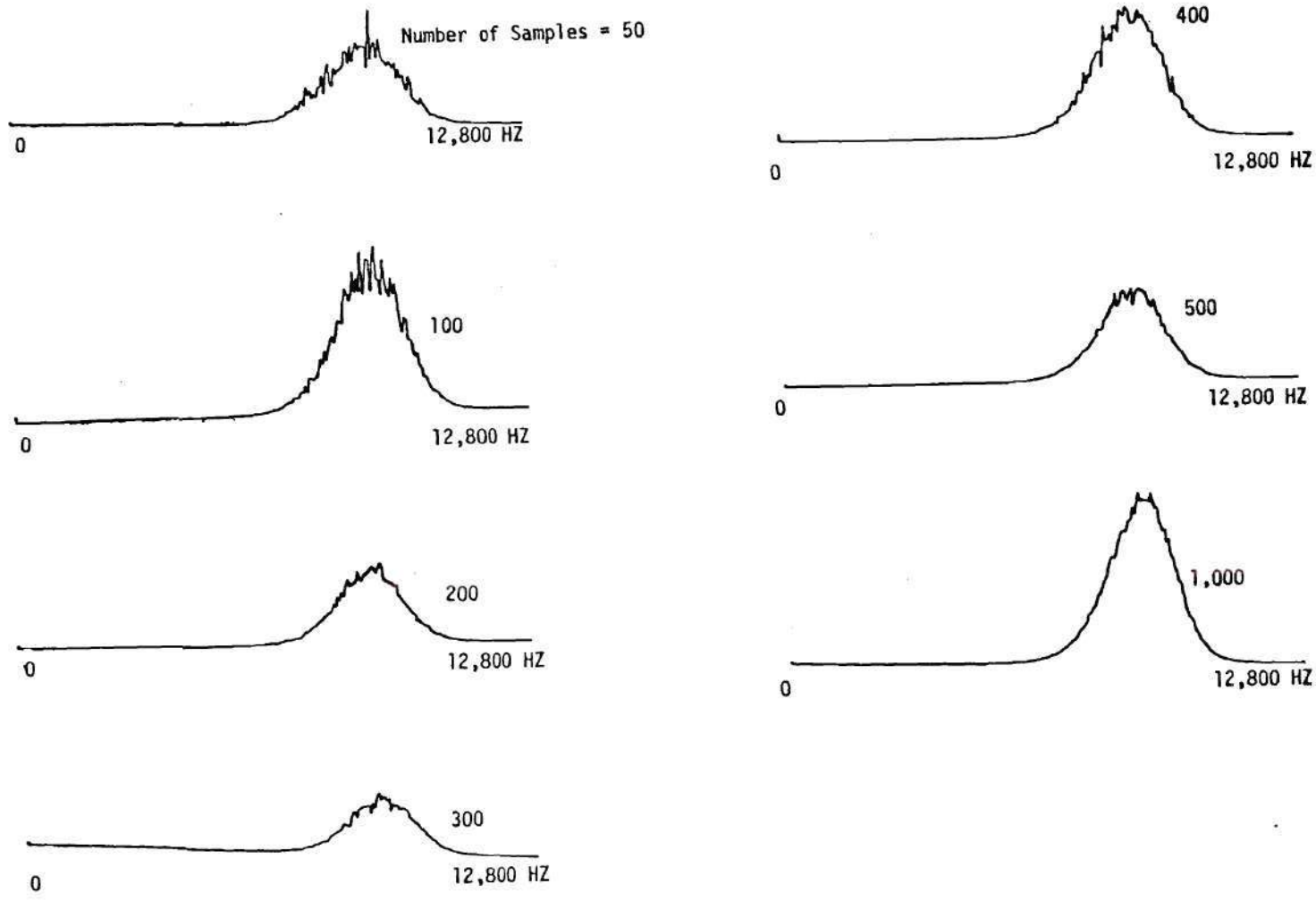

Figure 15. Effect of Averaging of Doppler Power Spectrum at 118 cm/sec (Each sample is 20 ms long)

Table 4. The Effect of Number of Samples Used in Estimating Mean Velocity (cm/sec) by DFM's

Number Samples	DFM Method		ZCF
	a	b	
1	16.0	16.0	15.4
5	15.6	15.6	14.8
10	14.8	14.8	14.7
20	14.3	14.2	14.3
50	13.8	13.7	14.3

as the time taken by the computational loop is greater than that required for sampling for reasonable frequency response for velocity. Thus, the best that could be done was to obtain 'snapshots' of the flow and compute the spatially-averaged velocity every few seconds - no turbulence estimates could be made.

This requirement for continuous processing of the Doppler audio signal, therefore was deemed to be of vital importance to the present study in order to measure turbulence. Several attempts of increasing complexity were made to this end and are listed below.

1. The program used to compute the power spectrum and first moment made use of keyboard callable functions in the Fourier Analyzer. Efforts were made to increase its efficiency, but still using the keyboard functions. All these efforts, unfortunately, proved to be unsuccessful.

2. It was felt that the part of the above program used in first moment computation was requiring the longest time, as the part related with power spectrum calculation makes use of microinstructions stored in Writeable Control Store (WCS) as explained in Chapter II. Therefore, a FORTRAN subroutine was written to do the former, making use of certain user-callable subroutines in the operating system of the minicomputer. This then was made part of the operating system, and was user-callable through the keyboard.

This resulted in a tremendous saving of computational time (from a few seconds to approximately 200 ms), but still was insufficient to fulfill the requirement of continuous sampling at rates fast enough to give high frequency response in velocity.

3. An assembly language, subroutine then was tried which interfaces directly with the operating system rather than communicating with it through user-callable subroutine as the FORTRAN one. This also resulted in saving of computational time, and yet proved insufficient.

4. At this stage, the use of a mass store device was deemed inevitable in order to store the Doppler signal digitized at any desired sampling rate and later, process it leisurely. For this, efforts were made to make use of a HP 2100 computer system available in the Aerospace Engineering school. This system is a time-sharing one and comes equipped with many peripherals (card reader, line printer, magnetic tape, discs, etc.). This was to be used as a central computer, with the Fourier Analyzer as its satellite. In this manner, all the data (Doppler Signal) from the ADC could be transmitted via the satellite computer to the

central one and written on the disc associated with the latter (HP 7900A model), and later retrieved sample by sample to be processed. After development of such a system, however, it was discovered, that this data transfer rate was not fast enough due to the several special-purpose subroutines that come into operation by the use of the satellite system.

5. Henceforth, there was no alternative but to acquire a mass-store device for the Fourier Analyzer itself for it was thought impractical to prepare analog tape for each experiment, and then transfer it to the central computing facility of Georgia Tech (which may have provided continuous Doppler signal processing at required fast rate). Therefore, a rigid, high-speed disc mass storage (HP 7900A) was added to the Fourier Analyzer. This did indeed allow for storage of digitized Doppler signal at sufficiently fast rates continuously and was used thereafter.

CHAPTER V

SIMULATED FLOW STUDIES

5.1 Purpose

After the preliminary experimentation described in the previous chapter to test the basic premise of the theoretical formulation of the model, the logical next step was to acquire an insight into the fundamental strengths and limitations of the proposed Digital measurement scheme as far as velocity accuracy and velocity frequency response are concerned.

For such an evaluation of the proposed demodulator, it is necessary to test it with Doppler signals of known parameters. These Doppler signals can be synthesized using standard laboratory electronic equipment such as waveform generators, noise generators, voltage controlled oscillators, filters and mixers, thus allowing us to study the performance of the digital scheme on a wide variety of flow situations without actually having to produce them in a fluid dynamic experiment. This is advantageous in two respects: first, the signal characteristics are completely known and controllable, i.e., Doppler signals can be idealized to any desired degree: effects of non-ideal sample volume, finite transit time of scatterers through it, and Doppler ambiguity can be eliminated or incorporated at will. This enables one to study the distorting effect of each of the above degrading factors individually. The second advantage of simulating flows was that working

with an actual flow system was avoided; the flow systems tend to be finicky, ungovernable and, often, messy. A further incentive for creating such a synthesizer was that it would be useful in any further studies.

In the present study effects of Doppler ambiguity were not taken into account, though those due to non-ideal sample volume were incorporated, thus somewhat idealizing the simulated PD velocimeter. This is desirable if it is noted that the Doppler ambiguity effects can be minimized by proper redesign of the PDV whereas those caused by non-ideal scattering will always be present in real life situations.

5.2 Basis for Synthesis

The Doppler shifted signal carries information about the flow in its frequency. Thus, the Doppler signal is essentially a frequency-modulated one with its 'carrier' proportional to the spatially-averaged velocity in the sample volume, and its frequency fluctuations related to the disturbances in this velocity. In addition, as a consequence of several non-idealities in the sample volume (discussed in Sections 3.3 and 3.4) there may occur aperiodic drop-out in its amplitude. Thus, in effect, two kinds of signals could be synthesized:

a) an 'ideal' Doppler signal which emanates from an 'ideal' sample volume, namely cylindrical in shape with uniform acoustic intensity within, and containing small, primary radiators. Such a Doppler signal shall only be frequency modulated (corresponding to the velocity variations within the sample volume) without any dropout in

amplitude.

b) a Doppler signal originating from a real sample volume. Consequently, in addition to being frequency modulated, it is also amplitude modulated. Furthermore, this amplitude modulating component will be random in nature.

The basic Doppler detection is extraction of velocity information from a FM signal, i.e., that of frequency-to-voltage conversion. Synthesis of a Doppler signal is, thus, an inverse problem of voltage-to-frequency conversion and can be accomplished by means of a Voltage Controlled Oscillator (VCO).

The output of a VCO is given by

$$x(t) = A \cos[\omega_c t + \alpha(t)] \tag{5.1}$$

where $\omega_c t + \alpha(t)$ is the instantaneous phase. Moreover,

$$\omega_c = \text{carrier frequency}$$

and

$$\alpha(t) = \int_o^t K_v\, u'(t) + \alpha_o$$

is the additional phase due to instantaneous velocity fluctuation, $u'(t)$ K_v is the VCO constant given in Hz/volt, and α_o is a constant phase which may be set to zero without any loss in generality. For the particular example of a sinusoidal variations velocity (about a mean U) given by:

$$u'(t) = u'_{max} \sin 2\pi f_u t \tag{5.2}$$

the VCO output changes as

$$x(t) = A \cos \left[\omega_c t + \frac{K_v u'_{max}}{2\pi f_u} \cos 2\pi f_u t \right] \quad . \tag{5.3}$$

The instantaneous phase then is

$$\omega_c t + \frac{u'_{max} K_v}{2\pi f_u} \cos 2\pi f_u t$$

giving the instantaneous frequency,

$$f(t) = \omega_c + u'_{max} K_v \sin 2\pi f_u t \tag{5.4}$$

which is the instantaneous Doppler frequency. Since the Doppler constant, K_D from Equation (3.5) relates the frequency to velocity, we may write the instantaneous velocity as

$$f(t) = K_D u(t) \quad .$$

Decomposition of the total velocity u(t) into its components of mean (U) and fluctuations about the mean (u') yields

$$f(t) = K_D(U + u')$$

a comparison with Equation (5.4) readily yields

$$\omega_c = K_D U$$

and

$$u'_{max} K_v \sin 2\pi f_u t = K_D u'$$

the latter of which, in comparison with (5.2) leads to:

$$K_V = K_D$$

that is, the VCO constant in our Doppler synthesis should be set equal to the Doppler constant.

For the sake of completeness, it may be noted that the VCO output of Equation (5.3) may alternately be written as series of Bessel functions of the first kind:

$$x(t) = A \sum_{n=-\infty}^{\infty} J_n(\beta) \cos(\omega_c + 2\pi n f_u)t \qquad (5.5)$$

whose power spectrum over infinitely long time period is a series of impulses at $f_c \pm n\, f_u$ with amplitudes equal to the magnitude of Bessel functions. The present problem, however, is not to compute this power spectrum, but rather a series of 'instantaneous' spectra in order to determine 'instantaneous' frequency, f(t), which in turn, shall give 'instanteous' velocity, u(t).

5.3 Doppler Synthesizer-Block Diagram

A schematic diagram of the overall Doppler signal synthesis system is given in Figure 16. A signal corresponding to a velocity fluctuations u'(t) (sinusoidal or turbulent) is generated by wave generator or white noise-generator — low pass filter combination, respectively, and is added with a signal representing the mean velocity U(t) (sinusoidal or steady). This total velocity signal is, then, used

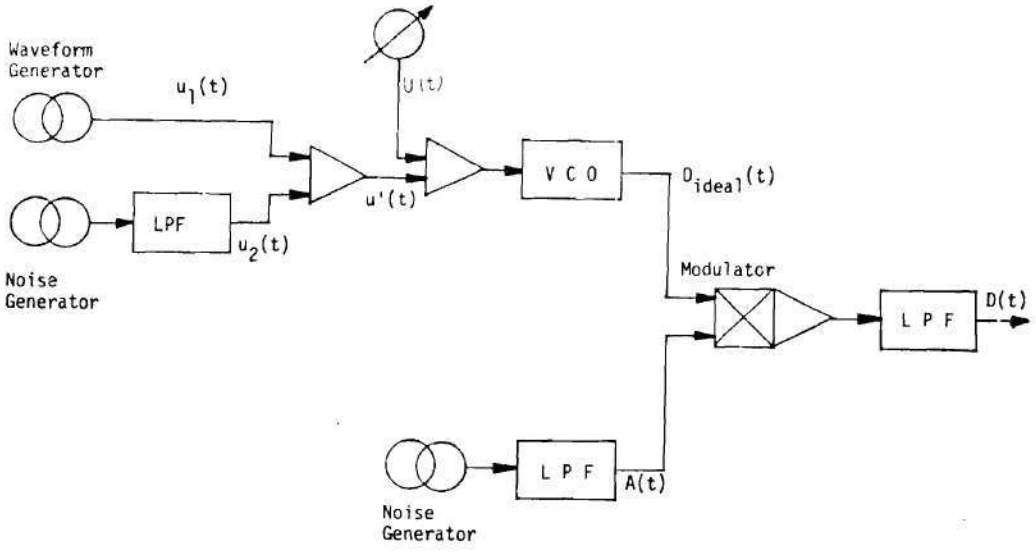

Figure 16. Block Diagram of Doppler Synthesizer

to drive a VCO whose output is the so-called 'ideal' Doppler signal, i.e., a signal of constant amplitude with its instantaneous frequency proportional to the instantaneous velocity.

If desired, the effect of non-idealities in the sample volume can be approximated by further amplitude modulating this 'ideal' Doppler signal. This modulating signal A(t) (also termed the 'envelope' of the 'real' Doppler signal), is produced with the help of another noise generator-low pass filter combination. This, and the ideal Doppler signal are subsequently mixed and filtered to give the Doppler signal which includes the effects of signal dropout due to Rayleigh fading occurring during the scattering process.

The system described above is capable of generating Doppler signal simulating a wide variety of flow situations occurring in real life (and many more than don't!). However, the present study was limited to:

i) steady flow, i.e., U(t) = constant and ($u_1 = u_2 = 0$),

ii) oscillating laminar flow ($u_2 = 0$), and

iii) steady turbulent flow, ($u_1 = 0$).

For the first three cases, no amplitude modulation to simulate signal fading) was employed, i.e., A(t) = constant. For class iii) both sinusoidal and random modulations were made. The random modulation was tailored so that, statistically, it was similar to the envelope of the Doppler signals obtained from fluid dynamic experiments.

5.4 Procedure

5.4.1 Window Considerations

In the DFM scheme each point in the velocity time series is calculated employing a single sample of the digitized Doppler series by the use of Equation (3.4). In the Fourier Analyzer, the power spectrum of the Doppler signal sample is evaluated using DFT's. In order to improve the accuracy of the velocity time series, one would like to reduce the variance in the estimate of this DFT of a single sample. Unfortunately, this cannot be done by increasing the length of the sample - the variance in the estimate of power spectrum is independent of the sample length used (Jenkins and Watts, 1969).

This variance, however, can be decreased by any of the following approaches:

1. taking several samples and ensemble averaging their power spectra, or
2. smoothing a long, single sample spectrum by averaging several

adjacent spectrum points, or

3. using a window function to modify the basic rectangular window in which each data point is equally weighted; and
4. overlapping, or sliding the window along a long sample of the Doppler signal.

Approaches 1 and 2 are equivalent if the same amount of data is taken in each case, and result in reduced frequency resolution in the exchange for improved accuracy. The choice left, then is the use of an appropriate window function. It should be noted that windowing a Doppler sample is nothing but multiplying the Doppler sample obtained with rectangular window (i.e., equally weighted data points) by a weighting function. Since multiplication in the time domain corresponds to convolution in the frequency domain, windowing is therefore a form of smoothing the power spectrum.

According to the general theory of line shapes, if a discrete time window of finite duration produces N data points spaced Δt apart, then the DFT of this time window (line shape) will have N-1 zeroes in the complex frequency plane in the region bounded by $\frac{1}{\Delta t}(m - 1/2) < \mathrm{Re}(f) \leq \frac{1}{\Delta t}(m + 1/2)$, for each integer m. Thus, any number of line shapes can be found simply by moving the zeroes around in the complex frequency plane. A large number of window functions have been proposed, each improving the variance in estimate in some way. For example, zeroes are generally removed from the main lobe and:

a) placed at ∞ to increase the side lobe roll-off rate, or

b) placed among the near side lobes to reduce side lobe

amplitude, or

c) placed along the imaginary frequency axis to flatten the main lobe top.

The actual choice of the window depends on the type of the signal being treated, and desired information.

In the present treatment of the Doppler signal, four different windows (Figure 17) were considered from a set offered by HP (Potter, R.W.):

1. Rectangular window — occurs by default. It has the familiar sinc function line shape. The main lobe is narrow, but side lobes are very large and roll off slowly. Also, the main lobe top is quite rounded and can introduce large measurement errors.

2. Hanning Window — quite popular due to easy implementation. This line shape is constructed by moving a main lobe zero at s = 1 to 'infinity'. The first side lobes are large but the high roll off rate (60 dB/octave) is very helpful for good frequency resolution.

3. P 301: It has the maximum amplitude accuracy (0.1 percent) in presence of closely spaced spectral lines of all the windows presented. Also, it has a large dynamic range. The main lobe is very flat (thus high amplitude accuracy), and side lobes are small, but their roll off rate is slow (20 dB/octave).

4. P 310: This window minimizes leakage among the channels due to the dramatic drop of -93 dB from main lobe to side lobes. However, frequency resolution and amplitude accuracy are not as good as P 301.

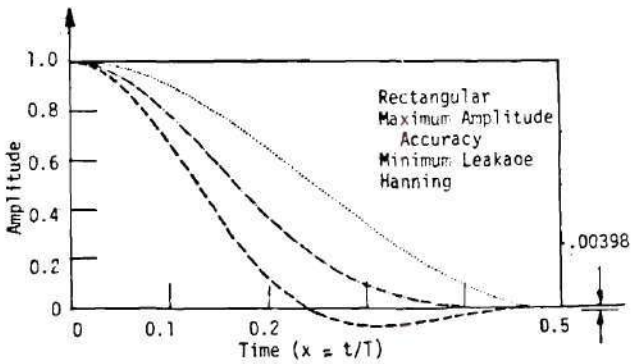

Figure 17. Shapes of Various Windows discussed in Section 5.4.1

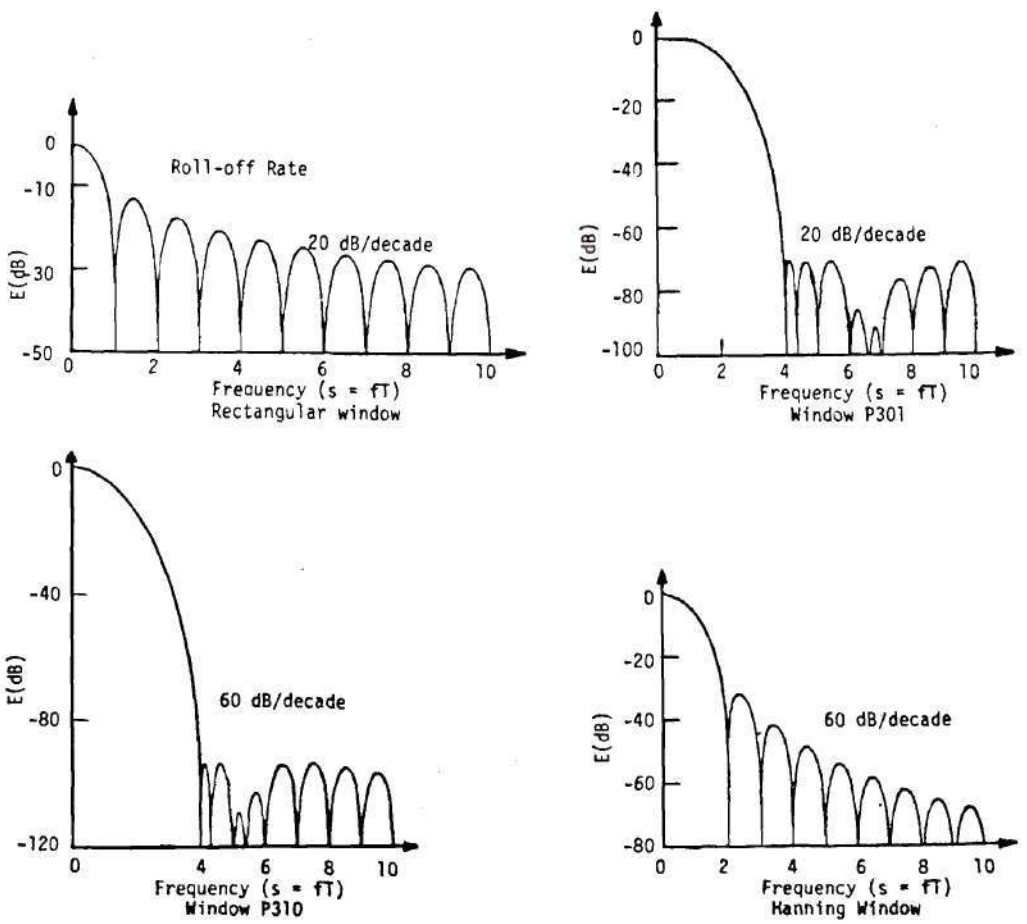

Figure 18. Line Shape and other Parameter of Windows in Figure 17.

The line shape and other data about these windows are given in Figure 18.

5.4.2 Sampling Parameters

For the PD velocimeter available to us in the fluid dynamics laboratory, the Doppler constant, K_D in Equations (3.5) is:

$$K_D = 102.6 \text{ Hz/cm per sec.}$$

for a beam inclination angle, $\theta = 0^o$. From Section 3.7, the desired velocity accuracy, and its maximum frequency response impose two conflicting requirements on the sampling rate of the Doppler signal. Choice of one of these determines the other automatically. Under these restrictions, the choice of a velocity accuracy of 2 cm/sec seems to be reasonable.

From Equation (3.16) this results in the Doppler frequency resolution of 205.2 Hz, and Equation (3.18) then gives the sample length of the Doppler signal as

$$T = 4.87 \text{ ms} \quad .$$

The number of equally spaced data points can then be adjusted to obtain the desired maximum frequency expected in the Doppler signal. In these studies, a sample of the Doppler signal was divided into 128 data points yielding maximum measurable frequency of 13,133 Hz. This satisfactorily brackets the range of Doppler shifts corresponding to velocities up to 100 cm/sec. This also leads to a sampling rate, Δt of 38.1 μs.

Finally, the specified Doppler sample length of 4.87 ms corresponds

to [from Equation (3.11)] a maximum frequency response, F_{max}, (in measuring velocity fluctuations) of 102.6 Hz.

5.4.3 Program Description

The processing the the Doppler signal consists of digitizing and storing it at desired rates (refer to Section 4.5), and later processing individual samples to find spatial-averaged 'instantaneous' mean velocity within the sample volume. A program listing with key may be found in the Appendix. The flow chart (Figure 19) and a brief outline are given below:

1. Since the length of the complete program exceeds the available program storage space in the Fourier Analyzer, it is implemented as a series of segments which are automatically loaded in sequence from the disc as required.

2. The disc file pointers are first initialized and the ADC turned on to begin digitizing the Doppler signal. For maximum throughput rate, a sample of 2048 data points is digitized at a time, and copied directly into the ADC Throughput File. This is done continuously using buffers until the file (which occupies almost half of the disc) is completely filled. The time taken depends, of course, on the sampling rate. For the rate decided upon in the last section, it is approximately 68 seconds.

3. The raw data are broken into consecutive samples of 128 points in accordance with the maximum frequency requirements of the Doppler signal described in the last section.

4. The DFM method is now applied to each sample, with the

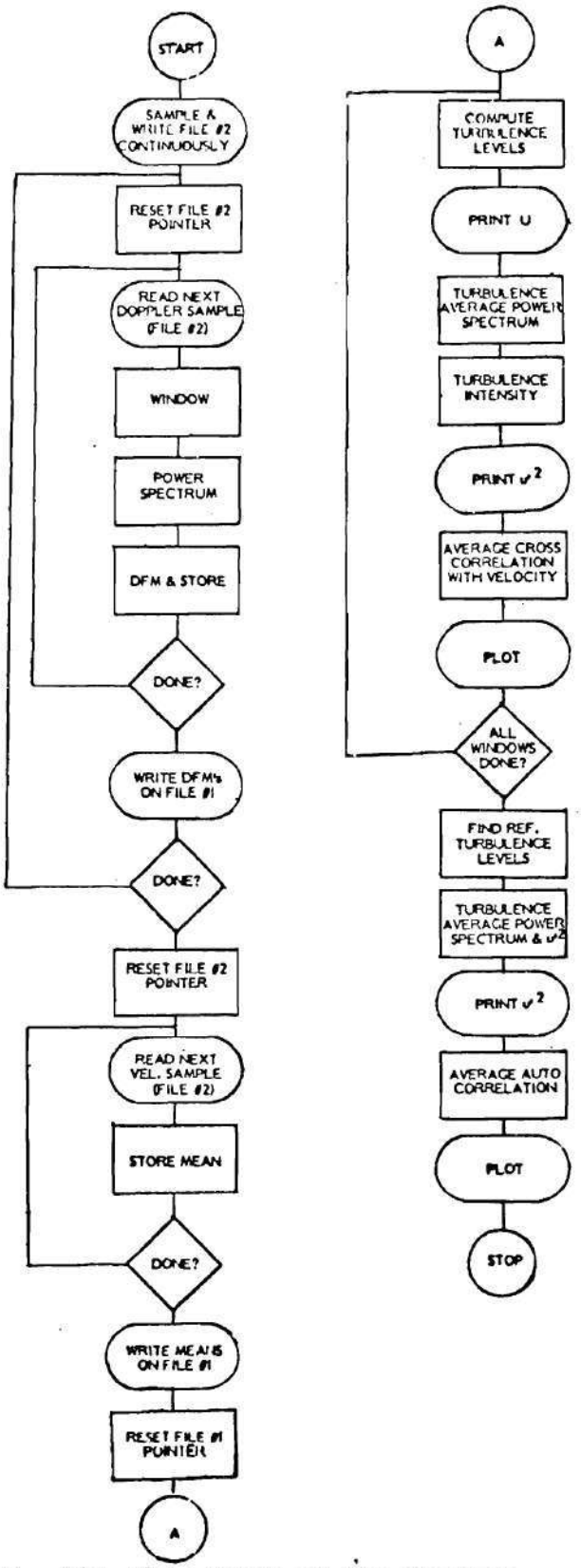

Figure 19. The Flow Chart of the Program

several windows decided upon earlier, in order to estimate the 'instantaneous' Doppler frequency shift. This consists of multiplication of the sample by the window function, power spectrum calculation, and determination of its first moment by the use of a user-defined special purpose subroutine. The consecutive values of these first moments (i.e., 'instantaneous' mean velocities) are stored in a section of the memory. This time history of velocity is continuously displayed while the computations are in progress so as to give a feedback to the observer.

5. After all the stored Doppler signal is processed, the stored velocity values are written into another disc file, and are available for any desired further analysis. For example, the mean turbulence intensity and turbulence power spectrum are next calculated and plotted. In addition, if the velocity input to the VCO was simultaneously recorded with the Doppler signal (which may be done as the ADC is dual channel), cross correlation functions may also be calculated and plotted, or

6. Sample the velocity signal at different rate in order to avoid aliasing and compare with the output of another demodulator, the PLL. The velocity series thus obtained are also stored on the disc for turbulence intensity and power spectrum computations.

5.5 Laminar Flow Results

A laminar flow through the sample volume causes scattering particles moving within it to shift the frequency of incident radiation by a constant amount in accordance with the Doppler equation (Equation 2.1). The received signal, therefore, will ideally be of a single

frequency at any instant of time which will man fest itself in the power spectrum as a single line. In these simulated laminar flow studies such a Doppler signal was used, i.e., effects of non-idealities causing spectral broadening were not considered.

5.5.1 Steady Laminar Flow

Here there is no variation in velocity (i.e., frequency of the Doppler signal) with time. Consequently the single line in the Doppler power spectrum remains invariant with time, and any sampling parameters can be used. Here, sampling parameters decided in Section 5.4.2 were used.

The results (Table 5) conclusively demonstrate the accuracy of the DFM method. The performance of the phase-locked-loop is also excellent as the Doppler signal is extremely narrowband (only the 'carrier' is present!). The frequency response, of course, cannot be measured here as the velocity is invariant with time.

Table 5. Measurement of Velocity in Simulated Steady Laminar Flows

Velocity Signal cm/sec	Mean Velocity, U ZCF cm/sec	DFM cm/sec	PLL cm/sec
12.7	12.7	12.7	12.7
30.3	30.3	30.3	30.3
38.4	38.4	38.4	38.4
49.0	49.0	49.0	49.0
66.3	66.3	66.3	66.3
93.1	93.1	93.1	93.1

5.5.2 Oscillating Laminar Flow

These experiments were conducted in order to determine the frequency and amplitude detection accuracies of the DFM method. Tests were carried out on a selection of discrete frequency 'components' of a turbulent flow, as outlined in Section 3.7. Conceptually, then, each of these components corresponds to a steady flow superimposed upon which is a sinusoidal variation in velocity. This, in turn, means that all the scatterers in the sample volume have sinusoidally varying velocity resulting in a Doppler signal with sinusoidal variation in frequency. Two cases were tried with the objective of seeing how well the DFM method 'tracks' these sinusoids:

1. Sinusoids of different frequencies were generated whose amplitude matched with a typical power spectrum of turbulence in pipe flow at a Reynolds' number of 15,000. (Resch 1970). (Figure 20) The Reynolds nubmer, Re of a flow is defined as

$$Re = \frac{U.D.\rho}{\mu} \tag{5.5}$$

where

U is the mean velocity of the flow

D is some characteristic dimension of the flow, here the pipe diameter

ρ is the density of the fluid

μ is the coefficient of viscosity of the fluid.

Furthermore, the turbulence power spectrum in Figure 20 is displayed in non-dimensional coordinates

$$E^* = \frac{F.U}{2\pi D} \tag{5.6}$$

and

$$N_s^* = \frac{2\pi Df}{U} \tag{5.7}$$

where

f is the frequency of velocity fluctuation in Hz, and

F dimensional power density function defined as

$$F(f) = \frac{E(f)}{\int_0^\infty E(f)\, df} \tag{5.8}$$

where E(f) is the measured power spectrum. Thus, for any given frequency, f, its power content E(f) can be determined, and hence the peak amplitude of the sinusoid.

Table 6 shows the performance of DFM method at several frequencies in the form of frequency and disturbance velocity power u'^2_{rms} (in Euqation 5.2) compared to the prescribed velocity signal whose Doppler signal was being synthesized (i.e., u' in Figure 16). The velocity waveform was reconstructed from every 4.87 ms of the Doppler signal using only the rectangular window in the DFM scheme. The performance of the scheme is clearly excellent, especially for velocity frequency detection. The large error near the extrema can be attributed to:

a) at the low frequency end the product $V \cdot f_v$ is large enough

Table 6. Measurement of Frequency and Power of Velocity Fluctuations in Simulated Oscillating Laminar Flows derived from Figure 20

Velocity Signal		DFM Results		Error	
Frequency Hz	Power $u'^2 \times 10^6$ rms	Frequency Hz	Power $u'^2 \times 10^6$ rms	Frequency %	Power %
2.10	17,060	2.19	17,380	4.37	1.42
2.96	17,000	3.06	17,410	3.17	2.42
9.57	14,030	9.64	14,440	0.73	2.94
18.2	12,720	18.3	12,960	0.39	1.89
32.1	8,387	32.2	8,684	0.12	3.54
50.5	4,152	50.4	4,334	0.22	4.38
65.7	3,597	65.5	3,733	0.30	3.77
80.2	2,079	79.6	2,153	0.75	3.57
94.0	1,526	93.1	1,631	0.96	6.86

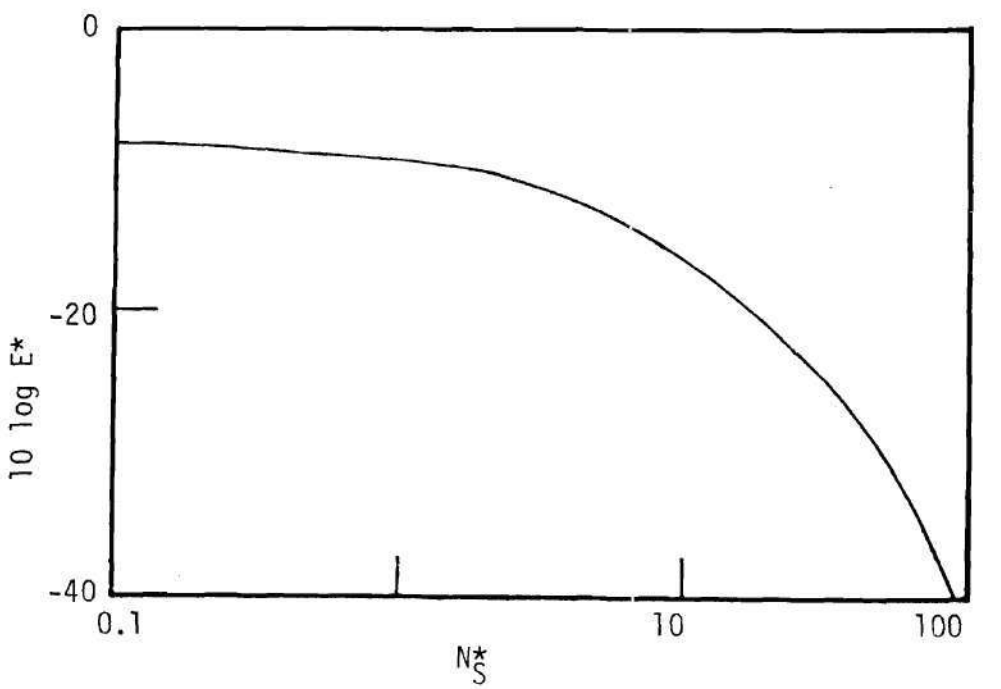

Figure 20. Typical Power Spectrum of Turbulence in Pipe Flow (Re ≃ 15,000)

to demand smaller sampling times than 4.87 ms,

b) toward the high frequency ends, less and less number of points are taken each cycle thus introducing errors. At the extremal case of 94 Hz there are only about two points per cycle, the minimum required by the sampling theorem, thus causing comparatively high error in power measurement.

c) Errors are also caused by spectrum 'wrap-around' at the limits caused by the inability of the system to reject large out-of-channel leakage power resulting from the use of rectangular window.

2. As outlined earlier (in Section 3.7) the DFM method performance depends on the frequency-peak amplitude product of the sinusoidal variations in velocity. The present series of tests, therefore, used different sinusoids with this product constant. Thus, the simulated oscillating velocity had an amplitude that varied as 1/f.

Also, to improve the performance of the digital scheme, use of windows was decided on. As discussed earlier in Section 5.4.1, the use of windows decreases the variance in the estimate of the power spectrum of a single sample. Three windows designated in numerical order were selected from a compilation of windows in a HP bulletin. They are:

Window 1: Maximum amplitude accuracy in a large dynamic large ($\pm$ 0.1%) (P301)

Window 2: Minimum sidelobe leakage (mainlobe-sidelobe drop - 93 dB) P(310)

Window 3: Hanning window

Their properties have been described in Section 5.4.1.

Tables 7 and 8 show the performance at various frequencies in comparison with the actual velocity signal. The use of windows definitely improves the performance of our scheme; Frequency accuracies (Table 7) are excellent; in fact, there are almost no errors with windows. The accuracies in power measurements (Table 8) are comparable for windows 1 and 2, and are somewhat better than Hanning window (window 3). Figures 21 and 22 display power spectra of disturbance velocity waveforms reconstructed from the Doppler Signal by the DFM mehtod, and bear out the above conclusions graphically.

As expected, aliasing occurs when the frequency of disturbance velocity oscillations exceed the maximum measurable frequency limit set by the sampling rate (in this case, 102.6 Hz). Table 9 demonstrates the almost mirror-like reflection of the line power spectra from this limit. Table 10 shows the expectedly increasing errors in the power measurements with increasing frequency.

5.6 Turbulent Flow Results

Studies done so far deal with single line spectra whose amplitudes were adjusted to match the amplitude of the turbulent pipe flow power spectrum. This way, errors associated with frequency and power measurement of each frequency 'component' of the turbulent flow have been determined. Now it remains to assess the DFM performance in the simulataneous presence of all these components, i.e., with fully turbulent flow conditions.

Table 7. Measurement of Frequency of Velocity Fluctuations in Simulated Oscillating Laminar Flows with Constant Peak Amplitude-frequency Product

Velocity Signal	Rectangular Window		Window 1		Window 2		Window 3	
Frequency Hz	Frequency Hz	Error Percent	Frequency Hz	Error Percent	Frequency Hz	Error Percent	Frequency Hz	Error Percent
1.62	1.64	0.5	1.62	0	1.63	0	1.63	0
10.1	10.3	1.9	10.1	0	10.1	0	10.1	0
20.2	20.7	2.9	20.2	0	20.2	0	20.2	0
40.7	40.2	1.2	40.7	0	40.7	0	40.7	0
59.9	58.3	2.7	59.9	0	59.9	0	59.9	0
80.5	69.9	13	80.5	0	80.5	0	80.5	0
90.2	67.8	25	90.1	0.1	90.1	0.1	90.1	0.1
96.3	67.7	30	96.2	0.1	96.2	0.1	96.2	0.1

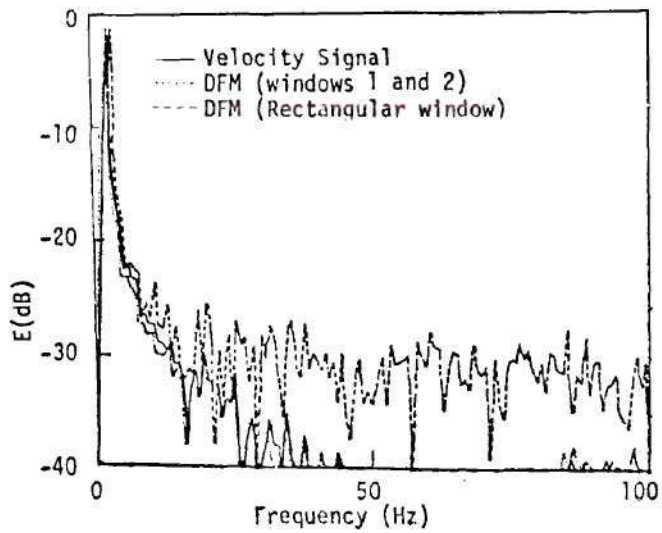

Figure 21. Performance of DFM in Measuring Oscillating Laminar Flow - low Frequency of Oscillation

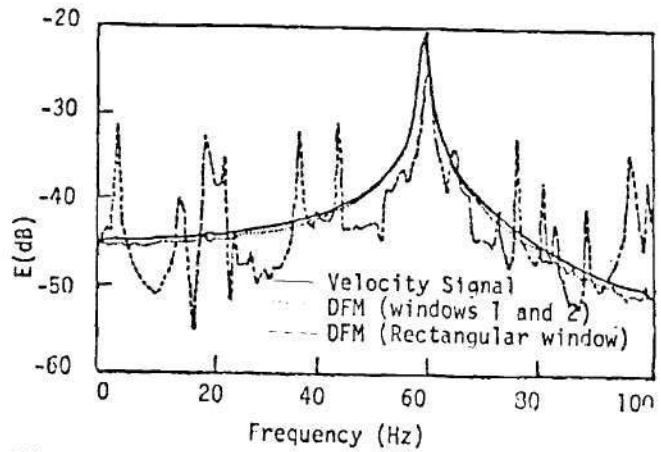

Figure 22. Performance of DFM in Measuring Oscillating Laminar Flow - high Frequency of Oscillation

Table 8. Measurement of Power of Velocity Fluctuations in Simulated Oscillating Laminar Flows with Constant Peak Amplitude-frequency Product

Velocity Signal		Rectangular Window		Window 1		Window 2		Window 3	
Frequency	Power	Power	Error	Power	Error	Power	Error	Power	Error
Hz	$u'^2_{rms} \times 10^6$	$u'^2_{rms} \times 10^6$	Percent	$u'^2_{rms} \times 10^6$	Percent	$u'^2_{rms} \times 10^6$	Percent	$u'^2_{rms} \times 10^6$	Percent
1.63	5,640,000	5,474,000	2.90	5,547,000	1.60	5,544,000	1.70	5,539,000	1.80
10.1	137,000	129,400	5.50	134,700	1.70	134,400	1.90	134,100	2.10
20.2	34,270	30,260	11.7	33,570	2.00	33,610	1.90	33,390	2.80
40.7	8,188	6,605	19.3	8,055	1.60	8,048	1.70	7,803	4.70
59.9	3,844	3,807	0.90	3,370	2.90	3,623	5.70	3,504	8.80
80.5	1,718	3,007	75.0	1,606	6.50	1,564	8.90	1,464	14.8
90.2	1,342	2,666	91.5	1,290	7.30	1,245	10.6	1,162	16.5
96.3	1,151	2,390	108	1,061	7.80	1,005	12.7	923	19.8

Table 9. Measurement of Frequency of Velocity Fluctuations in Simulated Oscillating Laminar Flows beyond the Aliasing Limit of the DFM Method

Velocity Signal	Rectangular	Window 1	Window 2	Window 3
Hz	Hz	Hz	Hz	Hz
111.3	86.9	89.9	89.9	89.9
119.8	77.3	80.4	80.4	80.4
150.3	53.0	49.8	49.8	49.8

Table 10. Measurement of Power of Velocity Fluctuations in Simulated Oscillating Laminar Flows beyond the Aliasing Limit of the DFM Method.

Frequency	Velocity Signal	Rectangular Window		Window 1		Window 2		Window 3	
Hz	$u'^2_{rms} \times 10^6$	$u'_{rms} \times 10^6$	Percent Error	$u'^2_{rms} \times 10^6$	Percent Error	$u'^2_{rms} \times 10^6$	Percent Error	$u'^2_{rms} \times 10^6$	Percent Error
111.3	32,930	10,980	66.7	29,960	9.0	28,590	13.2	25,370	23.0
119.8	28,430	8,540	70.0	29,380	3.2	27,910	1.83	24,120	15.2
150.3	29,890	3,830	87.2	28,220	5,6	25,760	13.8	20,500	31.4

5.6.1 'Ideal' Doppler Signal

As discussed in Section 5.2, an 'ideal' sample volume gives rise to an 'ideal' Doppler signal viz., a signal of constant amplitude, only frequency modulated by random velocity fluctuations inside the sample volume. Such a situation arises if the sample volume were of uniform shape and insonation, and all scatterers were acting as primary radiators. This, then, is the case that is examined next.

The Doppler signal is generated by appropriately low pass filtering white noise to simulate turbulence and using it to frequency modulate the 'carrier' (i.e., mean velocity) as illustrated in the Doppler Synthesizer (Figure 16). The signal A(t) is kept constant so as to have constant amplitude.

In order to compare the DFM method results with the total velocity signal (input to the VCO) as closely as possible, both were sampled simultaneously. However, the sampling rates were different: 38.1 μs for the Doppler signal and 4.87 ms for the velocity signal. All the four windows used in the previous studies with separate 'components' of turbulent flow were used here too, in order to test them in the simultaneous presence of a range of spectral lines.

Table 11 shows the performance of the DFM method for different degrees of turbulence intensity. This time, window 3 has considerably poorer performance in relation to window 1 or 2 which, again, are comparable. The rectangular window performance is almost equal to that of windows 1 and 2 since now a comparatively wideband signal is being processed and spectrum leakage is less of a problem. Figures 23-25

Table 11. Measurement of Simulated Turbulent Flow using 'ideal' Doppler Signal

	Velocity Signal	Rectangular Window		Window 1		Window 2		Window 3	
U cm/sec	u'_{rms}/U Percent	u'_{rms}/U Percent	Error Percent	u'_{rms}/U Percent	Error Percent	u'_{rms}/U Percent	Error Percent	u'_{rms}/U Percent	Error Percent
62.6	4.70	4.64	1.27	4.64	1.27	4.66	1.25	4.64	1.27
63.4	8.45	8.33	1.42	8.34	1.30	8.30	1.34	8.34	1.30
63.2	15.1	14.7	2.52	14.9	1.33	14.9	1.33	14.0	7.64

display these results graphically: note that power spectra of turbulence with windows 1 and 2 are identical between them and are comparable to that obtained directly from the velocity signal, even with unrealistically high degrees of turbulence being tested (approximately 15 percent as opposed to usual three to five percent for pipe flows). Therefore, from now on only one of them, namely, window 1 (P301) shall be used in the estimation of the Doppler power spectra.

It should be noted here, however, since the DFM method is capable of measuring frequencies only up to 102.6 Hz, (i.e., F_{max} = 102.6 Hz) its results displayed in Figures 23 through 25 are its aliased versions. But since the DFM's and the velocity signal were sampled at the same rate (Δt = 4.87 ms), both of them are aliased, and the excellent agreement between them demonstrates the accuracy of the DFM method. The errors at high frequencies can be explained as follows — the velocity signal, being sampled directly retains all of its power when aliased;

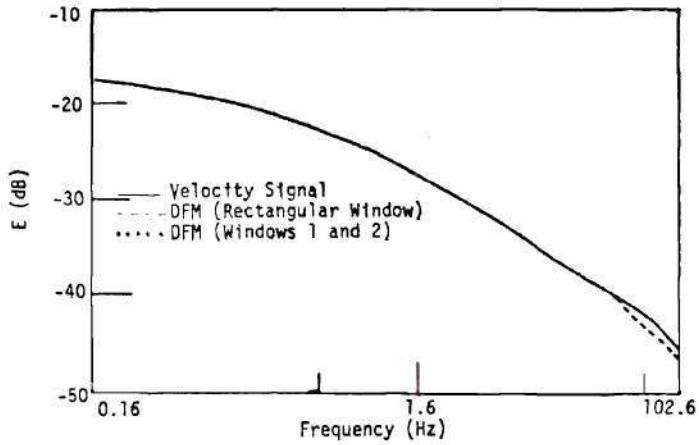

Figure 23. u'_{rms}/U = 4.70 percent

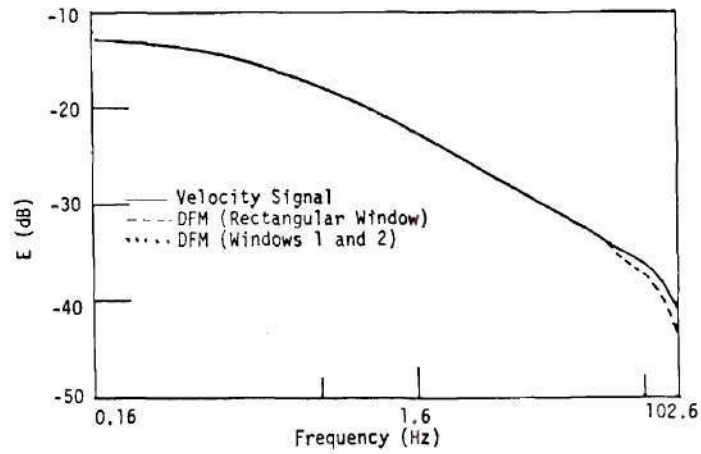

Figure 24. u'_{rms}/U = 8.45 percent

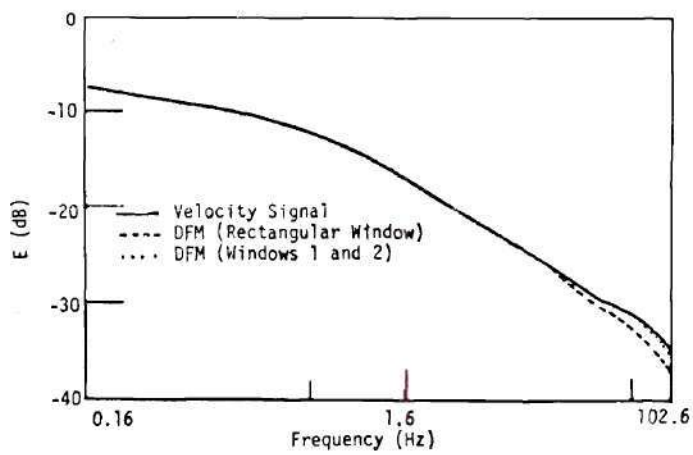

Figure 25. u'_{rms}/U = 15.1 percent

Performance of DFM Method in Measuring Simulated Turbulent flow with 'ideal' Doppler Signal

but the DFM's lose their power during alising as demonstrated in Table 10 for individual harmonics. The DFM power spectrum, therefore, falls below that of the velocity signal. This is not visible in the low frequency range due to extremely small amplitudes being folded back there. It is clear, then, that if the DFM method was implemented with higher F_{max}, even this small error can be eliminated. However, here we are trying to simulate the PD velocimeter available to us (with which F_{max} greater than 102.6 cannot be achieved).

5.6.2 Sinusoidal Amplitude Modulation

So far, the simulated Doppler signal has had constant amplitude. However, in a practical situation this hardly occurs: the Doppler signal almost always has random amplitude modulation i.e., signal fading. In order to make a preliminary evaluation of the effect of signal fading, the Doppler signal was amplitude modulated with sinusoids of different frequencies:

$$A(t) = A_0 \text{ Cos } \alpha\, w_c t$$

where w_c is the Doppler shift corresponding to time-averaged mean velocity, and α ranged from 0 to 0.8. Thus, the amplitude modulation frequency is adjusted to various fractions of the 'carrier' of the Doppler signal.

Table 12 shows the results for a simulated turbulence power spectrum. Again the DFM's and the velocity signal were sampled at the same rate for the purpose of comparison. Clearly, the DFM's are insensitive to sinusoidal amplitude modulation of the Doppler signal at low to moderate values for modulation frequency. Only at values

of $\alpha \simeq 1$ does the error increase, but as will be shown later, this condition is not observed with real Doppler signals. Figures 26 to 28 compare the power spectra of the velocity signal and DFM's for three of the cases listed in Table 12.

Table 12. Measurement of Simulated Turbulent Flow using Doppler Signal with Sinusoidal Amplitude Modulation

	Velocity Signal	DFM with Window 1		
α	u'_{rms}/U	U	u'_{rms}/U	error
	Percent	cm/sec	Percent	Percent
0	8.57	65.8	8.49	0.08
0.04	8.70	66.3	8.56	0.14
0.1	9.29	65.7	9.21	0.08
0.2	9.34	65.9	9.18	0.16
0.3	9.14	66.3	8.85	0.29
0.4	9.14	66.8	8.65	0.49
0.5	10.1	66.6	9.45	0.68
0.6	9.39	67.5	8.51	0.88
0.7	8.86	68.9	8.11	0.75
0.8	9.24	68.9	17.8	8.56

5.6.3 Random Amplitude Modulation

In a practical situation, the Doppler signal coming from a flow is amplitude modulated not sinusoidally but randomly. In order to simulate this, experiments were conducted on pipe flows, and Doppler signals for different velocities were recorded. These then, were passed through an envelope detector (essentially a full-wave rectifier and an

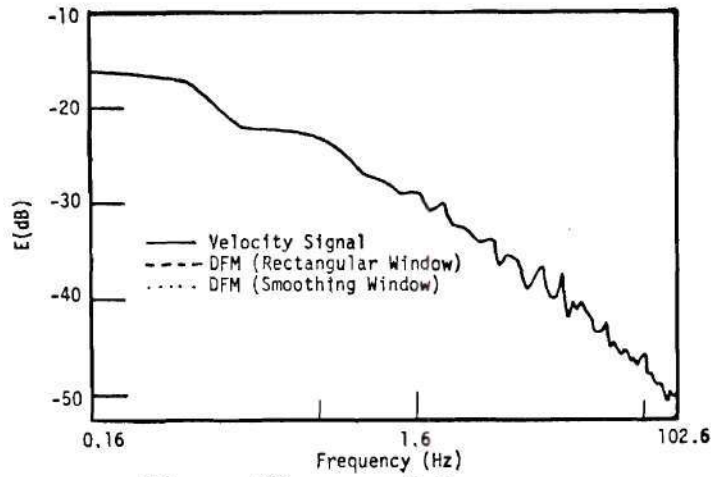

Figure 26. α = 0.1

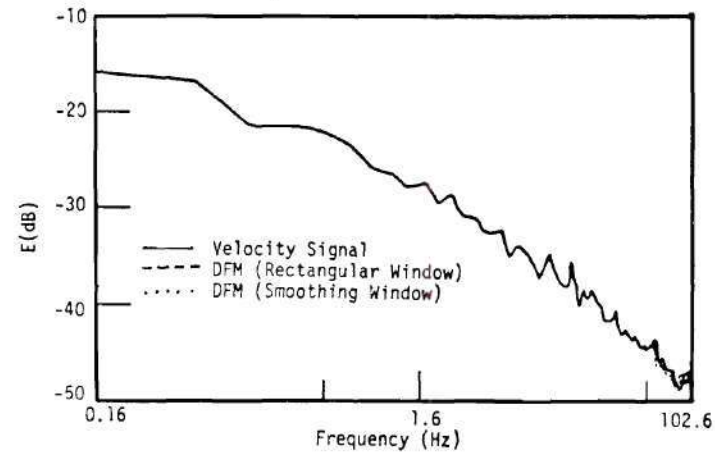

Figure 27. α = 0.5

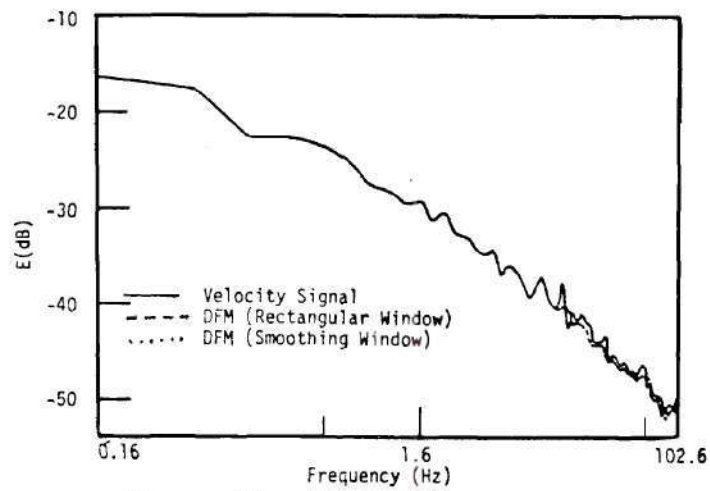

Figure 28. α = 0.8

Performance of DFM method in Measuring Simulated Turbulent flows using Doppler Signal with Sinusoidal Amplitude Modulation

RC circuit) to extract the amplitude modulating signal, whose average power spectrum was recorded. The noise generator-LPF combination at the bottom of the figure of the Doppler synthesizer (Figure 16) was used to generate a signal A(t) having the power spectrum of the detected envelope of the real Doppler signal. Figure 29 shows a comparison of power spectra of real and simulated envelopes, and Figure 30 illustrates the resulting synthesized and measured real Doppler signals. Thus, when the 'ideal' Doppler signal is amplitude modulated by the synthesized envelope, we get a Doppler signal which is similar in appearance to that obtained in fluid dynamic experiments.

By varying the dc offset of the envelope and/or its magnitude, the ideal Doppler signal can be amplitude modulated to give imperceptible variations in amplitude to very large excursions in it (with a large degree of signal drop-out. A modulation factor, therefore, was defined to quantify the degree of severity of the drop-out:

$$e = \frac{(v_m)_{rms}}{(v_m)_{avg}} \tag{5.9}$$

where v_m refers to the amplitude modulating signal.

Clearly, large values of e correspond to large modulation levels, or large excursions in the Doppler signal amplitude. As $v_{rms} \to 0$, and $v_{avg} \to 0$, the factor approaches 0, and there is no modulation (i.e., A(t) = constant). Thus, the 'ideal' Doppler signal has e = 0.

5.6.4 Doppler Signal with Random Amplitude Modulation

The amplitude modulation described above was used in the Doppler

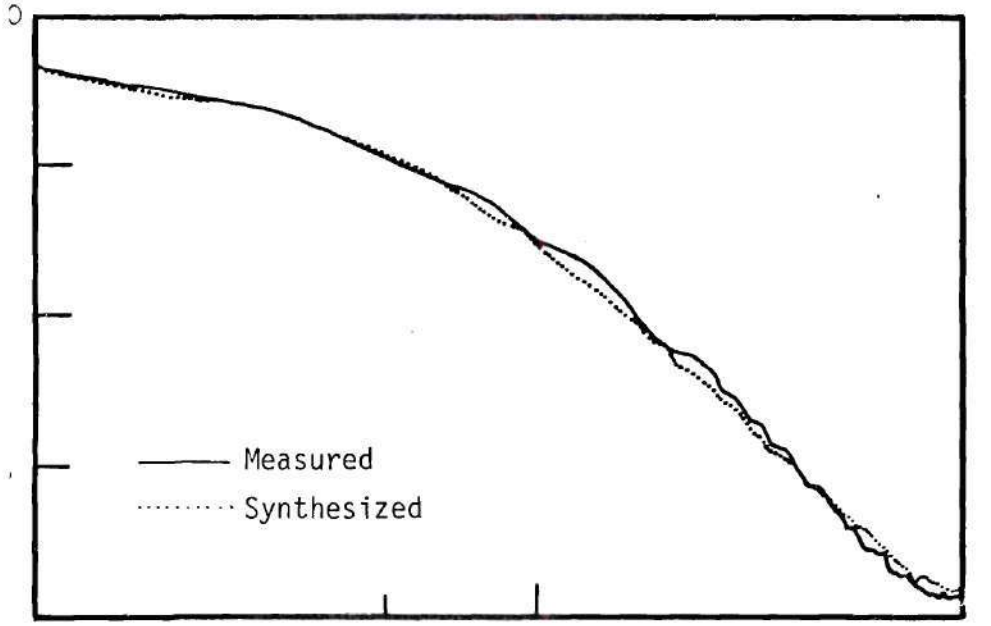

Figure 29. Comparison of Envelopes of Measured and Synthesized Doppler Signals

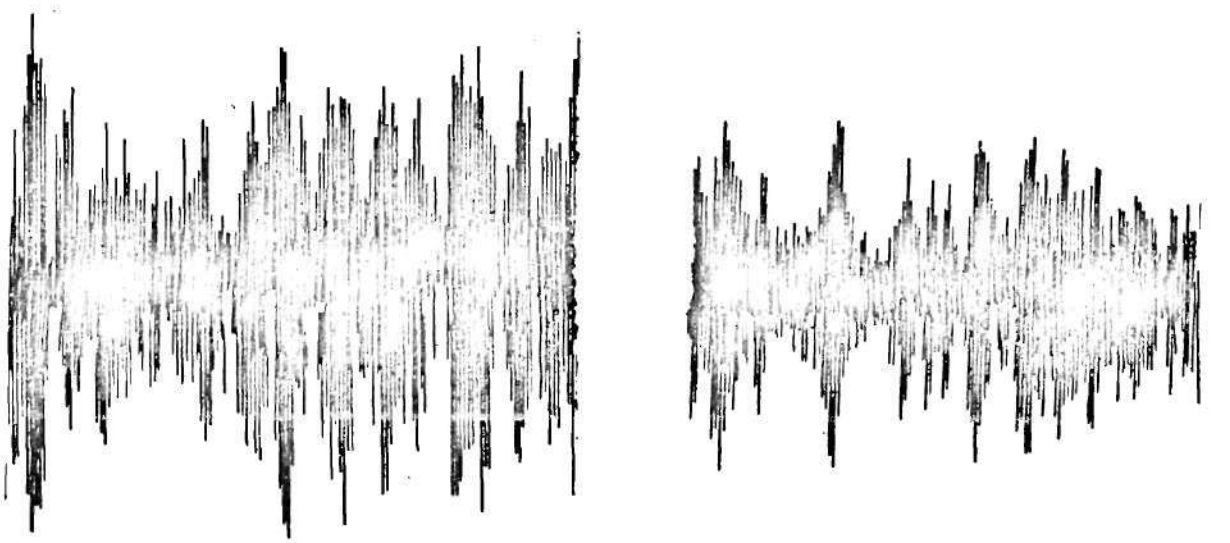

Figure 30. Comparison of Real and Synthesized Doppler Signals.

synthesizer to evaluate the DFM performance on the synthesized Doppler signal. Three levels of amplitude modulation were tried:

a) no amplitude modulation, e = 0,

b) modulation factor, e = 0.407, same as that observed with the pipe flows experiments,

c) the most severe dropout the instrument was capable of generating.

The turbulence power spectrum first simulated was that measured using Laser Doppler Velocimeter in pipe flow at Re $\tilde{}$ 10,000, Figure 31. Table 13 displays the error in measurement of turbulence intensities and Figures 32 to 34 show the freuqency response with the DFM method. Clearly, the use of the smoothing window improves the DFM performance considerably, especially in the situation with high signal dropout rate.

In all the studies done so far, the performance of the DFM scheme was evaluated against the velocity signal (an absolute reference), and was shown to be an excellent velocity estimator. It was felt that some comparison with the existing demodulators may prove to be beneficial. In current use, the msot popular demodulator is the zero-crossing frequency meter (ZCF), with the phase-locked-loops (PLL) being tried recently. Of these two, the former has been judged by many workers to be a very poor estimator of mean velocity inside the sample volume, and also of being incapable of measuring turbulence (Flax, et al., 1971, Bordy 1972). For this reason, we shall compare the performance of the DFM method and the PLL against each other, and the velocity signal being input to the VCO in the Doppler signal synthesizer.

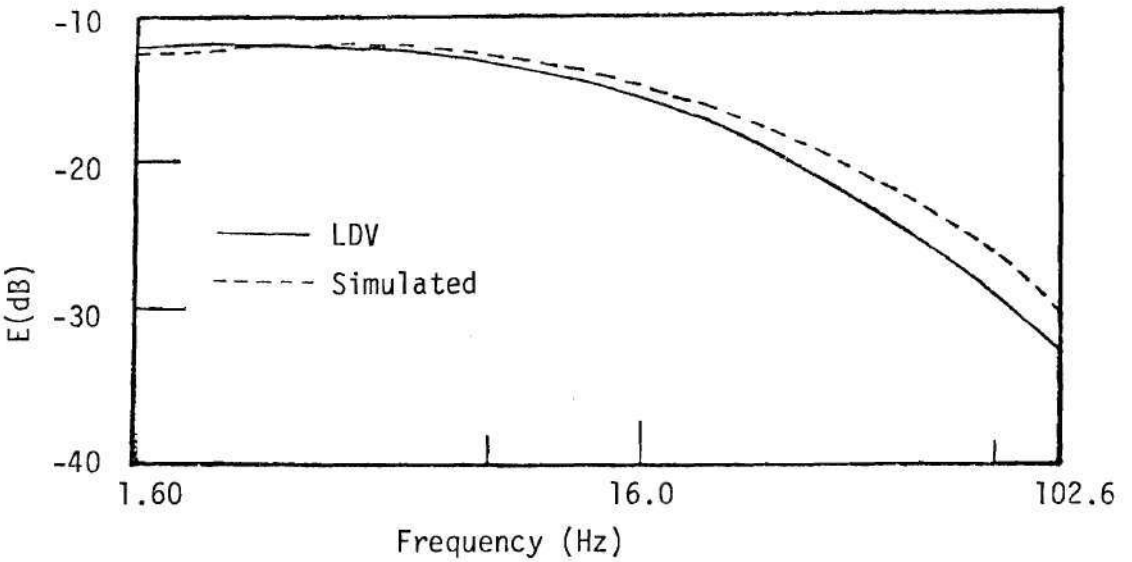

Figure 31. Comparison of Measured and Simulated Turbulence Power Spectra at Re ≃ 10,000

Table 13. Measurement of Simulated Turbulent Flow using Doppler Signal with Random Amplitude Modulation (Re ≃ 10,000)

e	Velocity Signal	DFM					
		Smoothing Window			Rectangular Window		
	u'_{rms}/U	U	u'_{rms}/U	error	U	u'_{rms}/U	error
	Percent	cm/sec	Percent	Percent	cm/sec	Percent	Percent
0	13.7	64.6	13.5	1.53	64.6	13.1	4.96
0.407	13.6	64.4	13.3	1.55	64.4	13.0	3.28
0.734	13.5	65.2	13.3	2.07	65.2	12.9	4.58

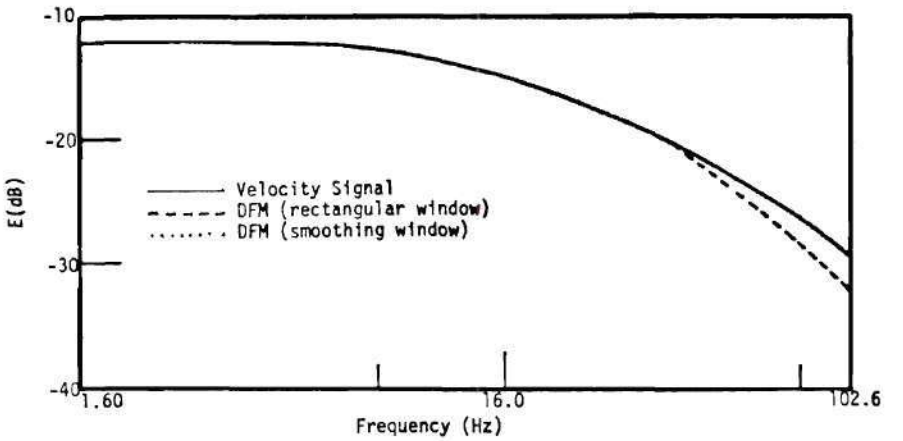

Figure 32. e = 0

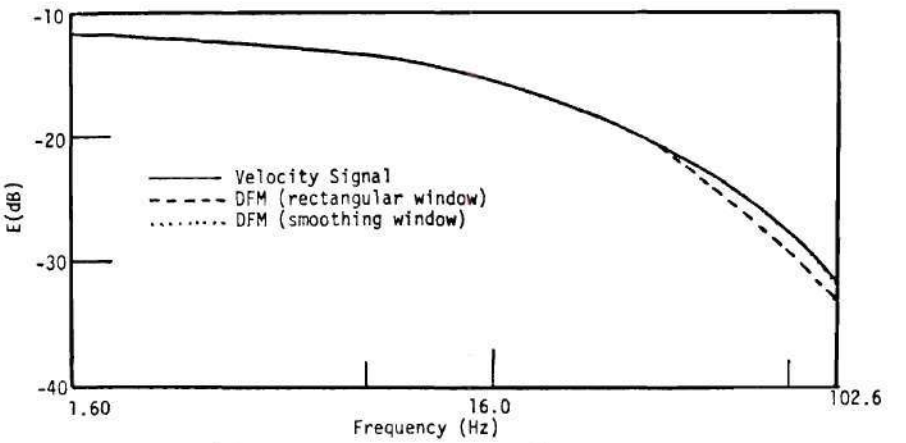

Figure 33. e = 0.407

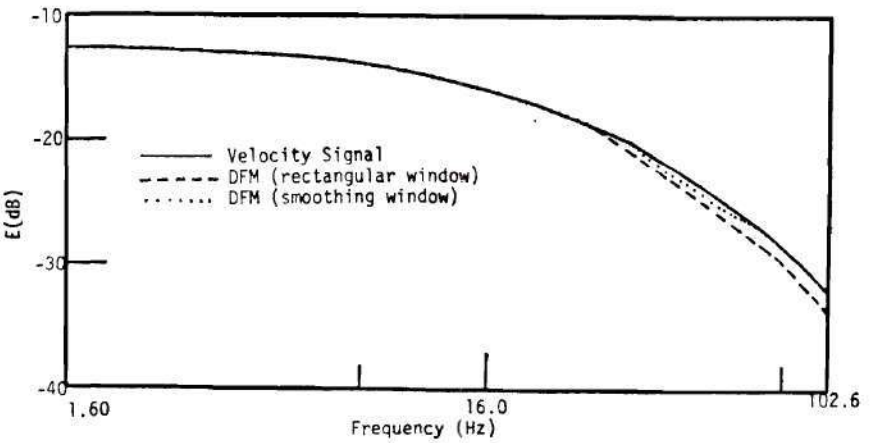

Figure 34. e = 0.734

Performance of DFM Method in Measuring Simulated Turbulent Flow using Doppler Signal with Random Amplitude Modulation (Re ≃ 10,000)

Two turbulence power spectra were chosen to be simulated - both obtained with steady pipe flow using Laser Doppler Velocimeter. Figure 35 and 36 show the comparison between the power spectra of the measured, and simulated flows for cases of a low and a high Reynolds number (approximately 5,000 and 15,000 respectively).

The procedure consisted of sampling the velocity signal, and the PLL output with a maximum frequency response, F_{max} of 500 Hz, and comparing the power spectra, and turbulence intensity predictions in that range. For the purpose of comparison with the DFM method output, the velocity signal was sampled with F_{max} of 102.6 Hz thus introducing similar aliasing errors already present in DFM's. A block diagram of the procedure is shown in Figure 37. Also, to make these comparisons of the two demodulators with the velocity signal as general as possible, two windows (rectangular and smoothing) were used with the DFM scheme, and three bandwidth settings (2%, 4% and 8%) with the PLL.

Tables 14 and 15 demonstrate the performance of the DFM and PLL methods of demodulating the Doppler signal. As will be explained later, the four percent bandwidth results of the PLL should be compared with the DFM for the low Reynolds number case (Table 14). The performance of the two scheme here appears to be equivalent. However, an examination of predicted turbulence power spectra tells a different story:

Figures 38 through 40, and 41 through 43 display the PLL and DFM method performances respectively for the low Reynolds number case (Re $\simeq$ 5,000). The performance of both deteriorates with increasing degree of severity of amplitude modulation (i.e., distortion of the

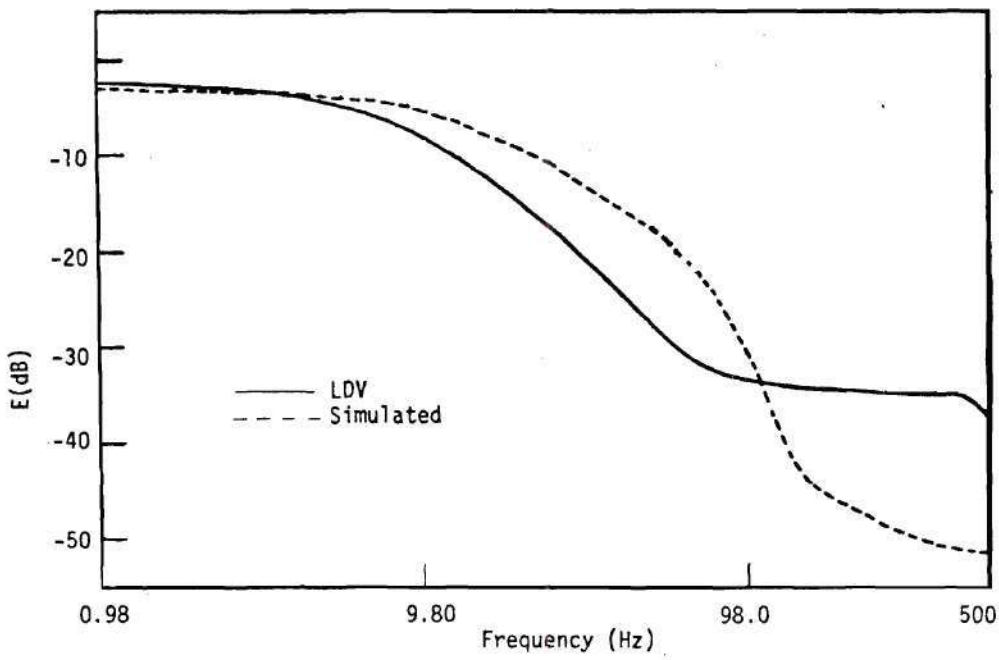

Figure 35. Comparison of Measured and Simulated Turbulence Power Spectra at Re ≃ 5,000

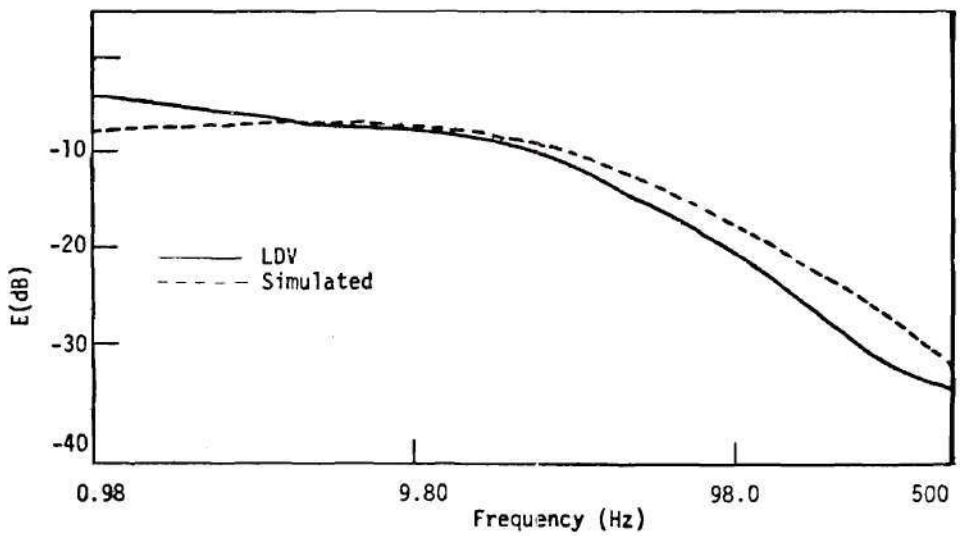

Figure 36. Comparison of Measured and Simulated Turbulence Power Spectra at Re ≃ 15,000

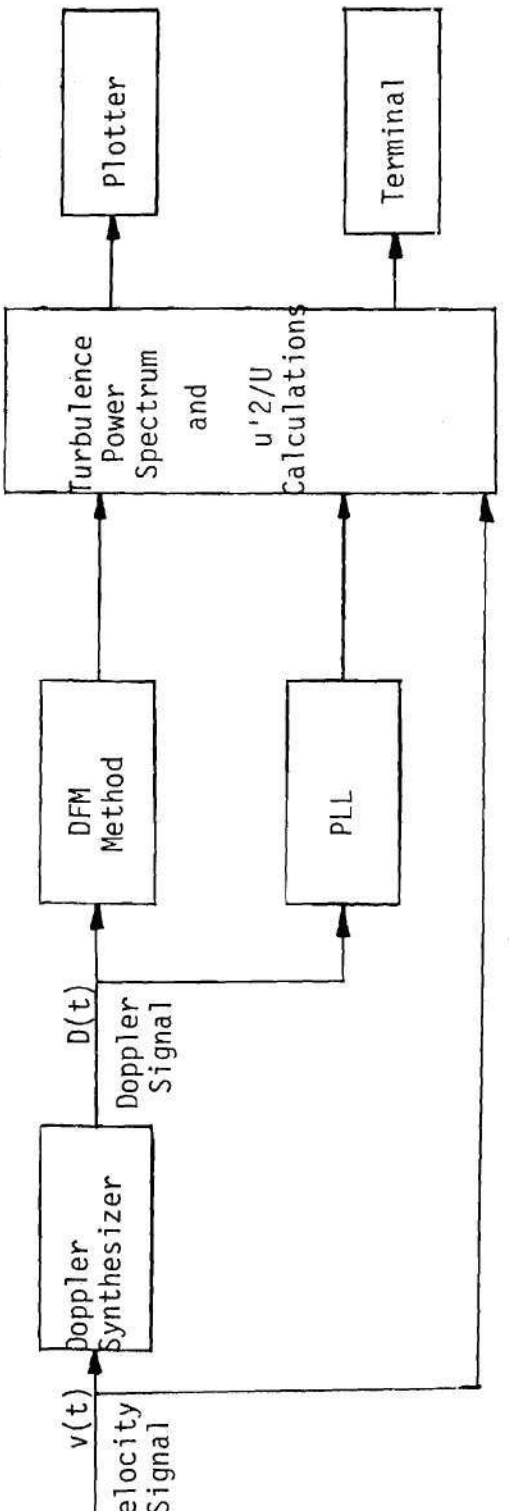

Figure 37. Block Diagram of Computations

Table 14. Measurement of Simulated Turbulent Flow using Doppler Signal with Random Amplitude Modulation (Re ≃ 5,000)

e	DFM									PLL					
	Smoothing Window			Rectangular Window			2 Percent			4 Percent			8 Percent		
	U	u'_{rms}/U	Error	U	u'_{rms}/U	Error	U	u'_{rms}/U	Error	U	u'_{rms}/U	Error	U	u'_{rms}/U	Error
	cm/sec	Percent	Percent	cm/sec	Percent	Percent	cm/sec	Percent	Percent	cm/sec	Percent	Percent	cm/sec	Percent	Percent
0	63.4	4.23	1.62	63.5	4.10	4.65	63.8	4.25	6.80	64.0	4.31	5.48	63.9	4.51	1.09
0.407	63.4	4.20	2.32	63.5	4.00	6.98	63.9	3.85	15.5	63.7	4.18	8.33	63.5	4.47	1.97
0.734	63.0	4.16	3.26	63.3	3.94	8.37	64.1	3.74	18.0	63.9	4.33	5.04	64.1	4.35	4.60

Table 15. Measurement of Simulated Turbulent Flow using Doppler Signal with Random Amplitude Modulation (Re ≃ 15,000)

e	DFM									PLL					
	Smoothing Window			Rectangular Window			2 Percent			4 Percent			8 Percent		
	U	u'_{rms}/U	Error	U	u'_{rms}/U	Error	U	u'_{rms}/U	Error	U	u'_{rms}/U	Error	U	u'_{rms}/U	Error
	cm/sec	Percent	Percent	cm/sec	Percent	Percent	cm/sec	Percent	Percent	cm/sec	Percent	Percent	cm/sec	Percent	Percent
0	62.2	4.27	2.00	62.2	4.17	4.38	62.9	3.46	23.5	62.7	4.29	5.09	62.7	4.38	3.10
0.407	62.2	4.19	3.82	62.2	4.08	6.43	62.8	3.03	33.0	62.7	3.94	12.83	62.5	4.24	6.19
0.734	61.0	4.10	5.90	61.5	3.85	11.6	63.1	3.00	33.6	62.7	3.90	13.7	63.0	4.16	7.96

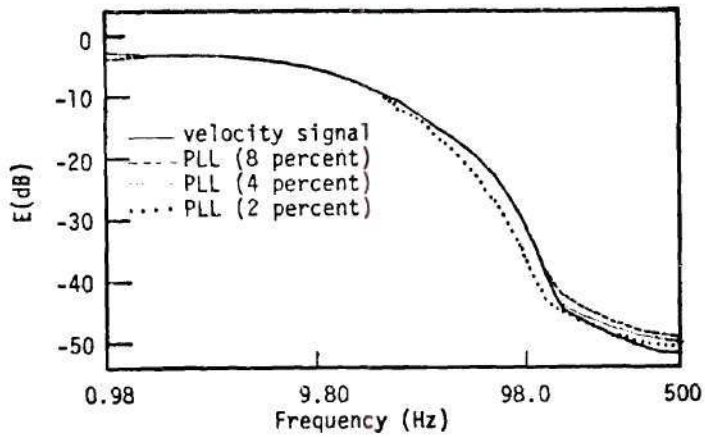

Figure 38. e = 0

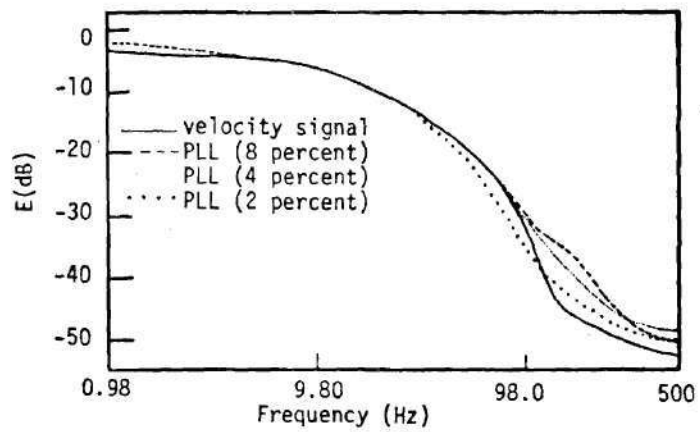

Figure 39. e = 0.407

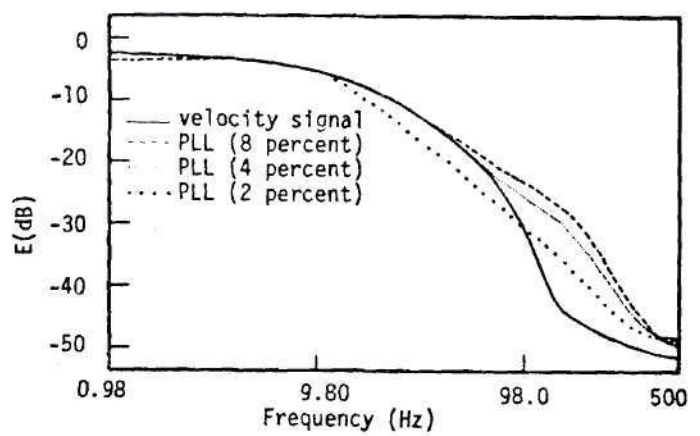

Figure 40. e = 0.734

Performance of PLL in Measuring Simulated Turbulent Flow using Doppler Signal with Random Amplitude Modulation (Re ≃ 5,000)

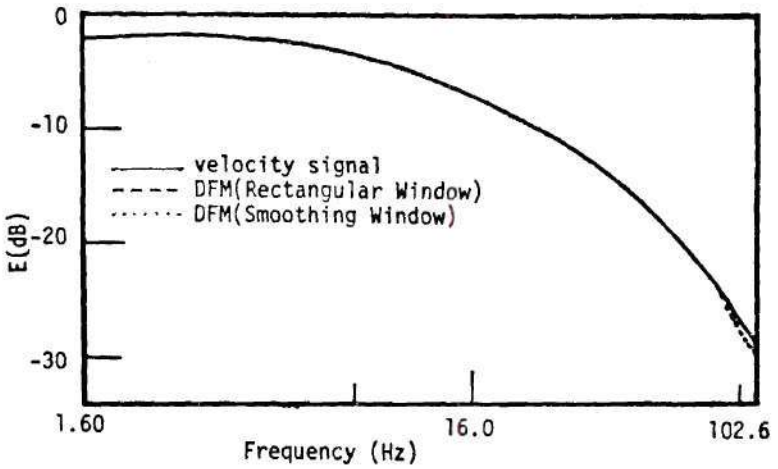

Figure 41. e = 0

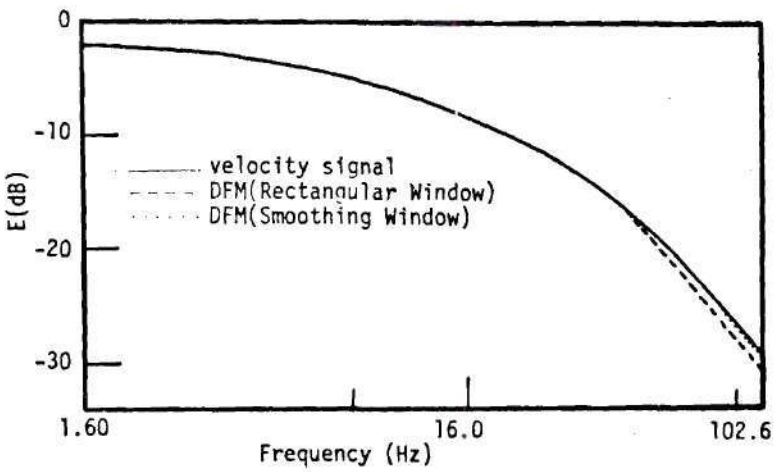

Figure 42. e = 0.407

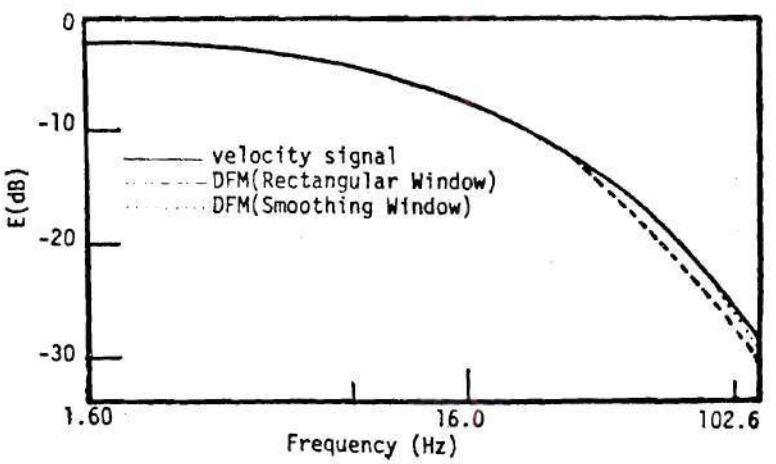

Figure 43. e = 0.734

Performance of DFM Method in Measuring Simulated Turbulent Flow using Doppler Signal with Random Amplitude Modulation (Re ≃ 5,000)

Doppler power spectrum). However, the DFM method outperforms the PLL in maximum frequency response in cases with amplitude modulation. The apparently better frequency response of the PLL with the 'ideal' Doppler signal may be attributed to the limitation of the DFM of not being able to detect frequencies higher than 102.6 Hz thus causing errors due to aliasing (see explanation on pp. 103). Had the PD velocimeter being simulated allowed a sampling rate prescribing F_{max} higher than this, say 500 Hz, the DFM would have shown a better performance than the phase-locked loop. Thus the DFM method performance is not limited by any inherent factor, but only by the PD velocimeter being used. Also note here that bandwidth of four percent yields the best comparison of PLL output and velocity signal, and it is for this reason that turbulence intensity predictions with this bandwidth should be used in comparison in Table 14.

The results with high Reynolds nubmer (Re $\tilde{=}$ 15,000) are shown in Figures 44 through 46 (PLL), and 47 through 49 (DFM). Again the performance of the DFM method is much better than that of the PLL as far as the frequency response is concerned. In this case of the flatter turbulence power spectrum, the PLL performance is best obtained with a bandwidth setting of eight percent. Thus the use of the PLL is frought with uncertainities -- one does not know what bandwidth is best suited in a particular velocity. This fact severely denigrates the importance of the PLL in cases where velocity is varying as no one bandwidth setting is suitable for all the velocities occurring in a cycle.

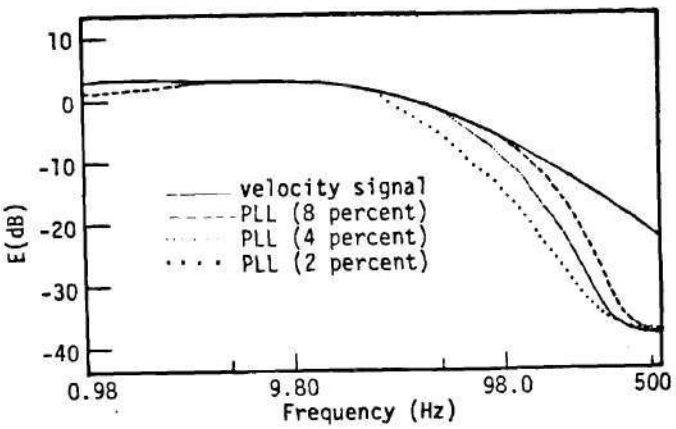

Figure 44. e = 0

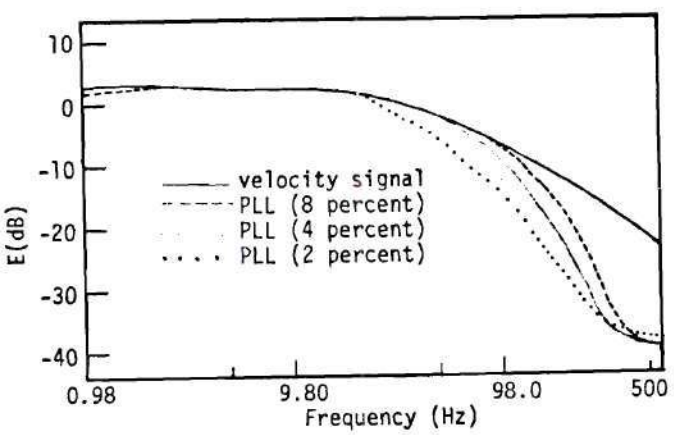

Figure 45. e = 0.407

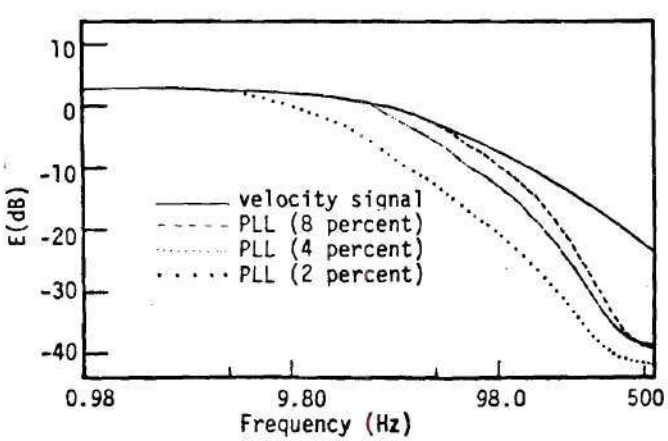

Figure 46. e = 0.734

Performance of PLL in Measuring Simulated Turbulent Flow using Doppler Signal with Random Amplitude Modulation (Re ≃ 15,000)

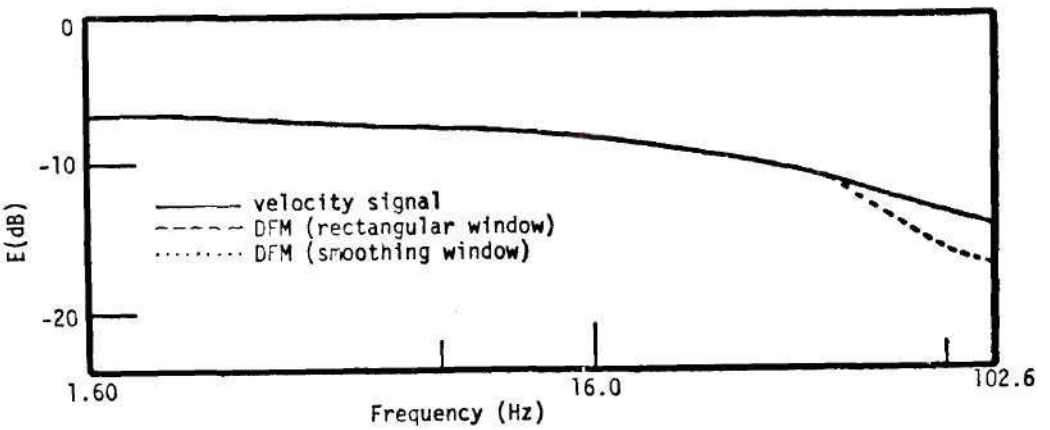

Figure 47. e = 0

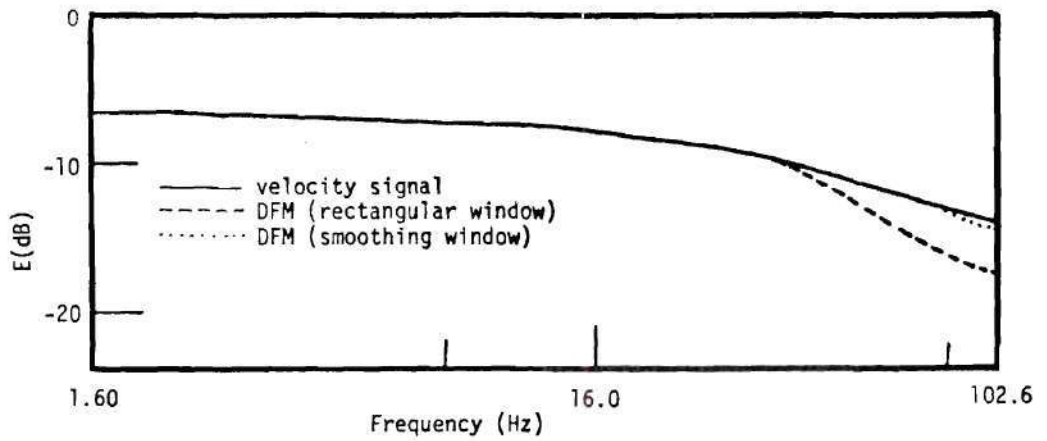

Figure 48. e = 0.704

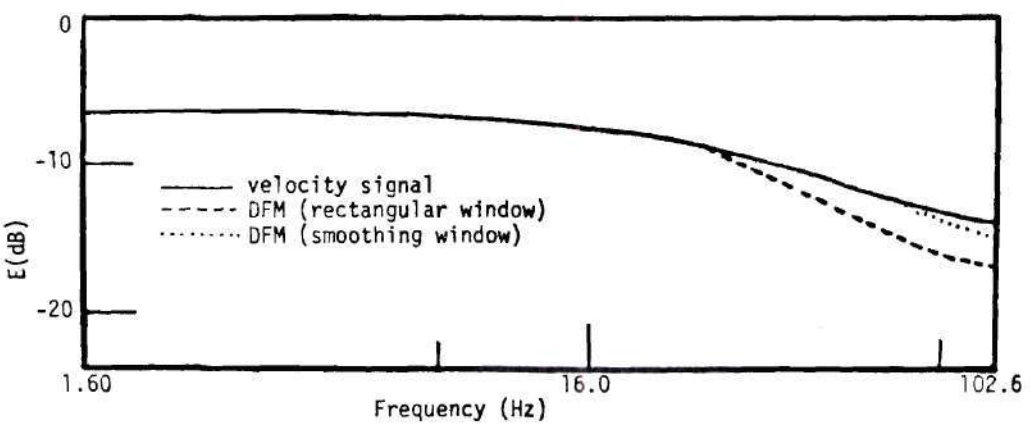

Figure 49. e = 0.734

Performance of DFM in Measuring Simulated Turbulent Flow using Doppler Signal with Random Amplitude Modulation (Re ≃ 15,000)

For the next phase of experimentation (turbulence measurements in real pipe flows), therefore, all the three bandwidth setting in the PLL shall be tried. Since the DFM method seems to yield the best results with the use of the smoothing window (previously referred to as P301 and Window 1), it will be used only with the smoothing window.

CHAPTER VI

FLUID FLOW EXPERIMENTS

6.1 Purpose

The results of the DFM method with simulated flow conditions as described in the previous chapter impart sufficient confidence to attempt its application in measuring turbulence in real-life situations. For this purpose three different velocity cases lying in the range of physiological interest were tried with the available PD velocimeter. These experiments were deemed necessary to predict the performance limit of the DFM method - PD velocimeter combination in real flow situations, to investigate the sources of errors, and to make recommendations for improvements.

6.2 The Flow System

Figure 50 shows a closed loop flow system used for this phase of experimentation. Water flows through a one inch diameter glass tube sufficiently long in order to give fully developed turbulent pipe flow at its exit. At the upstream end is a settling chamber which is replenished by the constant head reservoir through two centrifugal pumps. The flow rate through the tube is controlled by means of flow valves and variable speed pumps.

Measurements are made near the downstream end of the glass tube using both the PD and LD velocimeters. The PD probe was inserted

through the end, and kept at the centerline by means of plexiglass holders. The axial flow velocity was measured at a distance of 0.5 cm away from its tip. The length of the tube was enclosed in a rectangular plexiglass trough filled with water so that the laser beams strike at a normal plane surface, rather than the curved surface of the tube.

The scatterers used were silicon carbide particles. It was found from the previous experience that the size and concentration requirements for two velocimeters were different, thus excluding their simultaneous use. However, the simultaneous data from the two is not a desideratum as far as statistical measurement of the flow is concerned - if we accumulate data for long time intervals, the average values of mean velocity and turbulence energy distribution should be invariant.

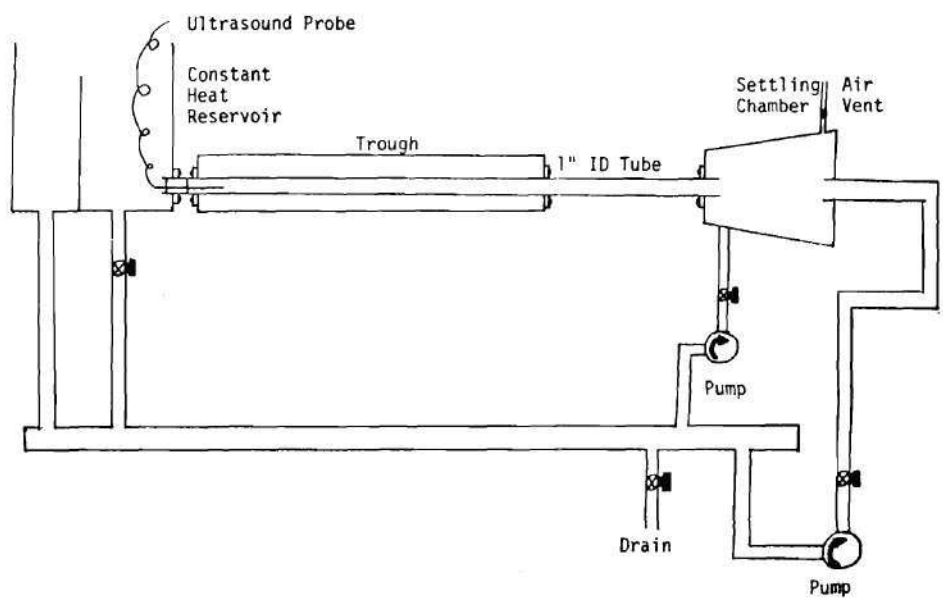

Figure 50. The Flow System

6.3 Procedure

Three different flow velocity cases were tried, corresponding to Reynolds numbers of approximately 5000, 10,000 and 15,000 respectively. For each case, the flow system was first filled with filtered water and seeded with 1 micron diameter silicon carbide particles for use with the LDV. After sampling and processing the LDV data, the water was heavily seeded with 10 micron silicon carbide particles in preparation for measurements with the PDV. The DFM program to sample, store and process the Doppler signal was then initiated on the minicomputer, and the results (DFM's) were stored. Lastly the PD Doppler signal was demodulated using the frequency tracker whose output was also sampled and stored.

The resultant three different velocity series were later processed as shown in the computational block diagram of Figure (where the simulated velocity signal from Chapter V is now replaced by the actual velocity signal measured by the LDV).

Two things should be noticed in the above procedure:

1. The LDV and PD velocimeter data were taken at different times due to conflicting seeding requirements. However, this does not jeopardize their comparison provided the pump characteristics, and therefore flow rate, remain invariant.

2. The real turbulent flow certainly has velocity fluctuations at frequencies in excess of 102.6 Hz, the highest measurable by the DFM. The DFM results will, therefore, be aliased. The output of the phase locked-loop and the LDV, on the other hand, can be sampled at any desired rate. Here it was chosen to be 1000 Hz, yielding a Nyquist

frequency (F_{max}) of 500 Hz).

6.4 Results

The first experiment was to assess the performance of the LDV, since PD/DFM and PD/PLL results will be compared against it. Figure 51 shows the comparison between the LDV output and another accepted standard (Resch, 1970) at Re $\simeq$ 15,000. This enhances the confidence in using the LDV as a reference.

Table 16 presents the turbulence intensity, and the mean velocity as determined by the different measuring systems used for the three cases tried. The performance of the PD/PLL combination is clearly good for the high velocity cases, but it deteriorates rapidly with decreasing velocity. The PD/DFM combination predicts surprisingly high turbulence intensities, the reasons for which shall be enumerated in the following discussion.

Figure 52 shows the comparison of the predicted turbulence power spectra by the PD/PLL and the LDV up to a maximum frequency of 500 Hz. (The power spectra in this figure, as well as in all the succeeding ones have been normalized for comparison using Equations 5.6). The DFM method result is compared next with the LDV output in the frequency range of 1.6 Hz to 102.6 Hz (Figure 53). Several observations can be made from these comparisons.

1. The LDV has an ambiguity in turbulence power spectrum measurement (i.e., the power spectrum becomes flat) beyond a certain frequency in accordance with the discussion of Doppler ambiguity in Section 3.5. The results beyond this limit (called the cut-off

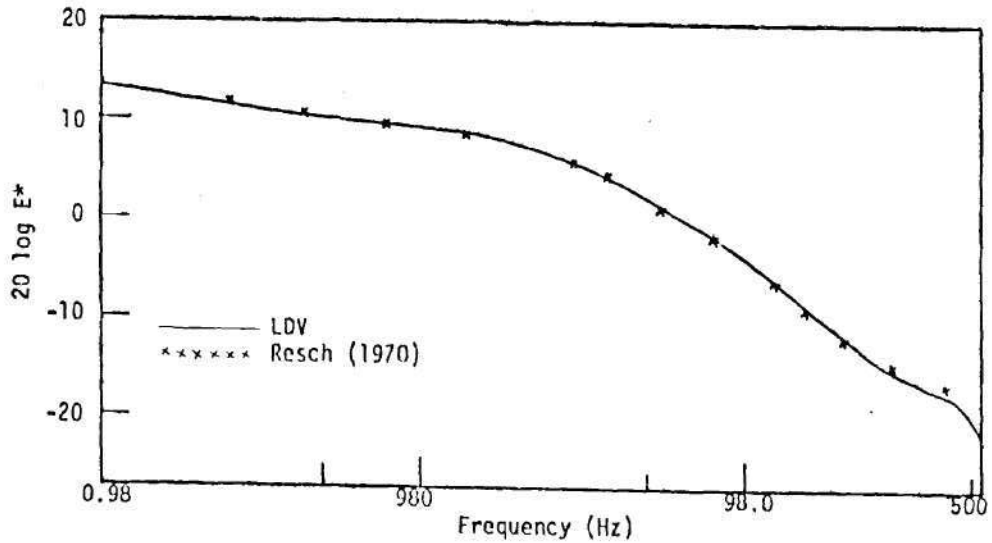

Figure 51. Comparison of Measured Turbulence Power Spectra

Table 16. Measurement of Turbulence in Pipe Flows

LDV		PLL									DFM		
		2 PERCENT			4 PERCENT			8 PERCENT			Maximum Amplitude Accuracy Window		
U	u'_{rms}/U	U	u'_{rms}/U	Error	U	u'_{rms}/U	Error	U	u'_{rms}/U	Error	U	u'_{rms}/U	Error
cm/sec	Percent	cm/sec	Percent	Percent	cm/sec	Percent	Percent	cm/sec	Percent	Percent	cm/sec	Percent	Percent
60.5	4.23	65.9	3.52	16.8	64.9	3.90	7.8	64.9	4.20	0.71	61.5	5.20	22.9
36.2	4.48	34.7	4.39	2.01	36.9	4.60	2.68	38.1	5.69	27.0	34.4	5.80	29.7
20.1	4.59	21.4	4.78	4.14	21.6	5.05	10.0	22.0	5.45	18.7	20.0	7.11	54.9

frequency, f*) are, therefore not trustworthy.

2. The PDV also has a similar limitation in turbulence power spectrum measurement. However, this cut-off frequency for the PDV is much lower than that for the LDV.

3. The maximum frequency response, F_{max} of the DFM method is constrained by sampling considerations (Section 3.7) to only 102.6 Hz, and consequently the turbulence power spectrum predicted by it is aliased.

These last two limitations compound their effects and severely distort the turbulence power spectrum predicted by PD/DFM combination. Nevertheless, the performance of this combination can be evaluated by investigating these causes of error and taking them into consideration. One may either attempt to correct the DFM results, or introduce the same errors in the LDV results before making a comparison. The latter approach will be used here.

4. Lastly, the apparent good comparison between the PD/PLL and the LDV outputs can be attributed to the rolling-off of the flat turbulence power spectrum (as measured by the PDV) due to the band-pass filter used in the frequency tracker. Here this filter roll-off rate and the turbulence power spectrum slope (as measured by the LDV) happen to be close resulting in apparently superior performance of the PLL. However, since this filter roll-off rate is fixed, this comparison will be degraded as the turbulence power spectrum shape changes with varying velocity. This, indeed, will be observed in the remaining two cases. Another important thing to note is that due

to the presence of this bandpass filter, the PLL is not making use of all the information present in the Doppler signal. This results in uncertainty as to what velocity in the sample volume is being measured. By increasing the passband of this filter, increasingly more information present in the Doppler signal is used, and consequently the PLL result should approach those predicted by the DFM. This trend is, indeed, observed in Figure 52: as the filter bandwidth is increased, the measured power spectrum tends to become flatter.

Combing back to comparing the PD/DFM performance with that of the LDV in turbulence pwoer spectrum measurement, we need to calculate the cut-off frequencies, f* of these two devices by the use of equations 3.11 and 3.12. For this, one must ascertain the minimum resolvable length in the mean flow direction. Following the arguments presented in Section 3.5 it is the sample volume dimension in that direction (.012 cm and .037 cm for the LDV and PDV, respectively). Using these, and other appropriate parameters, the cut-off frequencies for a velocity of 60 cm/sec are 440 Hz for the LDV, and 100 Hz for the PDV.

This phenomenon can, in fact, be observed for the LDV in Figure 52 at about 400 Hz with roll-off after it due to the low pass filter used. This agreement for the LDV enhances the validity of the predicted f* for the PDV. The Doppler ambiguity bandwidth, $\Delta\omega$, was measured from an averaged Doppler power spectrum and was found to be approximately 3200 Hz for a velocity of 60 cm/sec. The turbulence power spectrum predicted by the PDV, thus should follow the actual turbulence

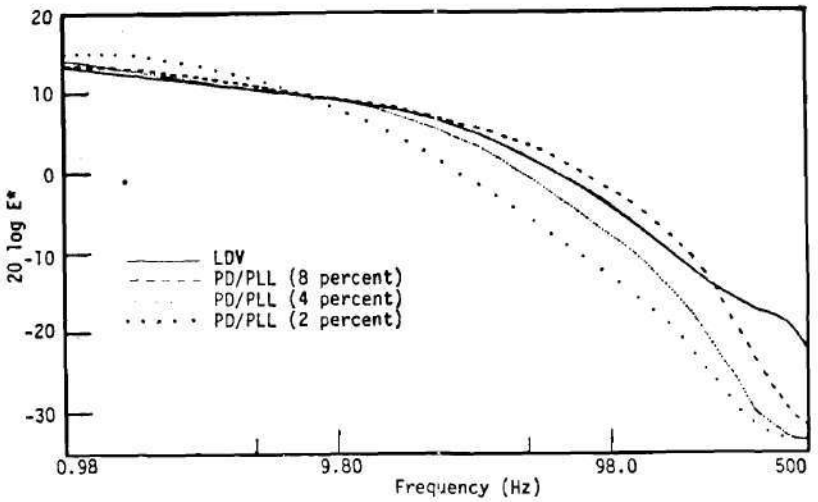

Figure 52. Performance of PD/PLL in Measuring Turbulent Pipe Flow at Re ≃ 15,000

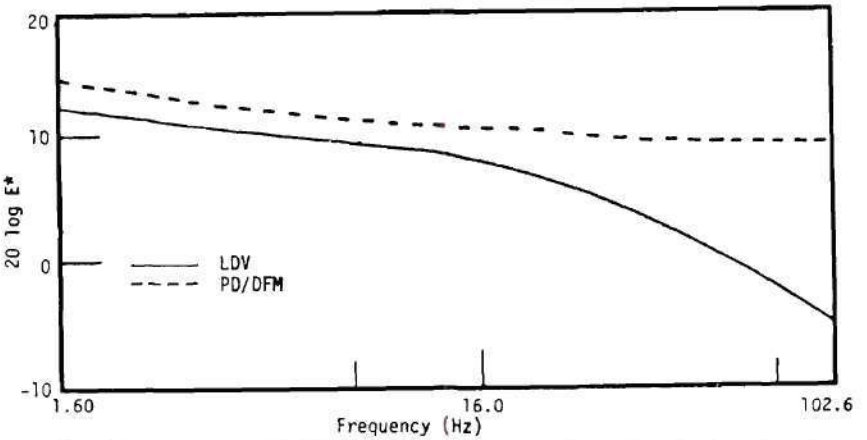

Figure 53. Performance of PD/DFM in Measuring Turbulent Pipe Flow at Re ≃ 15,000

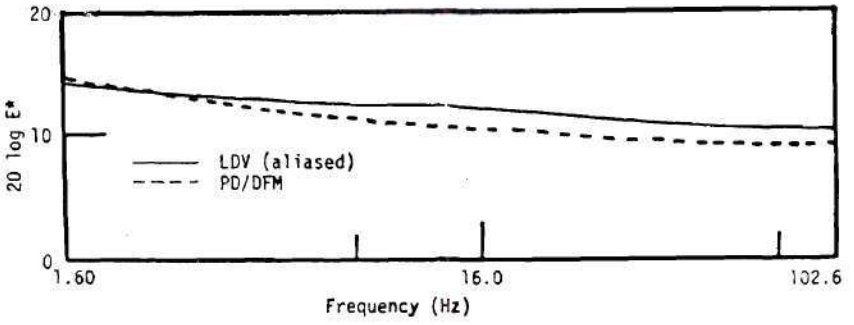

Figure 54. Comparison of Turbulence Power Spectra by PD/DFM and Corrupted LDV at Re ≃ 15,000

spectrum until about 100 Hz, then become flat and extend out to approximately 3200 Hz, (Figure 55). Clearly, the DFM method applied to measure such a spectrum will alias or 'fold back' all of the spectrum from 102.6 Hz to 3200 Hz into its measuring range, 1.6 to 102.6 Hz.

The above reasoning was applied to the turbulence power spectrum measured by the LDV, and the results compared with the prediction of the DFM method. The general agreement between them as shown in Figure 54 confirms the performance of the DFM method, at least within the constraints imposed by the PDV itself. It should be kept in mind, however, that the above predicted value of the cut-off frequency, f^* is an estimate resulting from various idealizing assumptions made in the derivation of equations on which these computations were based. Also, the measurement of the value of the Doppler ambiguity bandwidth, $\Delta\omega$ is also subjected to errors. In order to see what errors could be caused by inaccurate estimation of f^* and $\Delta\omega$, the aliased LDV power spectrum was computed for several of their values and the results are shown in Figures 56 and 57. It is apparent that variations in values of f^* and $\Delta\omega$ within a reasonable error margin do not affect the shape of the predicted spectrum significantly. Thus the correspondence between the spectrum measured by PD/DFM and the aliased version of that measured by LDV remains agreeable within a reasonable range of variation of f^* and $\Delta\omega$.

Figures 58 and 59 display the predicted turbulence spectra by the DFM method for remaining two velocity cases corresponding to

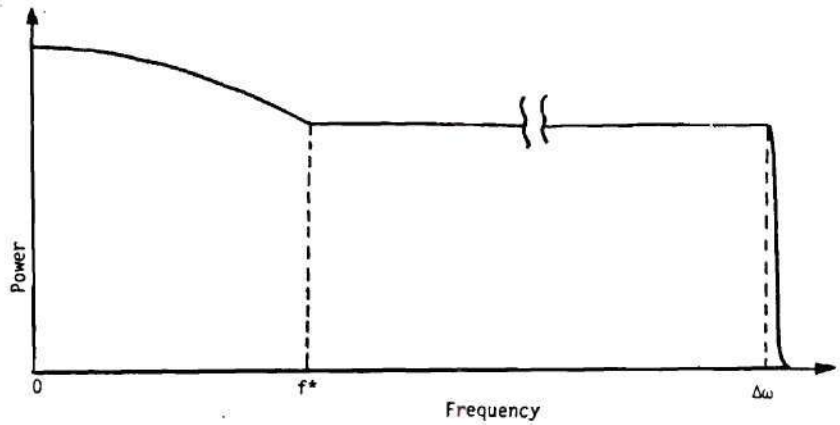

Figure 55. Ambiguity in Turbulence Measurement

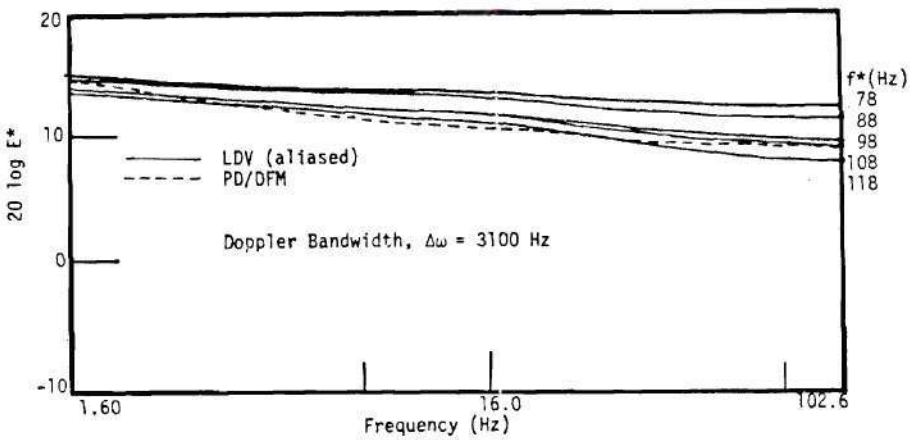

Figure 56. Effect of Variation in f^* on the Measured Turbulence Spectrum at Re ≃ 15,000

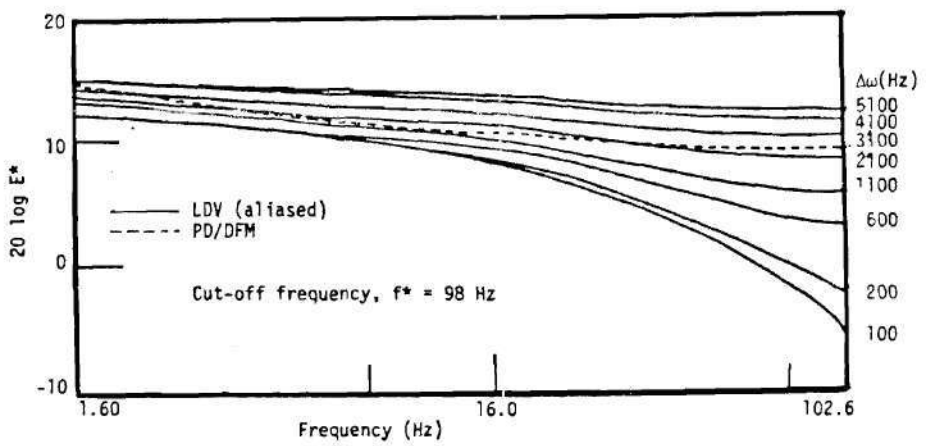

Figure 57. Effect of Variation in Δω on the Measured Turbulence Spectrum at Re ≃ 15,000

approximate Reynolds nubmers of 10,000 and 5,000 respectively. Again, the severe distortion in the PD/DFM spectra caused by aliasing is apparent. Following the same reasoning outlined above for Re $\simeq$ 15,000, the LDV data were appropriately modified and compared with the DFM results (Figures 60 and 61). There is an excellent agreement again for Re $\simeq$ 10,000. The discrepancy for the other case (Re $\simeq$ 5,000) can be attributed to errors in predictions of f* and $\Delta\omega$. Indeed, in this case small variations in estimation of f* and $\Delta\omega$ create significant changes in the aliased LDV power spectrum as demonstrated in Figures 62 and 63.

Lastly, Figures 64 and 65 show performance of the phase-locked loop for the above two flow cases. Its performance in the frequency measurement of velocity disturbances is decidedly insufficient. Also, as discussed earlier, since it is not clear as to what velocity it measures and the power spectra predicted by it depend on the roll-off rate of the bandpass filter in it, not only its results are incorrect but also any corrections to these are difficult to implement.

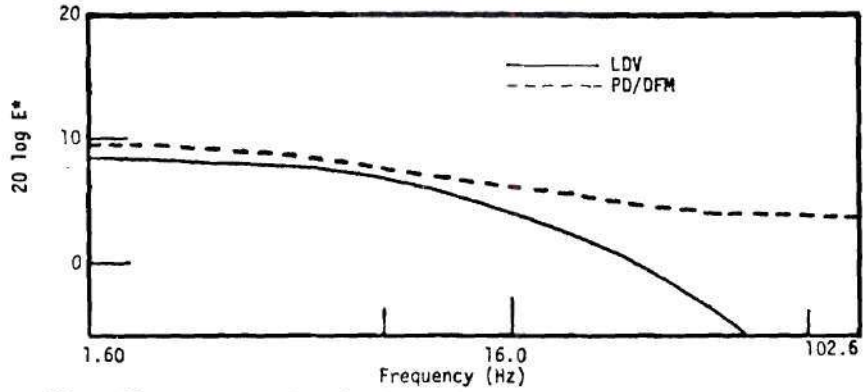

Figure 58. Measurement of Turbulent Pipe Flow by PD/DFM at Re ≃ 10,000

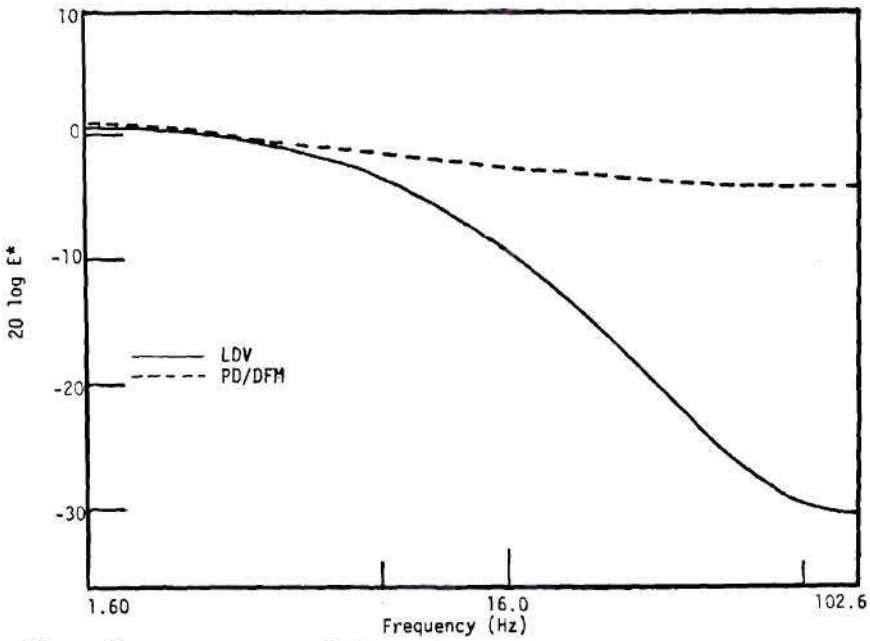

Figure 59. Measurement of Turbulent Pipe Flow by PD/DFM at Re ≃ 5,000

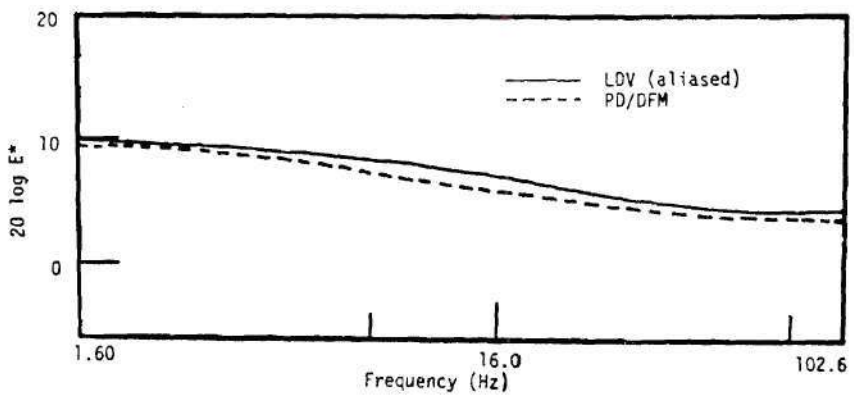

Figure 60. Comparison of Turbulence Power Spectra by PD/DFM and Corrupted LDV at Re ≃ 10,000

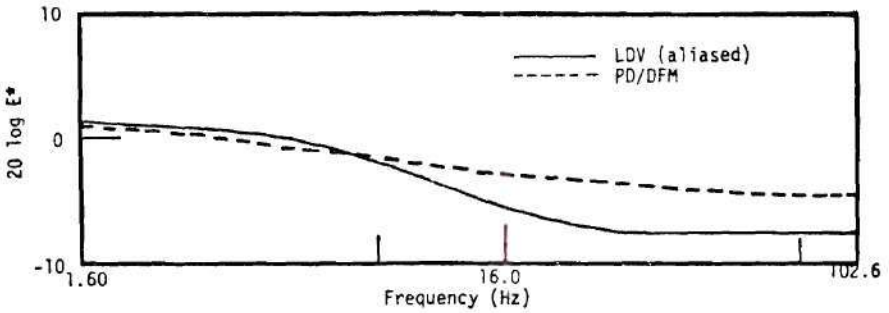

Figure 61. Comparison of Turbulence Power Spectra by PD/DFM and Corrupted LDV at Re ≃ 5,000

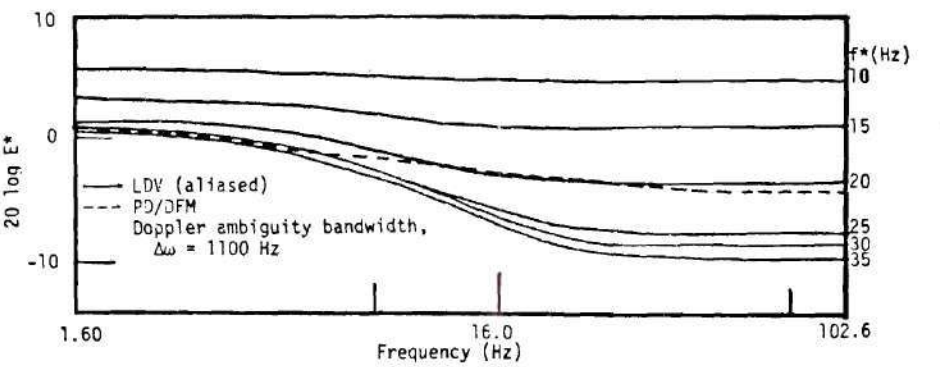

Figure 62. Effect of Variation in f^* on the Measured Turbulence Power Spectrum at Re ≃ 5,000

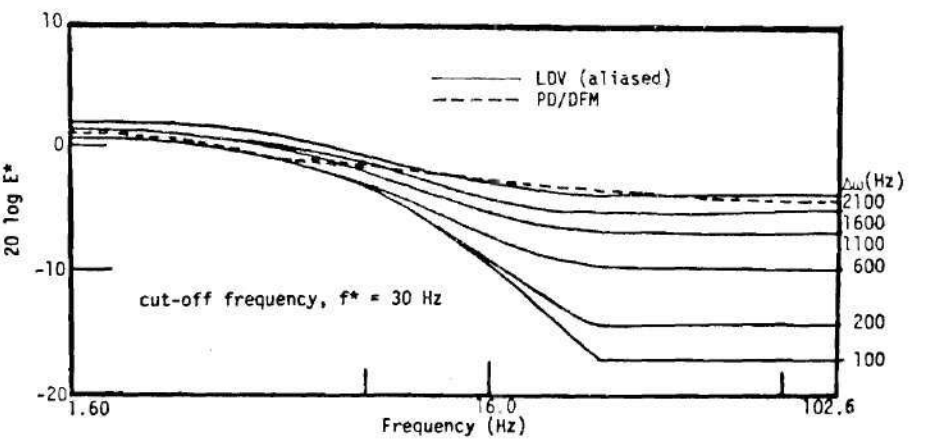

Figure 63. Effect of Variation in Δω on the Measured Turbulence Power Spectrum at Re ≃ 5,000

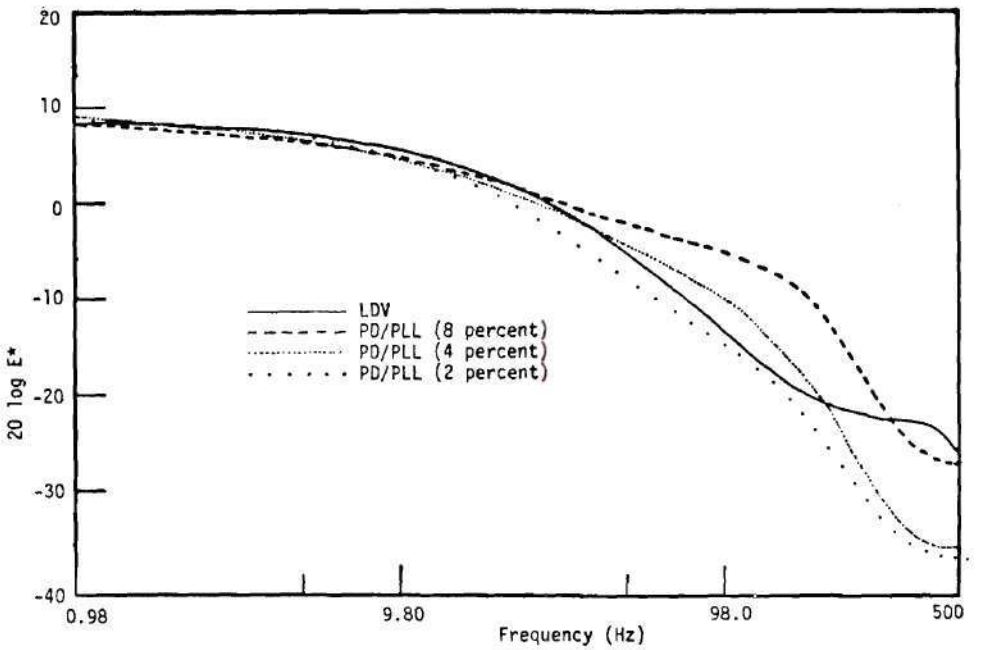

Figure 64. Performance of PD/PLL in Measuring Turbulent Pipe Flow at Re ≃ 10,000

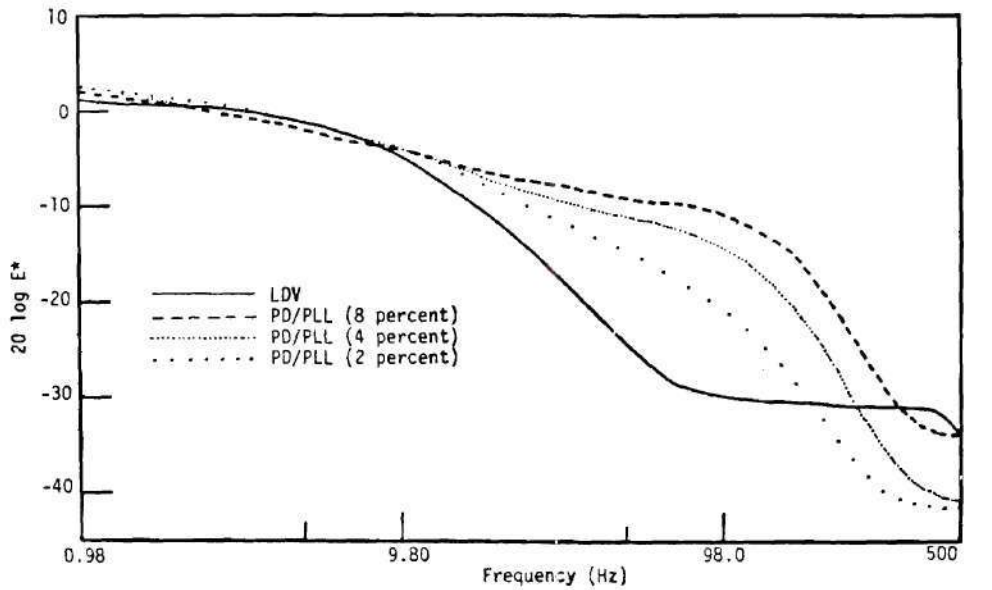

Figure 65. Performance of PD/PLL in Measuring Turbulent Pipe Flow at Re ≃ 5,000

CHAPTER VII

CONCLUSIONS AND DISCUSSION

At the outset of the present study, a model for determining the spatially-averaged 'instantaneous' velocity in a flow was hypothesized based upon consideration of ultrasound scattering from a large number of particles in the sample volume and upon statistical consideration of this phenomenon. The aim of the research was to test the validity and performance limits of the model through its realization by a digital scheme. Results of Chapter IV provided the preliminary testing of the proposed scheme - in the mean - with real pipe flows. Next, further extensive testing with several synthesized Doppler signals simulating different flow conditions yielded the basis for evaluation of the DFM method. This phase of experimentation was especially beneficial as the DFM performance was evaluated against known parameters, thus providing well-defined error margins. The DFM method was found to give superior performance in several cases compared to another accepted demodulator, the phase-locked-loop. Application of the hypothesized model to real pipe flows for turbulence measurements (Chapter VI) provided the final proof of the validity of the concept.

The goals of the present study have thus been attained. The DFM method has been demonstrated to be based on a valid concept and to provide excellent performance in measurement of turbulent flows. Its capabilities are impressive, and scope for improvements enormous.

As amply demonstrated by the last phase of experimentation, it is limited only by the design of the flowmeter being used. The severe distortion of the predicted turbulence power spectra is caused by design constraints of PD velocimeter and probe, and can be removed by appropriately taking into account the various sources of errors, in particular Doppler ambiguity, and aliasing.

In its present form, however, the proposed scheme is unsuitable for routine application in turbulence measurements. This can only be achieved by redesigning the PD device. Several suggestions immediately come to mind:

1. To decrease the effects of aliasing and to obtain high frequency response, F_{max}, in turbulence measurements the Doppler constant, K_D, in equation 3.5 must be increased. This can be realized by increasing the transmission frequency f_o. For example, with f_o equal to 23 MHz we shall have $F_{max} \simeq 300$ HZ, or triple its present value for the same velocity accuracy (2 cm/sec).

2. To improve the cut-off frequency, the sample volume size must be decreased. It has been shown that the velocity variations of extent smaller than the largest dimension of the sample volume are severely attenuated (George, 1971). Therefore, decreasing the minimum resolvable length in the direction of the mean flow is insufficient; all the dimensions must be decreased. This dictates a smaller size for the crystal and/or use of a focussed crystal. It is gratifying to note that the first requirements, namely, that of increasing the transmission frequency does allow for the use of smaller crystal while

still maintaining uni-directionality of the ultrasonic beam ($\lambda/d < 1$).

These two requirements, admittedly, imply considerable redesign of the existing PD device (or, perhaps a complete new design) involving large investment in effort and expenditure; but the motivation is great. The proposed scheme is suitable for turbulence measurements at any velocity, with variable frequency response and velocity accuracy. The existing demodulators are incapable of doing this; the zero-crossing frequencymeter has been shown to measure the second moment of the Doppler power spectrum (Rice 1945), thus yielding the rms rather than the mean velocity, its performance is severely degraded in the presence of noise, and it has been shown to be incapable of measuring turbulence (Flax et al., 1971). The phase-locked-loop, though providing good measurements at high velocities, is rendered almost useless at low velocities (See Figure 65). This can be a severe handicap in situations where the flow velocity is varying, for example, physiological situations. Also, there is the unresolved question of as to precisely what it does measure - e.g., the mean velocity, the maximum velocity, or the centerline velocity in the sample volume. These considerations thus make the development of the PD/DFM combination very desirable indeed.

3. So far we have only discussed possible (and highly desirable) modifications in the PD velocimeter design. There is however, another avenue for improvement: the digital scheme itself. In fact, this was the major factor for the digital implementation of the hypothesized model. The present study concentrated efforts only in testing of the

model through the use of the first moment of the power spectrum of the Doppler signal. Now that the validity has been established, this power spectrum can be further examined. For example, the second moment can be related to the rms velocity (and hence turbulence). Higher moments may provide yet more useful information, and the extension of the present program to calculate these can be achieved without redesigning the scheme, thus causing a tremendous saving in effort. The use of windows was demonstrated to give a better estimation of the Doppler power spectra, resulting in better estimation of velocity. Several other existing windows could be tried, or new windows could be designed more suitable for use with the Doppler signal (whose characteristics are roughly known). Another possible improvement is the use of a sliding window, thus providing more velocity points for same length of the digitized Doppler signal. This, in turn, improves the variance in the estimation of the turbulence power spectrum. Lastly, with respect to the response function correction, it may be noted that deconvolution in the frequency domain is difficult, time-consuming, and rather trying exercise. It may be possible through the use of a digital processing method (windowing, for example, in frequency or time domain, or both) to incorporate this correction, and still retain the speed of operation.

4. Lastly, it may be noted that since the objective of the present study was to hypothesize, test, and evaluate a model, an excessive amount of effort was not spent on making the method a real time operation; the Doppler signal was stored on a magnetic disc, and

later processed in an off-line mode. Now that the validity of the method has been proved, it may be made to operate in real time mode through making use of the continuing revolution in the electronic field.

In summary, thus, the DFM method seems to be a very attractive demodulator for the Doppler signal emanating from the Pulsed Ultrasound Doppler velocimeter. Its validity is established, its capabilities are impressive, and its potential enormous.

APPENDIX

PROGRAM LISTING

As explained in Section 5.4.3, the program is implemented as a series of records which are automatically loaded in the Fourier Analyzer memory in sequence from the disc. Below is the listing of a program used in Section 5.6.4 for applying the DFM method to the synthesized Doppler signal with random amplitude modulation. Here Doppler signal was sampled and stored in File 2, spectral analysis performed on it and resulting DFM's (with F_{max} = 102·6 Hz) stored in File 1. Later, the velocity signal and the PD/PLL output were sampled (with F_{max} = 500 Hz) one by one, and also stored in File 1. Finally, these three velocity series were recalled and turbulence intensity, mean velocity and turbulence power spectrum computed for each of them.

A note about the operation of Fourier Analyzer: computer data storage memory is divided in 'blocks'. The block size (BS) determines the length of the time series and is variable from 64 to 8192 data points. All the computations are done on whole blocks (i.e., individual data points are not accessibel to a keyboard user). For operation between two blocks (say, multiplication or correlation) one of them has to be ϕth block, and result of the operation also appear in this block.

PROGRAM SEQUENCE 1

COMPUTATION AND STORING OF DFM'S

STARTING CALL: JUMP Ø ENTER

```
L          99
MS         13                          READ NEXT PROGRAM SEQUENCE
D                                      DISPLAY BLOCK Ø AND WAIT
L           Ø                          STARTING POINT OF PROGRAM
BS       2Ø48                          FIX RECORD LENGTH IN FILE 2
MS         32                          INITIALIZE POINTER FOR FILE 2 FOR WRITING
MS         22        1       4ØØ      SAMPLE AND STORE 4ØØ RECORDS REAL TIME
BS        128                          MEMORY DIVIDED IN BLOCKS OF 128 DATA POINTS
Y ←         1        Ø                 INITIALIZE VARIABLE PARAMETER (VP1)
L          1Ø
CL          1D                         CLEAR 7Ø BLOCKS
Y  A+       1        1D                OF FOURIER ANALYZER MEMORY
#          1Ø        7Ø        Ø       EACH 128 POINTS LONG
MS         32                          REINITIALIZE POINTER FOR FILE 2 FOR READING
MS         35        1                 STORE CURRENT FILE POINTER VALUES
MS         25                          IN RECORD #1 OF FILE 5
MS         31      3ØØØ                READ RECORD # 3ØØØ OF FILE 1 CONTAINING
MS         11                          SMOOTHING WINDOW AND STORE IT
X>         7Ø                          IN BLOCK 7Ø
MS         35        1                 RESTORE THE ORIGINAL FILE POINTER
MS         15                          VALUES FROM FILE 5
Y        1ØØØ      -16                 BLOCK 16 IS DFM STORAGE STARTING POINT
Y ←         1        Ø                 INITIALIZE VP1 (# DFM DONE)
L           1                          STARTING POINT OF COMPUTATION LOOP
BS       2Ø48                          PREPARE FOR READING A FILE 2 RECORD
MS         12                          READ NEXT RECORD (DOPPLER SAMPLE 2Ø48 POINTS LONG)
Y ←         5        Ø                 # DFM COMPUTED IN A 2Ø48 POINTS LONG RECORD
BS        128                          BREAK READ RECORD INTO DOPPLER SAMPLES OF 128 POINT
L           3
X<         5D                          LOAD NEXT DOPPLER SAMPLE INTO BLOCK Ø
*          7Ø                          MULTIPLY BY WINDOW FUNCTION
F                                      TAKE ITS FOURIER TRANSFORM
*-                                     COMPLEX CONJUGATE MULTIPLY (POWER SPECTRA)
Y        1ØØØ        Ø                 COMPUTE DFM AND STORE STARTING FROM BLOCK 16
D           Ø        12                DISPLAY DOPPLER POWER SPECTRUM
Y  A+       5        5D                INCREMENT VP5 BY 1
Y  A+       1        1D                INCREMENT VP1 BY 1
#           3        16        Ø       FINISH ALL 16 DOPPLER SAMPLES OF 128 IN ONE RECORD
#           1      4ØØ         Ø       FINISH ALL 4ØØ RECORDS
Y  /L       1         1                WRITE # DFM DONE ON TTY
Y ←        5Ø        16
L           4                          MULTIPLY ALL STORED DFM'S BY 2
*        5ØD          2                (SINCE VCO CONSTANT = ½ DOPPLER CONSTANT)
MS         21       5ØD                AND WRITE THEM ON FILE 1
Y  A+      5Ø       5ØD                ON THE DISC
#           4        5Ø
J          99                          GO TO LABLE 99
.
```

PROGRAM SEQUENCE 2

SAMPLING AND STORING OF VELOCITY SIGNAL/PLL OUTPUT

```
L          99
MS         13                              READ NEXT PROGRAM SEQUENCE
D                                          DISPLAY BLOCK Ø AND WAIT
L           Ø                              STARTING POINT OF PROGRAM
Y  R     2ØØØ                              ACCEPT A MULTIPLICATION FACTOR FROM TTY
BS       2Ø48                              FIX RECORD LENGTH IN FILE 2
MS         32                              INITIALIZE POINTER 2 FOR WRITING
MS         22        1      6Ø             SAMPLE AND WRITE ON FILE 2 60 RECORDS
MS         32                              INITIALIZE POINTER 2 FOR READING
L           1                              STARTING POINT OF LOOP
BS       2Ø48                              PREPARE FOR READING A RECORD OF FILE 2
MS         12                              READ NEXT RECORD FROM FILE 2
*           Ø    2ØØØD                     MULTIPLY IT BY THE MULTIPLICATION FACTOR
Y ←        3Ø      Ø                      INITIALIZE VP3Ø
BS        256                              BREAK READ RECORD INTO BLOCKS OF 256 POINTS
L           3
MS         21     3ØD                      WRITE NEXT BLOCK IN FILE 1
D         3ØD      4                      DISPLAY THIS VELOCITY DATA ONCE
Y  A+      3Ø     3ØD                      INCREMENT VP3Ø
#           3       8      Ø               FINISH ALL 8 BLOCKS OF 256 IN ONE RECORD
#           1      5Ø      Ø               FINISH 5Ø SUCH RECORDS
J          99                              GO TO LABLE 99
.
```

PROGRAM SEQUENCE 3

COMPUTATION OF MEAN VELOCITY AND TURBULENCE

POWER SPECTRUM FROM DFM'S

```
L        99
MS       13                        READ NEXT PROGRAM SEQUENCE
BS       128                       PREPARE FOR READING DFM'S FROM FILE 1
Y ←      4Ø      4Ø                SET VP4Ø = 4Ø
L        Ø                         STARTING POINT OF THE PROGRAM
MS                                 LIST CURRENT FILE POINTERS LOCATIONS
CL       2                         CLEAR BLOCK 2
CL       4ØD                       CLEAR BLOCK VP4Ø
L        1                         STARTING POINT OF THE COMPUTATION LOOP
MS       11                        READ NEXT DFM RECORD FROM FILE 1
$                                  INTEGRATE - THE MEAN VALUE
:        Ø       128               IS 128TH DATA POINT
A+       2                         ADD TO AND
X>       2                         STORE IN BLOCK 2
#        1       5Ø      Ø         FINISH READING ALL DFM RECORDS
:        2       5Ø                FIND MEAN
←        2       127               AND FILL WHOLE
CL       2       1       127       OF BLOCK 2
$        2                         WITH THIS VALUE
W        2       Ø                 WRITE THIS MEAN VELOCITY VALUE,U, ON TTY
MS       31      -5Ø     1         MOVE BACK FILE 1 POINTER BY 5Ø RECORDS FOR
CL       1                         START READING DFM'S AGAIN
L        2                         STARTING POINT OF POWER SPECTRUM COMPUTATION LOOP
MS       11                        READ NEXT DFM RECORD FROM FILE 1
A-       2                         SUBTRACT MEAN TO GIVE FLUCTUATIONS
F
SP                                 AVERAGE POWER SPECTRUM OF TURBULENCE
#        2       5Ø      Ø         FROM THESE 5Ø DFM RECORDS
X<       1
CL       1       Ø                 MULTIPLY AMPLITUDE OF ALL
*        1       2                 FREQUENCIES BY 2 EXCEPT THE
CL       Ø       1       64        DC VALUE  ( SINCE POWER SPECTRA IN THE FOURIER
A+       1                         ANALYZER ARE COMPUTED AS 2-SIDED )
X>       4ØD                       STORE AVERAGE PS IN 4ØTH BLOCK
TL       4ØD                       CONVERT INTO LOG COORDINATES
$                                  INTEGRATE POWER SPECTRUM TO GET TURBULENCE
W        Ø       64                INTENSITY VALUE AND PRINT IT ON TTY
D        4ØD                       DISPLAY TURBULENCE POWER SPECTRUM TO PLOT IT
J        99                        GO TO LABLE 99
.
```

PROGRAM SEQUENCE 4

COMPUTATION OF MEAN VELOCITY AND TURBULENCE

POWER SPECTRUM OF VELOCITY SIGNAL/PLL OUTPUT

```
L          99
MS         13                          READ NEXT PROGRAM SEQUENCE
D                                      DISPLAY BLOCK Ø AND WAIT
L           Ø                          STARTING POINT OF PROGRAM
BS       4Ø96
CL          1                          CLEAR ALL DATA STORAGE MEMORY OF
CL          Ø                          THE FOURIER ANALYZER
BS        256                          PREPARE TO READ VELOCITY RECORDS FROM FILE 1
L           1                          STARTING POINT OF MEAN COMPUTATION LOOP
MS         11                          READ THE NEXT VELOCITY RECORD FROM FILE 1
$                                      INTEGRATE - THE MEAN VELOCITY VALUE
:           Ø    256                   IS 256TH DATA POINT
A+          8                          ADD TO AND
X           8                          STORE IN BLOCK 8
#           1    4ØØ      Ø           FINISH READING ALL VELOCITY RECORDS
:           8    4ØØ                  FIND MEAN VELOCITY VALUE,U
←           8    255                  AND FILL WHOLE OF
CL          8      1      255         BLOCK 2 OF 1Ø24 DATA POINTS
BS       1Ø24
$           2                          WITH THIS VALUE
W           2      Ø                   WRITE THIS MEAN VELOCITY VALUE,U, ON TTY
MS         31   -4ØØ      1           MOVE BACK FILE 1 POINTER BY 4ØØ RECORDS FOR
CL          1                          START READING VELOCITY AGAIN
L           2                          STARTING POINT OF POWER SPECTRUM COMPUTATION LOOP
BS        256                          PREPARE TO READ VELOCITY RECORDS FROM FILE 1
Y          1Ø      Ø
L           3                          READ 4 VELOCITY RECORDS OF SIZE 256 POINTS
MS         11     1ØD                  AND
Y  A+      1Ø     1ØD                  MERGE THEM INTO
#           3      4       Ø           ONE BLOCK OF
BS       1Ø24                          SIZE 1Ø24 POINTS
A-          2                          SUBTRACT MEAN TO GIVE TURBULENCE
F
SP                                     AVERAGE POWER SPECTRUM OF STORED
#           2    1ØØ                   4ØØ VELOCITY RECORDS IN FILE 1
X           1
CL          1      Ø                   MULTIPLY AMPLITUDE OF ALL
*           1      2                   FREQUENCIES BY 2 EXCEPT THE
CL          Ø      1      512          DC VALUE (SINCE POWER SPECTRA IN FOURIER ANALYZER
A+          1                          ARE COMPUTED AS 2-SIDED)
X           2                          STORE THE AVERAGE POWER SPECTRUM IN
TL          2                          BLOCK 2 AND CONVERT INTO LOG COORDINATES
$                                      INTEGRATE THE POWER SPECTRUM TO GET TURBULENCE
W           Ø    1Ø5                   INTENSITY VALUE AND PRINT IT ON TTY
D           2                          DISPLAY TURBULENCE POWER SPECTRUM TO PLOT IT
J          99                          GO TO LABLE 99
.
```

BIBLIOGRAPHY

1. Allen, H. W., J. W. Knutti, S. J. Gschwend, R. B. Martin, and J. D. Meindl, "An Implantable Integrated Circuit CW Doppler Flowmeter," 30th ACEMB, 1977, 6.1, pp. 44.

2. Arts, M. G. J., and J. M. J. G. Roevros, "On Instantaneous Measurement of Blood Flow by Ultrasound Means", Med. and Biol. Eng., 10, 1972, pp. 23.

3. Baker, D. W., et al., Proc. of ACEMB, 1964 pp. 76.

4. Baker, D. W., "The Doppler Shift Principle Applied to Flow and Displacement Measurement", 18th ACEMB, 1965, 23-6, pp. 172.

5. Baker, D. W. and D. W. Watkins, "A Coherent Pulse Doppler System for Cardiovascular Measurements", 20th ACEMB, 1967, pp. 27-2.

6. Baker, D. W., "Pulsed Ultrasonic Doppler Blood Flow Sensing", IEEE Trans. Son. and Ultra., SU-17, 3, July 1970.

7. Baker, D. W., J. E. Jorgensen and D. N. Campau, "The Characteristics of Pulsed Ultrasound Flowmeter", Flow - Its Measurement and Control in Science and Industry, 1, Part III, Ed. Dowdell, 1971, pp. 1389-1400.

8. Baker, D. W. and W. G. Yates, "Techniques for Studying the Sample Volume of Ultrasonic Doppler Devices", Med. and Biol. Eng., II, 6, November 1973, pp. 766-770.

9. Bert, L., James Frescura, D. Meindl, "An Implantable CW Directional Doppler Ultrasonic Flowmeter", 25th ACEMB, 1972, 7.2, pp. 32.

10. Brody, W. R., "Theoretical Analysis of the Ultrasonic Blood Flowmeter", Technical Reports #4951-1, *Stanford University*, October 1971.

11. Brody, W. R. and J. D. Meindl, "Theoretical Analysis of the Constant Wave Doppler Ultrasonic Flow meter", IEEE Trans. Biomed. Eng., BME-21, 3, May 1974, pp. 182-192.

12. Collins, J. T., B. Van Bellen, R. H. Dean, J. J. Bergen, and J. S. T. Yao, "Fourier Analysis of Doppler Shift Arterial Flow Signals", Proc. of 29th ACEMB, 1976, 11.2, pp. 71.

13. Dipietro, D. M., and J. D. Meindl, "An Implantable Ultrasonic Flowmeter", 23rd ACEMB 21-1, November 1970.

14. Durst, F., A. Melling and J. H. Whitelaw, Principles and Practice of Laser-Doppler Anemometry, Academic Press, 1976.

15. Edwards, R. V., J. C. Angus and M. J. French, "Spectral Analysis of the Signal from the Laser Doppler Flowmeter: Time Dependent Systems", J. Appl. Mech., 42, 2, February 1971, pp. 837-850.

16. Flax, S. W., J. G. Webster and S. J. Updike, "Theoretical and Experimental Evaluation of Doppler Blood Flow Information", 8th International Conference Med. Biol. Eng. 1969, pp. 108.

17. Flax, S. W., J. G. Webster and S. J. Updike, "Statistical Evaluation of the Doppler Ultrasound Flowmeter", ISA Transactions, 10, 1, 1971, pp. 1-20.

18. Flax, S. W., J. G. Webster and S. J. Updike, "Noise and Functional Limitations of the Doppler Blood Flowmeter", Cardiovascular Applications of Ultrasound ed. Reneman, North Holland 1974.

19. Fox, M. D., "A Multiple-Beam Ultrasound Doppler Velocimetry", IEEE Trans. Sonics and Ultrasonics, SV-25, 5, September 1978.

20. Franklin, D. L., D. W. Baker, R. M. Ellis and R. F. Rushmer, "A Pulsed Ultrasonic Flowmeter", IRE Transactions on Medical Electronics, December 1959.

21. Franklin, D. L., W. Shlegel and R. F. Rushmer, "Blood Flow Measured by Doppler Frequency Shift of Backscattered Ultrasound", Science, August 1961, pp. 564-565.

22. George, W. K., "An Analysis of Laser Doppler Velocimeter and its Application to the Measurement of Turbulence Ph.D. Thesis, Department of Mechanics, The John Hopkins University, 1971.

23. George, W. K., and J. L. Lumley, "The Laser Doppler Velocimeter and its Application to the Measurement of Turbulence", J. Fluid Mech., 60, Part 2, 1973, pp. 321-362.

24. Giddens, D. P., R. F. Mabon, and R. A. Cassanova, "Measurement of Disordered Flow Distal to Subtotal Vascular Stenoses in the Thoracic Aorta of Dogs", Circulation Research, 39, 1, July 1976.

25. Gosling, R. G., D. H. King and C. D. Side, "Spectrum Analysis and Arterial Ultrasound Doppler Shift: The Intensity Dilution Syndrome", 23rd ACEMB, 1970, pp. 21-14.

26. Green, P. S., "Spectral Broadening of Acoustic Reverberations in Doppler Shifted Fluid Flowmeters", The J. of the Acoustical Soc. of Am., 36, 7, July 1964, pp. 1383-1390.

27. Green, P. S., "Image Spreading Function in a Medium Containing Discrete Isotropic Scatterers", JASA, 56, 1966, pp. 607-610.

28. Griffith, J. M., and W. R. Brody, "Velocity Resolution in Ultrasonic Doppler Flowmeters", 28th ACEMB, 1-10, 1975, pp. 75.

29. Griffith, J. M., W. R. Brody and L. Goodman, "Resolution Performance of Doppler Ultrasound Flowmeters", JASA, 60, 1976, pp. 607-610.

30. Haase, W. C., W. S. Foletta and J. D. Meindl, "A Directional Ratiometric Ultrasonic Blood Flowmeter", Proc. IEEE Ultrasonic Symposium, November 1973, pp. 81-85.

31. Herrick, J. F., J. A. Anderson, "An Ultrasonic Flowmeter", IRE Transactions on Medical Electronics, December 1959, pp. 195.

32. Histand, M. B., E. R. Green, "Detection of Arterial Stenoses", 29th ACEMB, 11.8, 1976, pp. 77.

33. Jenkins, G. M., and D. G. Watts, "Spectral Analysis and its Applications", Holden-Day, 1969.

34. Jethwa, C. P., M. Kaveh, G. R. Cooper and F. Saggio, "Blood Flow Measurement Using Ultrasonic Pulsed Random Signal Doppler System", IEEE Trans. on Sonics and Ultrasonic, SU-22, 1, 1975, pp. 1-11.

35. Jethwa, C. P., and M. D. Olinger, "Blood Flow Measurement Using Random Signal Flowmeter", Ultrasound in Medicine, 2, ed. D. White and R. E. Brown, Am. Inst. of Ultrasound in Medicine, 1977, pp. 341-350.

36. Jorgensen, J. E., D. N. Campau, J. L. Gabrini and D. W. Baker, "Analytical Modelling of the Pulsed Ultrasonic Doppler Flowmeter", 25th ACEMB, 1972, pp. 7-5.

37. Jorgensen, J. E., D. N. Campau and D. W. Baker, "Physical Characteristics and Mathematical Modelling of Pulsed Ultrasonic Flowmeter", Med. and Bio. Eng., 1973, pp. 404-420.

38. Jorgensen, J. E., and J. L. Garbini, "An Analytical Procedure for the Calibration of the Pulsed Ultrasonic Doppler Flowmeter", Trans. ASME, 96, June 1974, pp. 158.

39. Kalmus, H. P., "An Electric Flowmeter", Rev. Sci. Inst. 75, 1954, pp. 201.

40. Laufer, J., and R. McClellan, J. Fluid Mechanics, 1, 1956, pp. 276.

41. Light, L. H., "Ultrasonic Doppler Techniques in Blood Velocity Measurement", Fluid Dynamic Measurements in the Industrial and Medical Environments, 1, ed. David J. Cockrell, Leicester University Press, 1972.

42. Lin, J. C., F. T. S. Yu, A. Tai, "Coherent Optical Analysis of Ultrasonic Blood Flow Spectrum", 29th ACEMB, 19:1, 1976, pp. 137.

43. Luque, J., D. E. Dick, F. D. McLeod, "Trandsducer Limitations on Random Signal Ultrasound", 29th ACEMB, 3.3, 1976, pp. 17.

44. MacIntosh: British Journal of Radiology, 45, 1972, pp. 320-327.

45. McGillem, C. D., G. R. Cooper and W. B. Waltman, "Use of Wide-band Stochastic Signals for Measuring Range and Velocity", EASCON Conf., 1969, pp. 305-311.

46. McLeod, F. D. Jr., "Directional Doppler Demodulation", 20th ACEMB, 1967, pp. 27-1.

47. McLeod, F. D., Jr., "Calibration of CW and Pulsed Doppler Flow-meters", 23rd ACEMB, 21.2, 1970, pp. 270.

48. McLeod, F. D., and N. Anliker, "Multiple Gate Pulse Doppler Flowmeter", Proc. of IEEE Ultrasonic Symposium, 1971.

49. McLeod, F. D., "Multichannel Pulse Doppler Techniques", Cardiovascular Applications of Ultrasound, ed. Reneman, North Holland, 1974

50. McLeod, F. D., C. W. Miller and R. E. Daigle, "Doppler Detection of Flow Disturbances", Ultrasound in Medicine, 1, ed. D. White and R. E. Brown, Am. Inst. of Ultrasound in Med., 1977, pp. 351.

51. Middleton, D., "A Statistical Theory of Reverberations and Similar First Order Scattered Fields", Part I: Waveforms and General Process", IEEE Trans. on Information Theory IT-13, 1967, pp. 372-392.

52. Miller, C. W., M. B. Histand, "An Evaluation of the Measure-ment of Flow Rate using a Pulsed Doppler Velocitymeter", 25th ACEBM, 7.6, 1972(a), pp. 36.

53. Miller, C. W., and M. B. Histand, "Transcutaneous Measurement of Blood Velocity Profiles and Instantaneous Flow:, 25th ACEMB, 1972(b), pp. 7.8.

54. Newhouse, V. L., and P. J. Bendick, "Analysis of Random Signal Blood Flow Measurement", Proc. of IEEE Ultrasonic Symposium, November 1973, pp. 94-97.

55. Newhouse, V. L., L. W. Varner and P. J. Bendick, "Transit Time Effects on Ultrasonic Doppler Blood Flow Measurement", 27th ACEMB, 1974, pp. 38.2.

56. Newhouse, V. L., P. J. Bendick and L. W. Varner, "Analysis of Transit Time Effects on Doppler Flow Measurement", IEEE Trans. Biomed. Eng., BME-23, 5, September 1976(b), pp. 381-387.

57. Newhouse, V. L., L. W. Varner and G. T. Mitchell, "The Effect of Geometrical Broadening on Ultrasonic Doppler Flow Measurement Systems", 29th ACEMB, 19.5, 1976(a), pp. 141.

58. Nippa, N J., "Ultrasonic Doppler Velocimeter for Quantitative Forward and Reverse Flow Velocities", Proc. Am. Inst. of Ultrasound in Medicine, October 1974, pp. 459-462.

59. Nippa, J. H., D. E. Hokansen, D. R. Lee, D. S. Summer and D. E. Strandess, Jr., "Phase Rotation for Separating Forward and Reverse Blood Flow Velocity Signals", IEEE Trans. on Son. and Ultrason., SU-22, 5, 1975, pp. 340-346.

60. Peronneau, P. A., and F. Leger, "Doppler Ultrasonic Pulsed Blood Flowmeters", 8th International Conference on Med. and Biol. Eng., 1969

61. Peronneau, P. A., M. M. Pellet, M. C. Xhaard and J. R. Kinglais, "Pulsed Doppler Ultrasonic Blood Flowmeter: Real-time Instantaneous Velocity Profiles", Symposium of Flow, Pittsburgh, PA, May 1971, pp. 1367-1376.

62. Potter, R. W., "Compilation of Time Windows and Line Shapes for Fourier Analysis", HP Bulletin.

63. Reid, J. M. R. A. Siegelman, M. G. Nasser and R. D. W. Maker, "Scattering of Ultrasound by Human Blood", 8th Intl. Conf. Med. and Biol. Eng., 1969.

64. Resch, F. J. "(1970) Hot Film Turbulence Measurements in Water Flow", Proc. Am. Soc. Civil Engineers, J of Hydraulic Division, 96, HY3, 1970, pp. 787-800.

65. Rice, S. O., "Mathematical Analysis of Random Noise", Bell System Technical Journal, 23:282, 1944, and 24:1, 1945.

66. Rushmer, R. F., D. W. Baker, H. F. Stegall and E. A. McCutcheon, "Application of Transcutaneous Doppler Flowmeters", 18th ACEMB, 1976, pp. 72.

67. Rushmer, R. F., D. W. Baker and H. F. Stegall, "Transcutaneous Doppler Flow Detection as A Non-Destructive Technique", J. of Appl. Physiol., 21, 1966, pp. 554-556.

68. Satomura, S., "Study of Flow Patterns in Peripheral Arteries by Ultrasonics", J. of Acoustical Society of Japan, 15, 1959, pp. 151-159.

69. Satomura, S., and Z. Kaneko, "Ultrasonic Blood Rheograph", Digest of 3rd International Conf. on Med. Electronics, London, 1960, pp. 254-258.

70. Siegel, B., R. J. Gibson, K. V. Amatineek, W. R. Felix, Jr., A. L. Edelstein, and G. L. Popky, "A Doppler Ultrasound Method for Distinguishing Laminar from Turbulent Flow - A Preliminary Report", Journal of Surgical Research, 10, 5, 1970, pp. 221-224.

71. Stegall, H. F., H. L. Stone, V. S. Bishop and C. Laenger, "A Catheter-tip Pressure and Velocity Sensor", 20th ACEMB, 1967.

72. Strandness, D. E., Jr. and D. S. Summer, "Application of Ultrasonic Flow Detector to the Study of Arterial and Venous Disease", 20th ACEMB, 1967(a), pp. 27.5.

73. Strandness, D. E., R. D. Schultz, D. S. Sumner, and R. F. Rushmer, "Ultrasonic Flow Detection -- A Useful Technique in Evaluation of Peripheral Vascular Disease", Am. Jr. Surgery, 113, 1967(b), pp. 311-320.

74. Stratton, J. A., Electromagnetic Theory, McGraw-Hill Book Company, New York, 1941.

75. Van Citter, R. L., and D. L. Franklin, "Blood Flow in Mesenteric Artery of Chimpanzee Monitored via Telemetry", Aerospace Medicine 38, 9, 1965(a), pp. 926-931.

76. Van Citter, R. L., O. A. Smith, Jr., D. L. Franklin, W. S. Kemper and N. W. Watson, "Radio Telmetry Blood Flow and Blood Pressure in Feral Baboons: A Preliminary Report", Paper read at the 2nd Symposium on Baboon and its Use as Experimental Animal, San Antonio, Texas, 1965(b)

77. Van Citter, R. L., D. L. Franklin, O. A. Smith, Jr., N. W. Watson and R. W. Elsner, "Cardiovascular Adaptations to Diving in Northern Elephant Seal, Mirounga Augosti rostris", Comp. Biochem. Physiol. 16:267, 1965(c).

78. Van Citter, R. L., E. Evonak and D. L. Franklin, "Blood Flow Distribution in Alaska Sled Dogs During Extended Exercises", Physiologist 9:310, 1966.

79. Van Citter, R. L., and D. L. Franklin, "The Doppler Ultrasonic Telemetry Flowmeter Applications in Animal Expts", 20th International Conference on Engineering in Medicine and Biology, 27.7, November 1967.

80. Varner, L. W., V. L. Newhouse and P. J. Bendick, "Application of Transit Time Effects to the Independent Measurement of Blood Flow Velocity and Angle", 28th ACEMB, B1.11, 1975, pp. 76.

81. Wehrmann, O. H., "Advances in Hot Wire Anemometry", AFOSR Number 68-1492, University of Maryland, 1968, pp. 194.

82. Wells, P. N. T., "A Range-gated Ultrasonic Doppler System", Med. and Biol. Eng., 7, 1969, pp. 641-652.

83. Wells, P. N. T., "The Possibility of Harmful Effects in Ultrasonic Diagnosis", Cardiovascular Applications of Ultrasound, ed. Reneman, North Holland, 1974.

84. Wiener, Norbert, Extrapolation, Interpolation and Smoothing of Stationary Time Series, John Wiley and Sons, New York, 1949.

85. Winter, D. C., M. K. Wells, R. J. Morgan, "Detection of Cardiovascular Flow Disturbances using Autocorrelograms", 28th ACEMB, E2a-6, 1975, pp. 300.

86. Winter, D. C., M. K. Wells and R. J. Morgan, "Ultrasonic Detection of Cardiovascular Flow Disturbances", 29th ACEMB, 19.4, 1976(a), pp. 140.

87. Winter, D. C., M. K. Wells, R. J. Morgan, "Ultrasonic Detection of Cardiovascular Flow Disturbances", ISA, BM 76319, 1976(b), pp. 101-105.

88. Yao, S. T., and T. N. Needham, "Frequency Analysis of Doppler Shift Blood Flow Signals by a Band-pass Filter: Preliminary Report", Biomedical Eng., Sept. 1970, pp. 438-442.

89. Yeh, Y., and H. Cummins "Localized Fluid Flow Measurements with He-Ne Laser Spectrometer", Appl. Phys. Lett., 4, 1964, pp. 176-178.

VITA

The author was born on 24 October 1952 in the town of Auriya, India and graduated from GBMS Inter College, Kanpur in 1969. He received a Bachelor of Technology degree in Aeronautical Engineering from Indian Institute of Technology, Kharagpur, India in 1974. In the Fall of the same year he joined Georgia Institute of Technology as a graduate student and was awarded Master of Science in Aerospace Engineering in August 1975.